

¹ Measurement of the Drell-Yan Absolute Cross-Section
² in pp Collisions with a 120 GeV Proton Beam at
³ Fermilab

⁴ Chatura Kuruppu¹, Stephen Pate¹

⁵ ¹New Mexico State University, Las Cruces, NM 88003, USA

⁶ October 2, 2025

⁷ **Abstract**

This analysis note reports on the determination of pp Drell-Yan absolute cross sections from data collected using the Roadset 67 trigger. We seek preliminary approval of these results, for presentation in upcoming conferences. Similar techniques will be used to determine the pd DY cross section, and then we will move on to include data from the other run 2-3 and 5-6 roadsets.

¹³ This work was supported in part by US DOE grant DE-FG02-94ER40847.

¹⁴ Contents

¹⁵ 1	Introduction	5
¹⁶ 2	Analysis Methodology	5
¹⁷ 2.1	Data and Monte Carlo Samples	5
¹⁸ 2.2	Event Selection	6
¹⁹ 2.3	Cross-Section Formalism	6
²⁰ 3	Acceptance and Efficiency Corrections	7
²¹ 3.1	Detector Acceptance Correction	7
²² 3.2	Reconstruction Efficiency Correction	24
²³ 3.2.1	Uncertainty Propagation	24
²⁴ 3.2.2	Efficiency Results	24
²⁵ 3.3	Trigger Efficiency	45
²⁶ 4	Systematic Uncertainties	45
²⁷ 5	Results: Double-Differential Cross-Section	46
²⁸ 6	Discussion and Conclusion	64
²⁹ 7	Acknowledgements	64
³⁰ A	Appendix: Event Selection Criteria	65
³¹ A.1	Positive Track Cuts (<code>chuckCutsPositive_2111v42</code>)	65
³² A.2	Negative Track Cuts (<code>chuckCutsNegative_2111v42</code>)	65
³³ A.3	Dimuon Cuts (<code>chuckCutsDimuon_2111v42</code>)	65
³⁴ A.4	Physics and Occupancy Cuts	65
³⁵ B	Appendix: Table of Systematic Errors	66
³⁶ C	Appendix: Table of $M^3 \frac{d^2\sigma}{dM dx_F}$ Cross-Section Values	70

37 **List of Figures**

38 1	Acceptance plots for $0.00 \leq x_F < 0.05$	8
39 2	Acceptance plots for $0.05 \leq x_F < 0.10$	9
40 3	Acceptance plots for $0.10 \leq x_F < 0.15$	10
41 4	Acceptance plots for $0.15 \leq x_F < 0.20$	11
42 5	Acceptance plots for $0.20 \leq x_F < 0.25$	12
43 6	Acceptance plots for $0.25 \leq x_F < 0.30$	13
44 7	Acceptance plots for $0.30 \leq x_F < 0.35$	14
45 8	Acceptance plots for $0.35 \leq x_F < 0.40$	15
46 9	Acceptance plots for $0.40 \leq x_F < 0.45$	16
47 10	Acceptance plots for $0.45 \leq x_F < 0.50$	17
48 11	Acceptance plots for $0.50 \leq x_F < 0.55$	18
49 12	Acceptance plots for $0.55 \leq x_F < 0.60$	19
50 13	Acceptance plots for $0.60 \leq x_F < 0.65$	20
51 14	Acceptance plots for $0.65 \leq x_F < 0.70$	21
52 15	Acceptance plots for $0.70 \leq x_F < 0.75$	22
53 16	Acceptance plots for $0.75 \leq x_F < 0.80$	23
54 17	Efficiency plots for the x_F bin $0.00 \leq x_F < 0.05$	25
55 18	Efficiency plots for the x_F bin $0.05 \leq x_F < 0.10$	26
56 19	Efficiency plots for the x_F bin $0.10 \leq x_F < 0.15$	27
57 20	Efficiency plots for the x_F bin $0.15 \leq x_F < 0.20$	28
58 21	Efficiency plots for the x_F bin $0.20 \leq x_F < 0.25$	29
59 22	Efficiency plots for the x_F bin $0.25 \leq x_F < 0.30$	30
60 23	Efficiency plots for the x_F bin $0.30 \leq x_F < 0.35$	31
61 24	Efficiency plots for the x_F bin $0.35 \leq x_F < 0.40$	32
62 25	Efficiency plots for the x_F bin $0.40 \leq x_F < 0.45$	33
63 26	Efficiency plots for the x_F bin $0.45 \leq x_F < 0.50$	34
64 27	Efficiency plots for the x_F bin $0.50 \leq x_F < 0.55$	35
65 28	Efficiency plots for the x_F bin $0.55 \leq x_F < 0.60$	36
66 29	Efficiency plots for the x_F bin $0.60 \leq x_F < 0.65$	37
67 30	Efficiency plots for the x_F bin $0.65 \leq x_F < 0.70$	38
68 31	Efficiency plots for the x_F bin $0.70 \leq x_F < 0.75$	39
69 32	Efficiency plots for the x_F bin $0.75 \leq x_F < 0.80$	40
70 33	Differential cross-section for x_F bin $0.00 \leq x_F < 0.05$	47
71 34	Differential cross-section for x_F bin $0.05 \leq x_F < 0.10$	48
72 35	Differential cross-section for x_F bin $0.10 \leq x_F < 0.15$	49
73 36	Differential cross-section for x_F bin $0.15 \leq x_F < 0.20$	50
74 37	Differential cross-section for x_F bin $0.20 \leq x_F < 0.25$	51
75 38	Differential cross-section for x_F bin $0.25 \leq x_F < 0.30$	52
76 39	Differential cross-section for x_F bin $0.30 \leq x_F < 0.35$	53
77 40	Differential cross-section for x_F bin $0.35 \leq x_F < 0.40$	54
78 41	Differential cross-section for x_F bin $0.40 \leq x_F < 0.45$	55
79 42	Differential cross-section for x_F bin $0.45 \leq x_F < 0.50$	56
80 43	Differential cross-section for x_F bin $0.50 \leq x_F < 0.55$	57
81 44	Differential cross-section for x_F bin $0.55 \leq x_F < 0.60$	58
82 45	Differential cross-section for x_F bin $0.60 \leq x_F < 0.65$	59
83 46	Differential cross-section for x_F bin $0.65 \leq x_F < 0.70$	60
84 47	Differential cross-section for x_F bin $0.70 \leq x_F < 0.75$	61
85 48	Differential cross-section for x_F bin $0.75 \leq x_F < 0.80$	62
86 49	Summary of double differential cross-section measurements	63

87 List of Tables

88	1	Average Efficiency and Errors for Bins in x_F and Mass	41
89	2	Detailed Systematic Error calculation for Bins in x_F and Mass	66
90	3	Detailed cross-section calculation for Bins in x_F and Mass	70

91 1 Introduction

92 The Drell-Yan process, where a quark from one hadron annihilates with an antiquark from
93 another to produce a lepton-antilepton pair ($q\bar{q} \rightarrow \ell^+\ell^-$), provides a clean and direct probe
94 of the antiquark structure of nucleons. Over the past several decades, Drell-Yan experiments
95 have been instrumental in mapping the parton distribution functions (PDFs) of the proton and
96 other hadrons. However, most existing data are concentrated at small to moderate values of
97 the parton momentum fraction, $x < 0.3$. The region of large x ($x > 0.3$) remains relatively
98 unexplored, yet it is crucial for understanding phenomena such as the flavor asymmetry of the
99 proton's light antiquark sea ($\bar{d}(x)/\bar{u}(x)$) and the fundamental mechanisms of non-perturbative
100 QCD that govern hadron structure.

101 The SeaQuest experiment (E906) at Fermilab was designed specifically to explore this high- x
102 frontier. By impinging a high-intensity 120 GeV proton beam from the Main Injector onto various
103 fixed targets, including liquid hydrogen (LH_2) and liquid deuterium (LD_2), SeaQuest measures
104 dimuon production in a kinematic region sensitive to antiquarks carrying a large fraction of the
105 nucleon's momentum.

106 This analysis presents a measurement of the absolute double-differential Drell-Yan cross-
107 section, binned in the dimuon invariant mass (M) and Feynman- x (x_F), using data collected
108 with the LH_2 and LD_2 targets. The p+p collisions are primarily sensitive to the \bar{u} distribution
109 in the proton, while the p+d collisions provide information on the sum of \bar{u} and \bar{d} . These results
110 provide stringent new constraints on modern PDF parameterizations in the valence-dominated
111 region.

112 The cross-section is presented in its scaling form, which, in the leading-order Drell-Yan
113 model, is independent of the center-of-mass energy, \sqrt{s} :

$$114 M^3 \frac{d^2\sigma}{dMdx_F} = f(\tau) \quad (1)$$

115 where $\tau = M^2/s$. The experimental determination of this quantity requires a precise under-
116 standing of the integrated luminosity, detector acceptance, and reconstruction efficiencies, which
117 are detailed in the subsequent sections of this document.

117 2 Analysis Methodology

118 The extraction of the Drell-Yan cross-section from the raw data involves several distinct steps:
119 selecting candidate dimuon events, subtracting backgrounds, calculating the integrated luminos-
120 ity, and correcting for detector- and reconstruction-related inefficiencies.

121 2.1 Data and Monte Carlo Samples

122 This analysis utilizes the "Roadset 67" dataset collected by the SeaQuest experiment. The
123 primary data files for the liquid hydrogen (LH_2) target and the corresponding empty "flask"
124 target runs are saved in:

125 `/seaquest/users/apun/e906_projects/rs67_merged_files/`

- 126 • **Data (LH_2 Target):** `merged_RS67_3089LH2.root`
- 127 • **Background (Empty Flask):** `merged_RS67_3089Flask.root`

128 The empty flask data are crucial for subtracting contributions from beam interactions with the
129 target vessel walls and other upstream material.

130 To correct for detector acceptance and reconstruction efficiencies, extensive Monte Carlo
131 (MC) simulations were employed. The simulations model the Drell-Yan process and propagate

132 the resulting muons through a Geant4-based model of the SeaQuest spectrometer. The primary
133 MC files used are:

- 134 • **Acceptance Study:** Drell-Yan events were generated over a 4π solid angle ("thrown")
135 and also processed through the full detector simulation and reconstruction chain ("ac-
136 cepted"). This study uses the *_M027_S001_* series of files saved in:

137 `/seaquest/users/chleung/pT_ReWeight/`

138

139 – `mc_drellyan_LH2_M027_S001_4pi_pTxFweight_v2.root`
140 – `mc_drellyan_LH2_M027_S001_clean_occ_pTxFweight_v2.root`
141 – `mc_drellyan_LH2_M027_S001_messy_occ_pTxFweight_v2.root`
142 – `mc_drellyan_LD2_M027_S001_4pi_pTxFweight_v2.root`
143 – `mc_drellyan_LD2_M027_S001_clean_occ_pTxFweight_v2.root`
144 – `mc_drellyan_LD2_M027_S001_messy_occ_pTxFweight_v2.root`

- 145 • **Efficiency Study:** To model the effect of high detector occupancy on track reconstruction,
146 simulated events were processed with ("messy") and without ("clean") the overlay of
147 random background hits from experimental data. This study uses the *_M027_S002_*
148 series of files also saved in the same location:

149 – `mc_drellyan_LH2_M027_S002_clean_occ_pTxFweight_v2.root`
150 – `mc_drellyan_LH2_M027_S002_messy_occ_pTxFweight_v2.root`

151 All MC samples are weighted on an event-by-event basis to match the transverse momentum
152 (p_T) distribution observed in the data.

153 2.2 Event Selection

154 A multi-tiered set of selection criteria is applied to isolate high-quality Drell-Yan dimuon events
155 from the large background of other processes.

- 156 • **Data Quality:** Only data from "good spills," as identified by standard run quality moni-
157 toring, are included in the analysis. A physics trigger condition (`MATRIX1 == 1`) is required,
158 selecting events consistent with the passage of two muons through the spectrometer.
- 159 • **Track and Dimuon Quality:** A set of stringent cuts, developed by the collaboration and
160 referred to as "Chuck cuts," are applied to ensure well-reconstructed positive and negative
161 muon tracks that form a high-quality common vertex. These cuts impose requirements on
162 track χ^2 , momentum, number of hits, and fiducial volume. The full details of these cuts
163 are provided in Appendix A.
- 164 • **Kinematic Selection:** The analysis focuses on the high-mass continuum, away from the
165 charmonium resonances ($J/\psi, \psi'$). A cut of $M_{\mu\mu} > 4.2$ GeV is applied. The analysis is
166 restricted to the kinematic range $0 < x_F < 0.8$.

167 2.3 Cross-Section Formalism

168 The double-differential cross-section in a given kinematic bin ($\Delta M, \Delta x_F$) is calculated as:

$$\frac{d^2\sigma}{dMdx_F} = \frac{N_{DY}}{\Delta M \Delta x_F \cdot \mathcal{L} \cdot \epsilon_{\text{total}}} \quad (2)$$

169 where:

- N_{DY} is the number of Drell-Yan events in the bin after subtraction of the combinatoric and empty flask backgrounds (see [2] DocDB 11322).

$$N_{DY} = N_{\text{LH2}} - N_{\text{LH2, mixed}} - \frac{I_{\text{LH2}}}{I_{\text{flask}}} (N_{\text{flask}} - N_{\text{flask, mixed}})$$

- 170 • \mathcal{L} is the integrated luminosity for the dataset.

- 171 • ϵ_{total} is the total correction factor, accounting for acceptance and inefficiencies.

172 The integrated luminosity, \mathcal{L} , is given by the product of the total number of protons incident
173 on the target and the number of target nuclei per unit area:

$$\mathcal{L} = N_{\text{incident}} \cdot \frac{N_A \rho L}{A} \cdot f_{\text{atten}} \quad (3)$$

174 Here, N_{incident} is the number of protons on target, N_A is Avogadro's number, ρ is the target
175 density, L is the target length, A is the molar mass, and f_{atten} is a correction factor for beam
176 attenuation within the thick target. For the $L = 50.8$ cm long LH₂ target, with a density of
177 $\rho_H = 0.0708$ g/cm³, the target thickness is 3.5966 g/cm² with a beam attenuation factor of
178 0.966.

179 The total correction factor, ϵ_{total} , is the product of three terms determined from MC simu-
180 lations:

$$\epsilon_{\text{total}} = \epsilon_{\text{acc}}(M, x_F) \cdot \epsilon_{\text{recon}}(M, x_F) \cdot \epsilon_{\text{trigger}} \quad (4)$$

181 where ϵ_{acc} is the geometric and kinematic acceptance of the spectrometer, ϵ_{recon} is the track
182 reconstruction efficiency (often called "kTracker efficiency"), and $\epsilon_{\text{trigger}}$ is the trigger efficiency.

183 The calculation of these three terms is detailed in the following sections.

184 3 Acceptance and Efficiency Corrections

185 3.1 Detector Acceptance Correction

186 The SeaQuest spectrometer has a finite geometric acceptance, which limits the fraction of pro-
187 duced dimuon events that can be detected. This acceptance depends strongly on the event
188 kinematics, primarily the dimuon invariant mass (M) and Feynman- x (x_F). The acceptance
189 correction factor is determined using MC simulations.

190 The acceptance, $A(M, x_F)$, is defined as the ratio of the number of simulated events that
191 are successfully reconstructed and pass all analysis cuts (N_{reco}) to the total number of events
192 generated in a given kinematic bin (N_{gen}):

$$\text{Acceptance (A)} = \frac{N_{\text{reco}}}{N_{\text{gen}}} \quad (5)$$

193 This calculation is performed in bins of M and x_F . The kinematic binning used for this study
194 is defined by the following edges:

- x_F Edges: $\{0, 0.05, 0.1, \dots, 0.8\}$ (16 bins)

- Mass Edges (GeV/c²): $\{4.2, 4.5, 4.8, 5.1, 5.4, 5.7, 6, 6.3, 6.6, 6.9, 7.5, 8.7\}$ (11 bins)

197 The following pages show the calculated acceptance as a function of mass for each of the
198 16 x_F bins. The plots show the acceptance for the LH₂ and LD₂ targets, their combined
199 average, and their ratio. The ratio is close to unity across the kinematic range, indicating that
200 target-dependent effects on the acceptance are small. In this case, we compare newly calculated
201 acceptance corrections to the existing acceptance calculations saved in Shivangi's file:

202 `./shivangi/work/analysis/R008/diffCross/v42/5770/looseCut/final/acceptance_h.root`

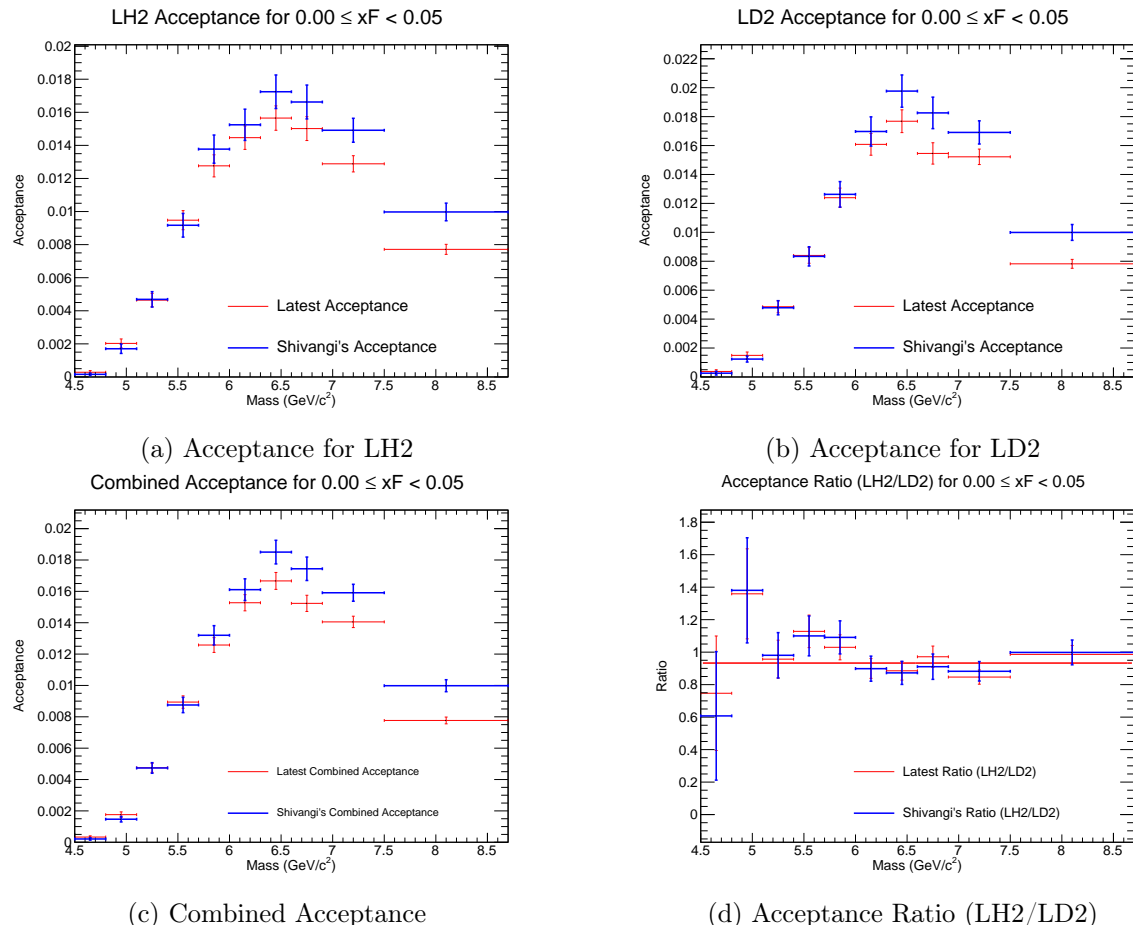


Figure 1: Acceptance plots for $0.00 \leq x_F < 0.05$.

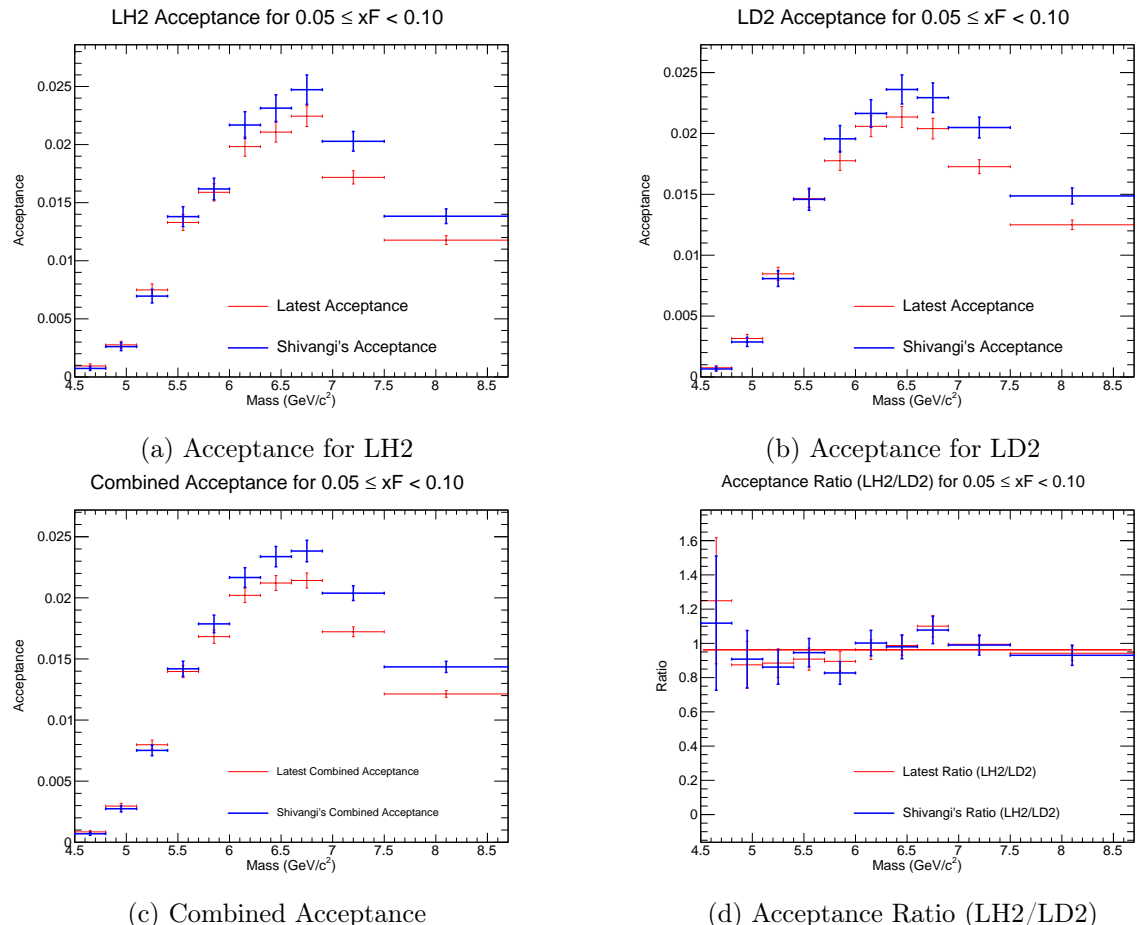


Figure 2: Acceptance plots for $0.05 \leq x_F < 0.10$.

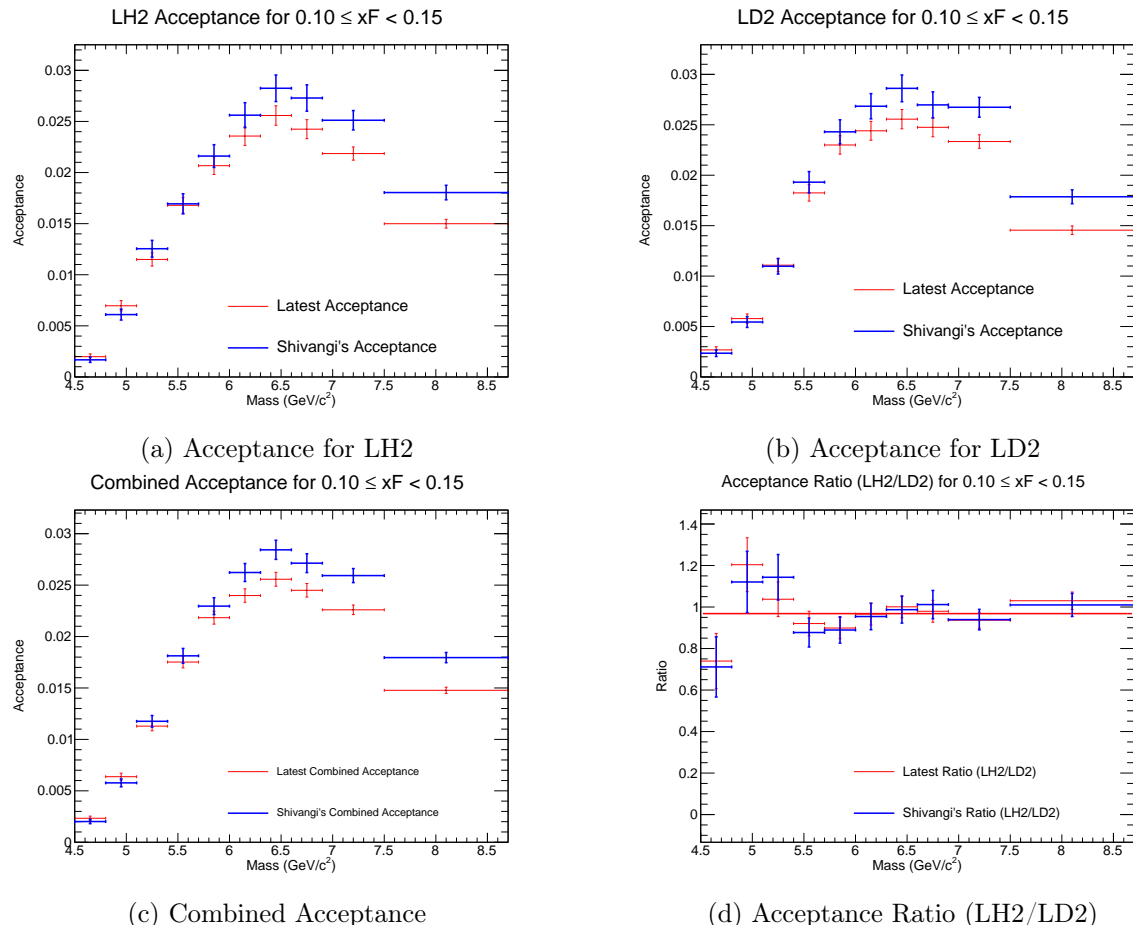


Figure 3: Acceptance plots for $0.10 \leq x_F < 0.15$.

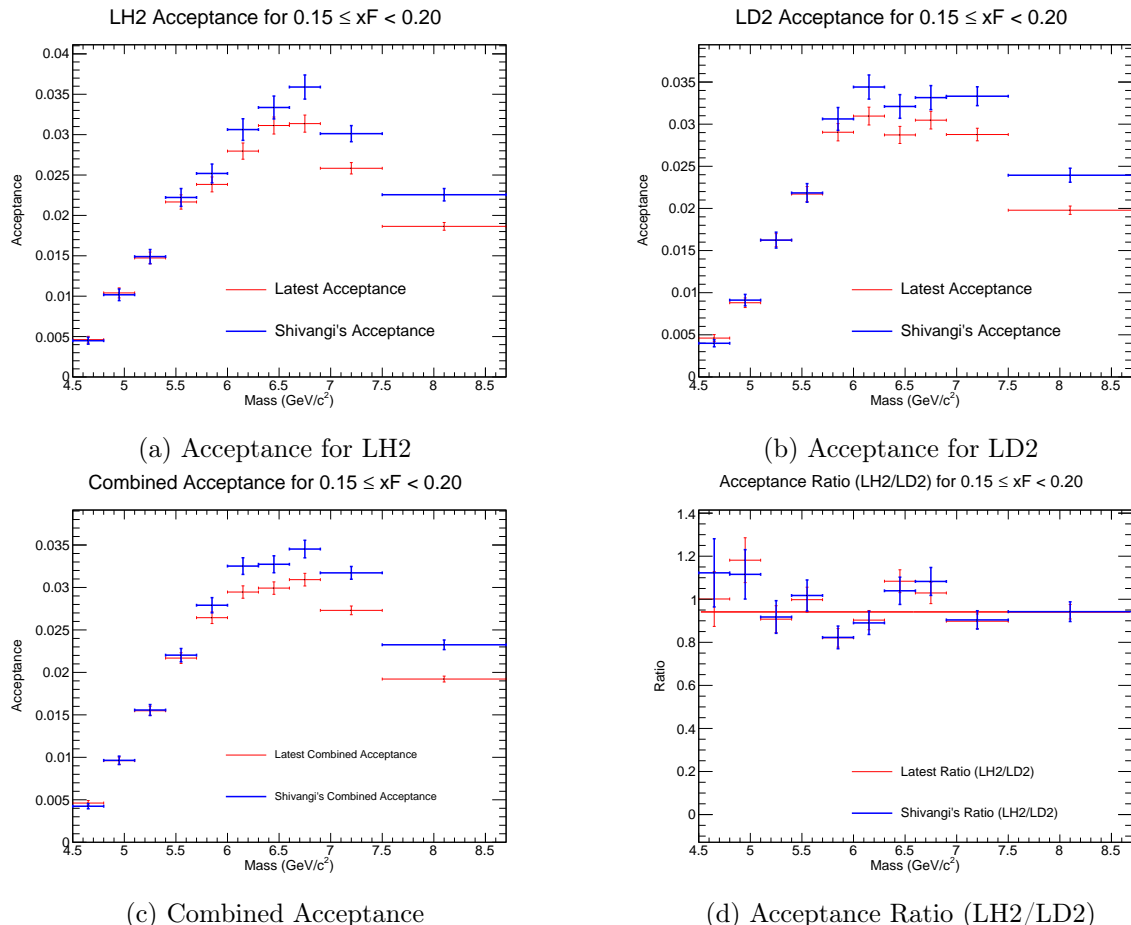


Figure 4: Acceptance plots for $0.15 \leq x_F < 0.20$.

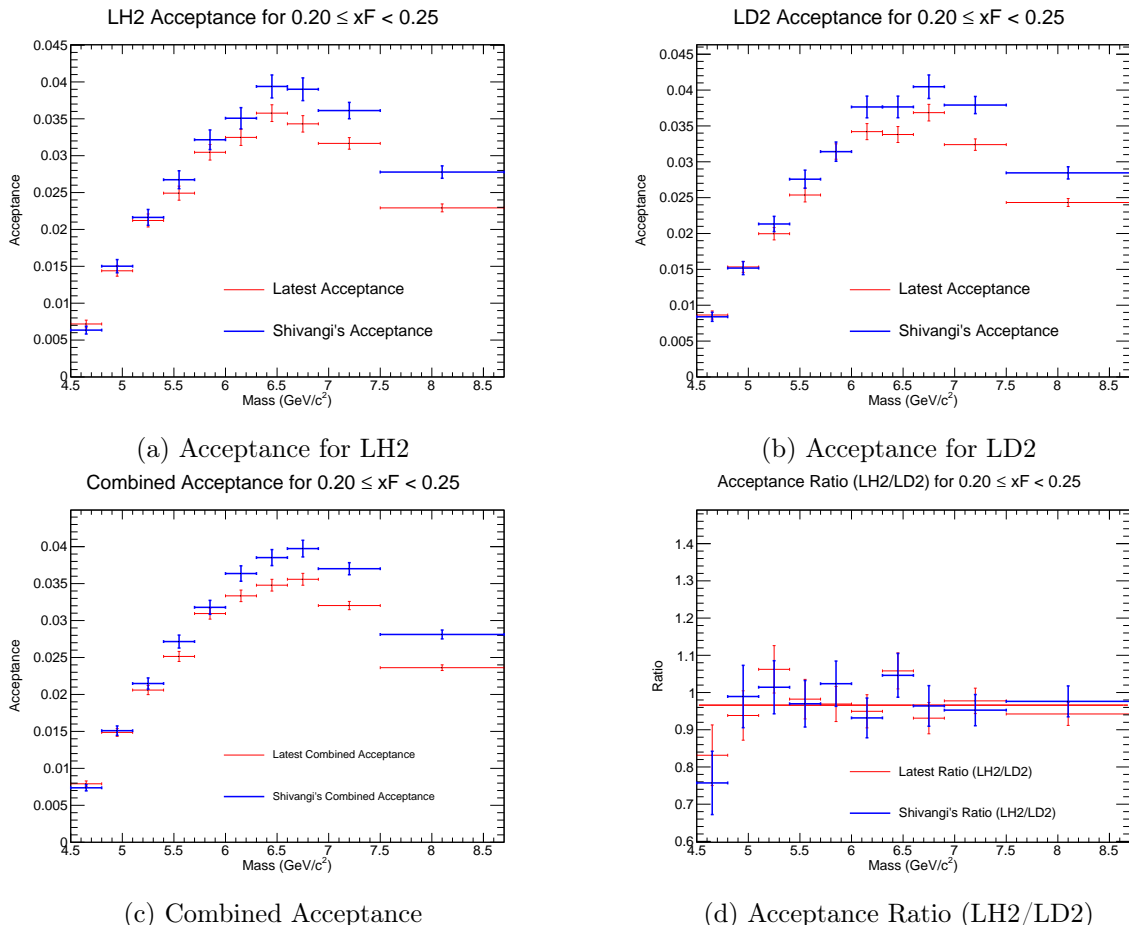


Figure 5: Acceptance plots for $0.20 \leq x_F < 0.25$.

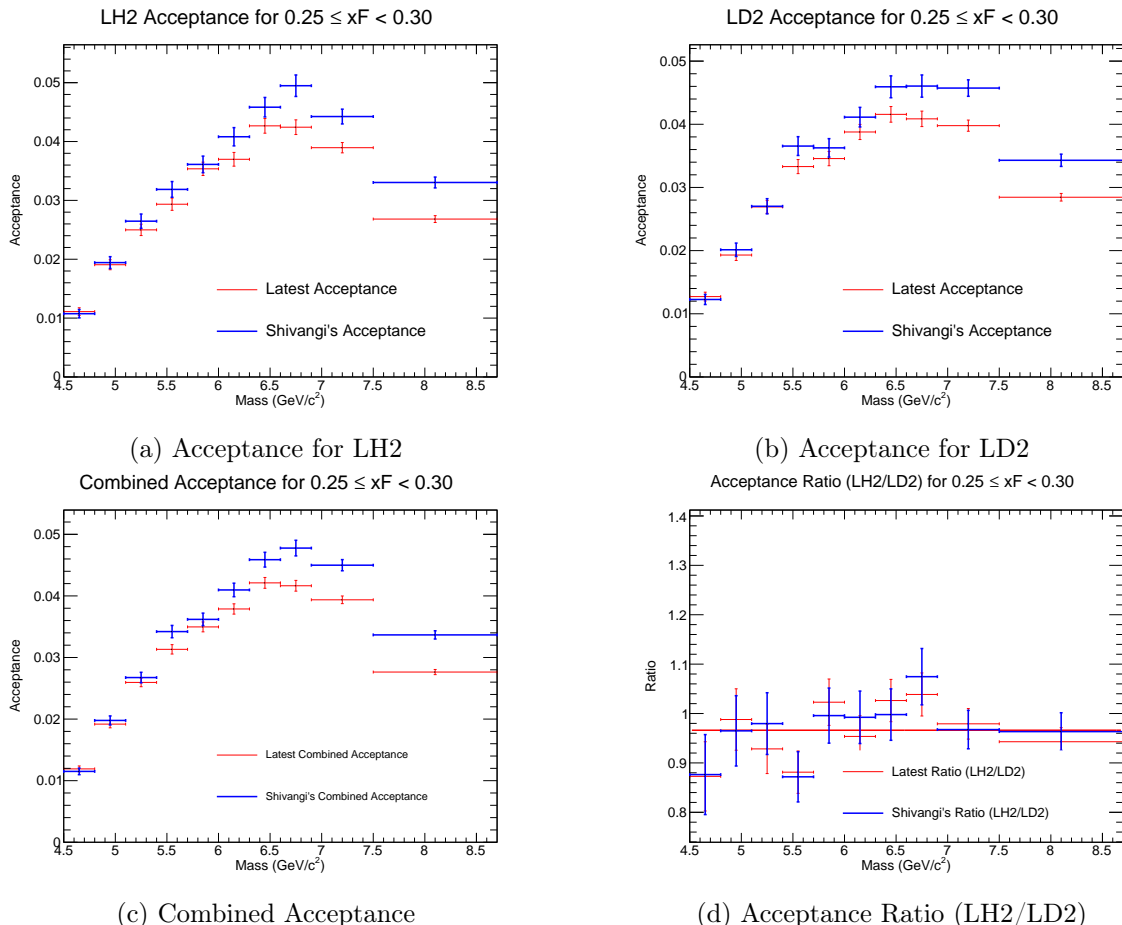


Figure 6: Acceptance plots for $0.25 \leq x_F < 0.30$.

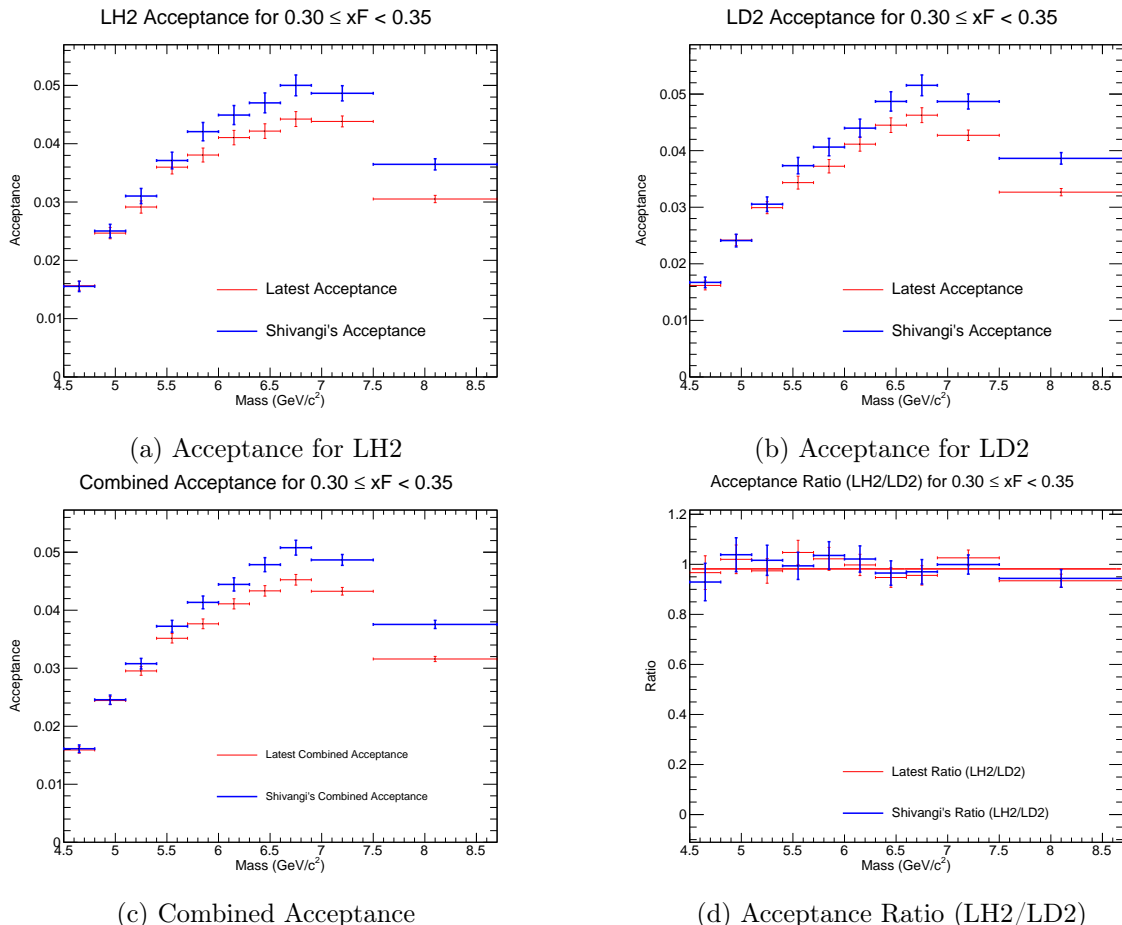


Figure 7: Acceptance plots for $0.30 \leq x_F < 0.35$.

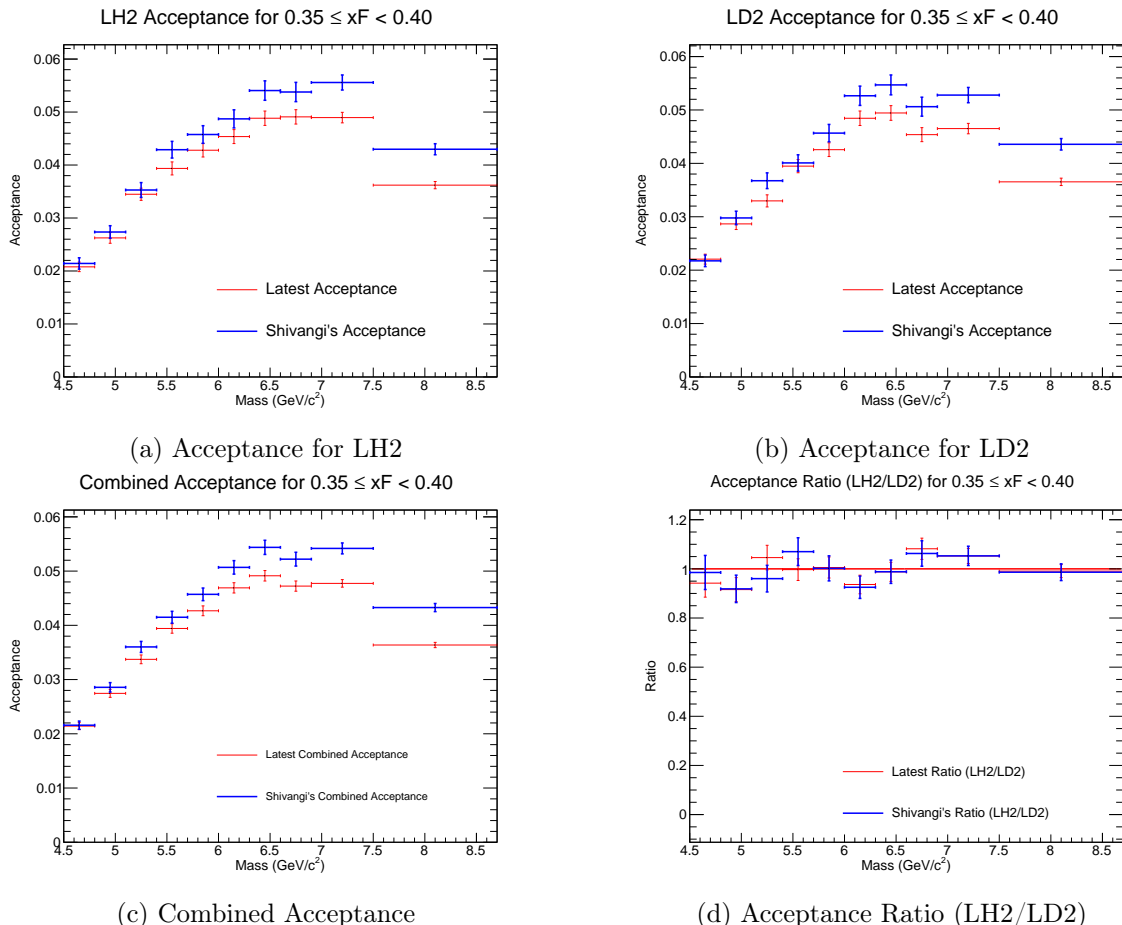


Figure 8: Acceptance plots for $0.35 \leq x_F < 0.40$.

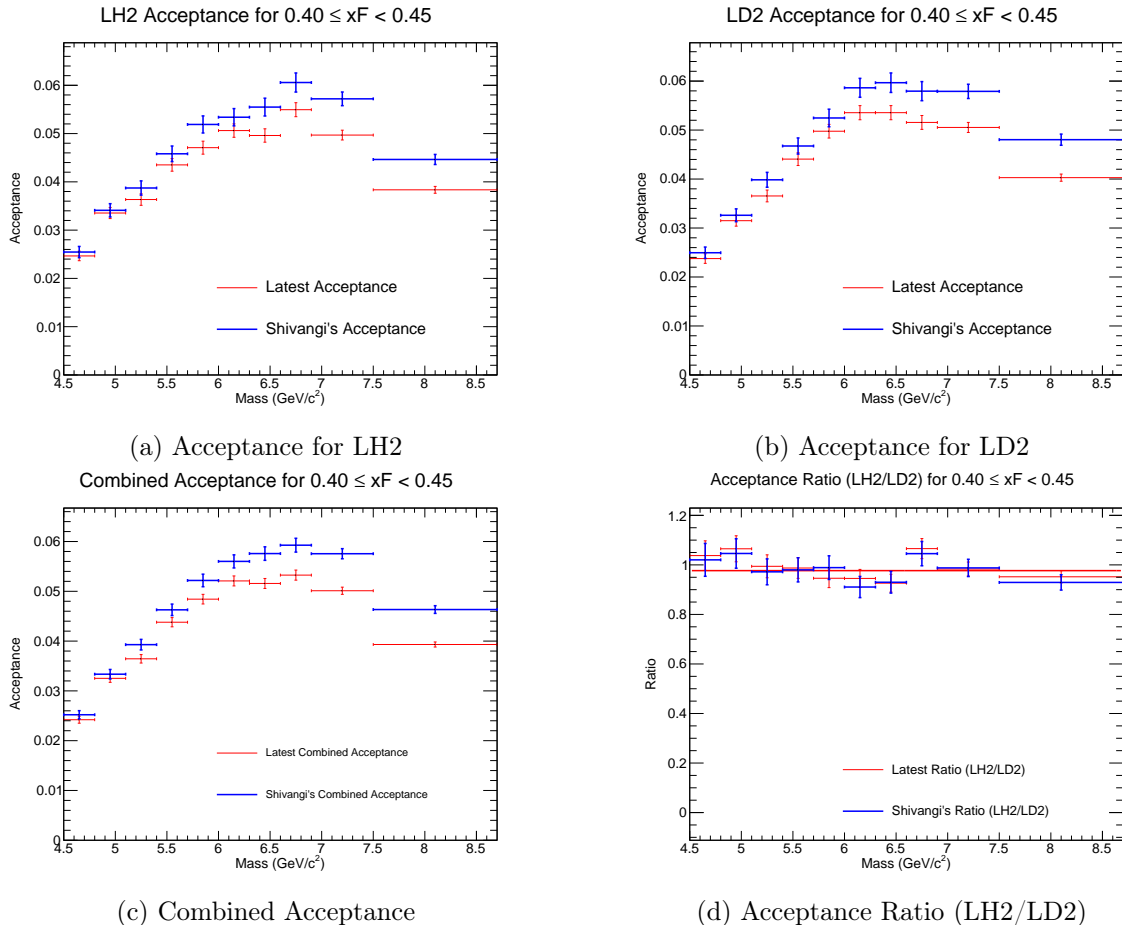


Figure 9: Acceptance plots for $0.40 \leq x_F < 0.45$.

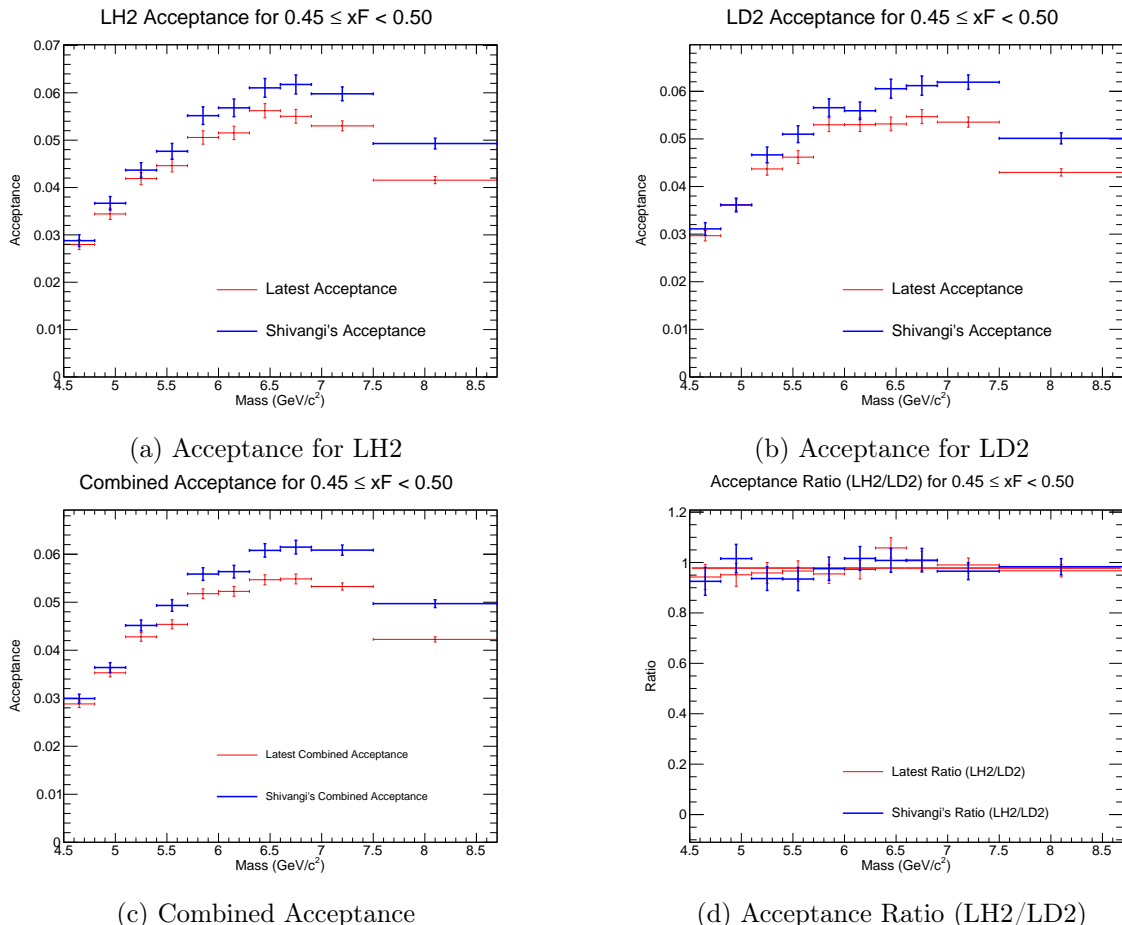


Figure 10: Acceptance plots for $0.45 \leq x_F < 0.50$.

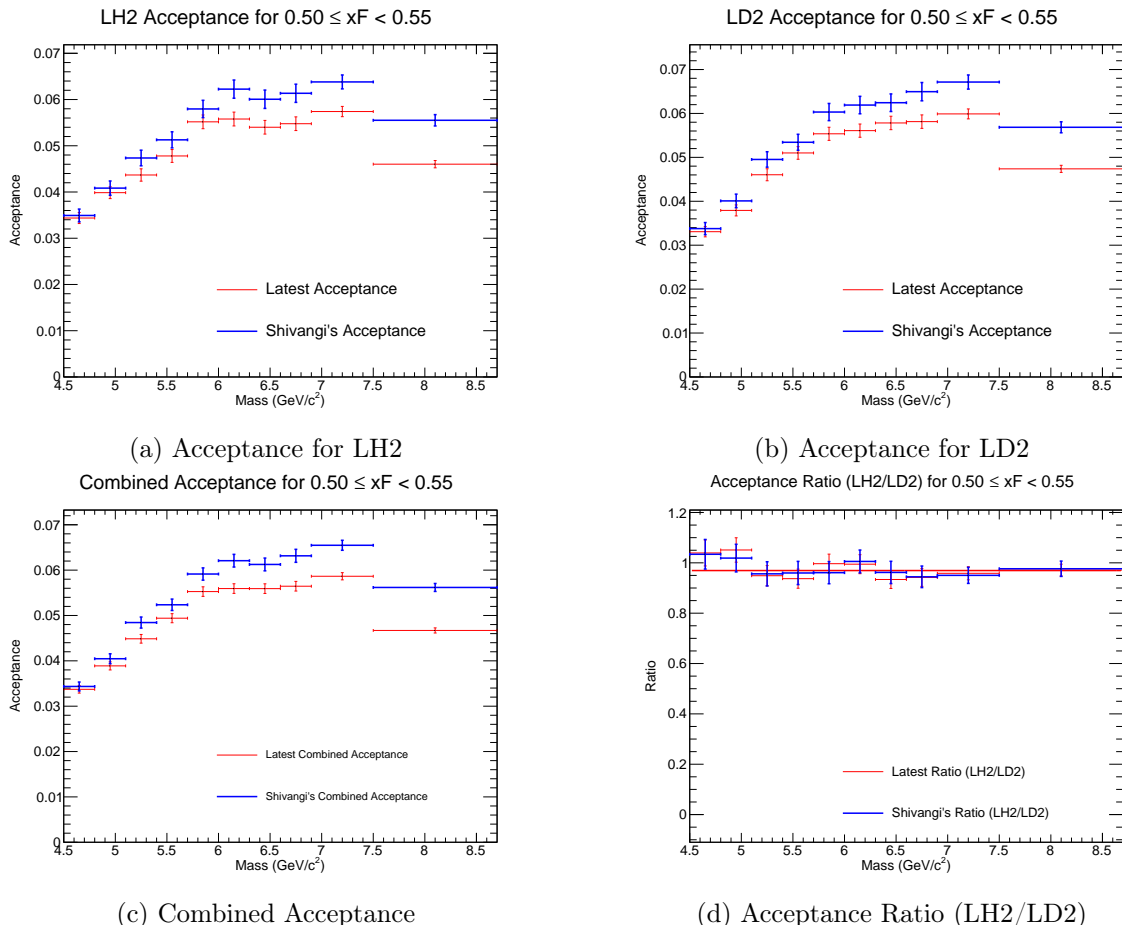


Figure 11: Acceptance plots for $0.50 \leq x_F < 0.55$.

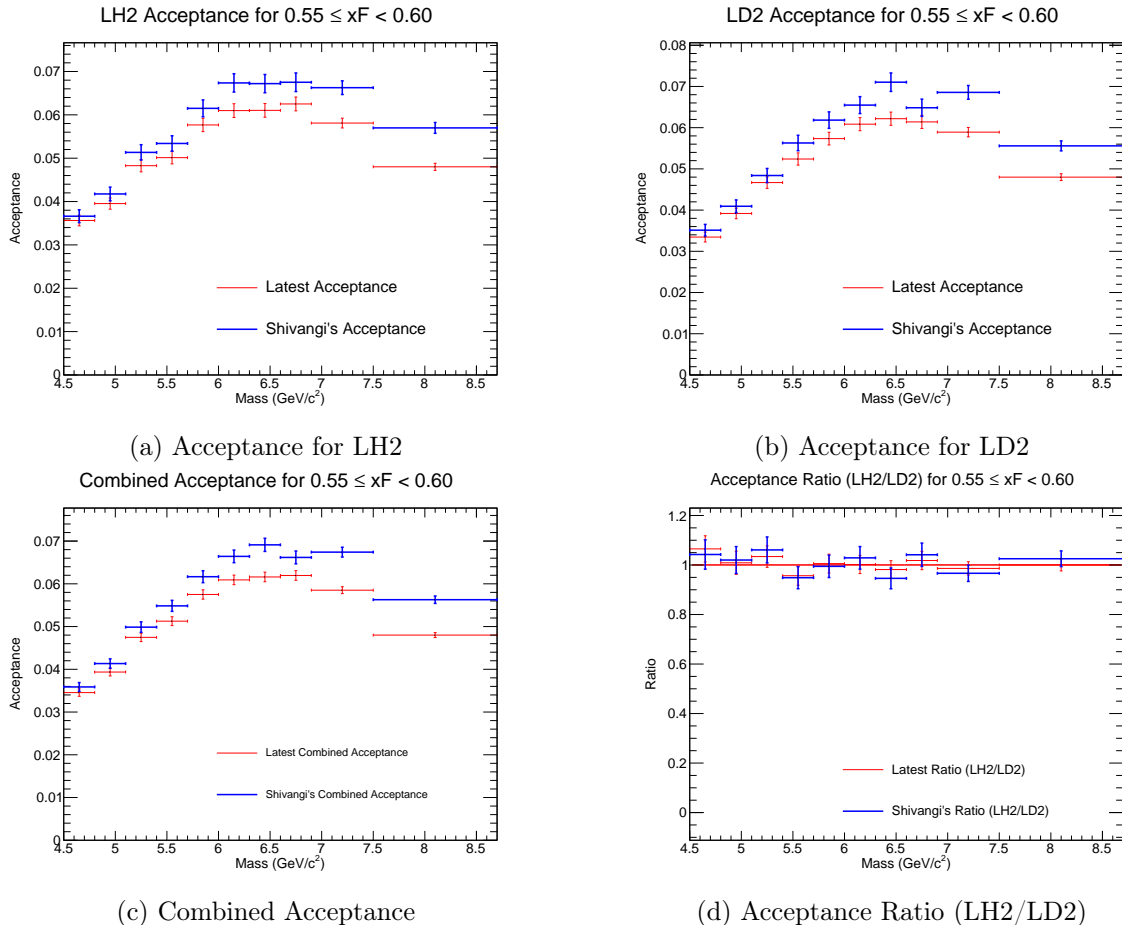


Figure 12: Acceptance plots for $0.55 \leq x_F < 0.60$.

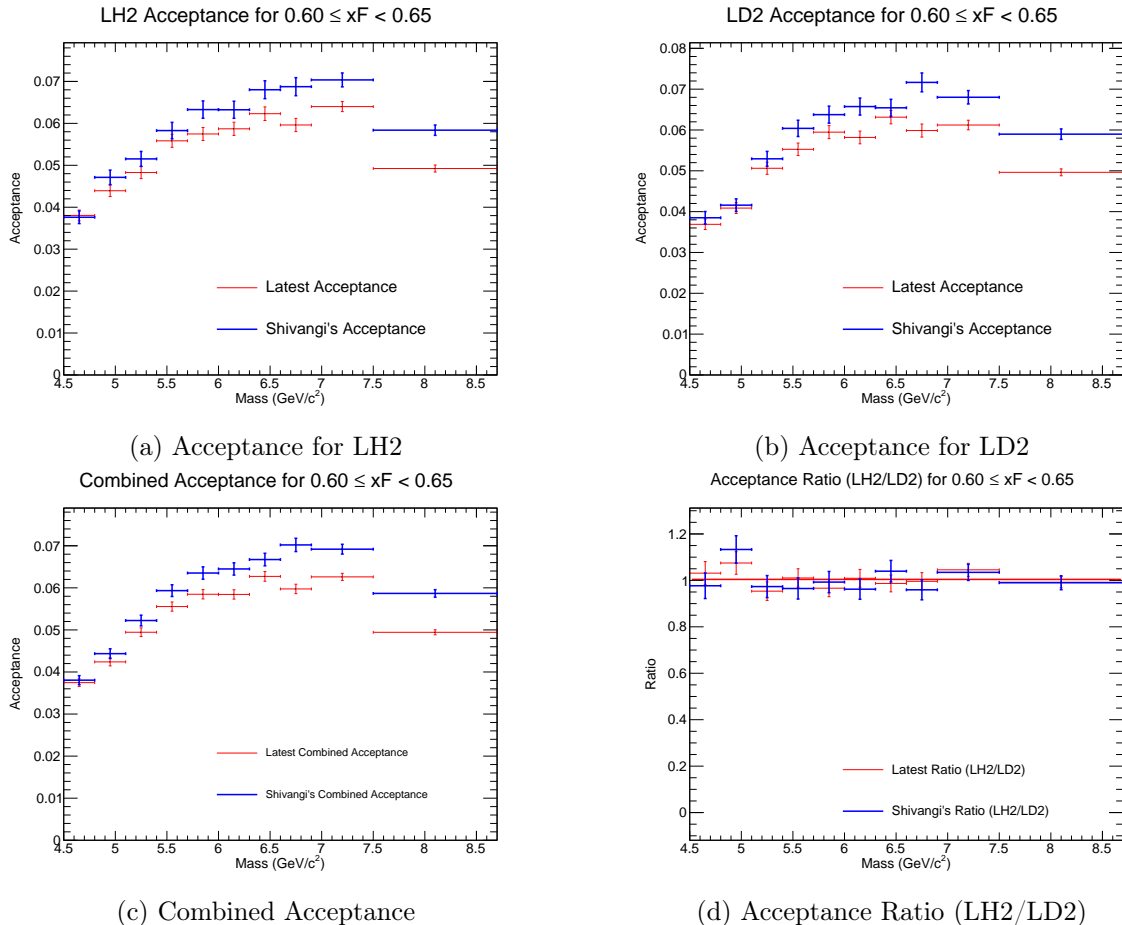


Figure 13: Acceptance plots for $0.60 \leq x_F < 0.65$.

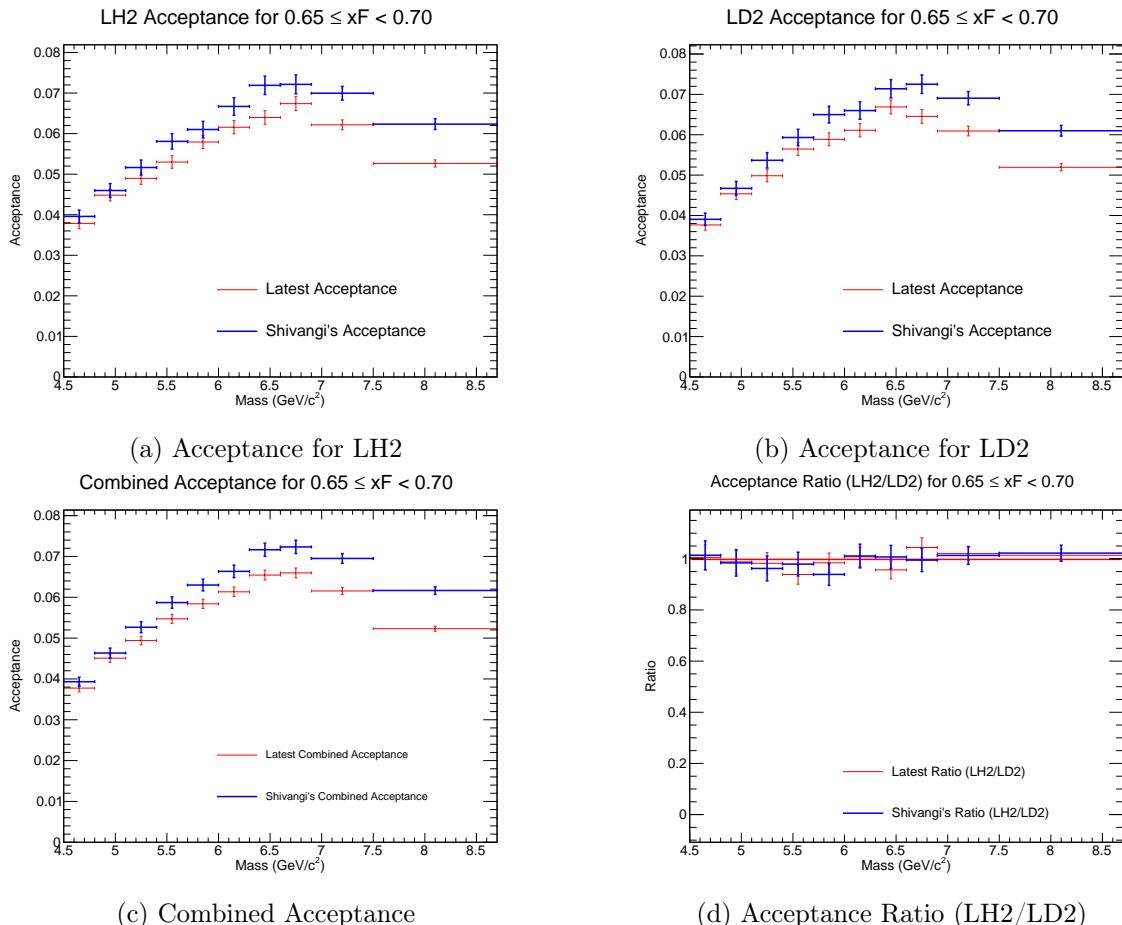


Figure 14: Acceptance plots for $0.65 \leq x_F < 0.70$.

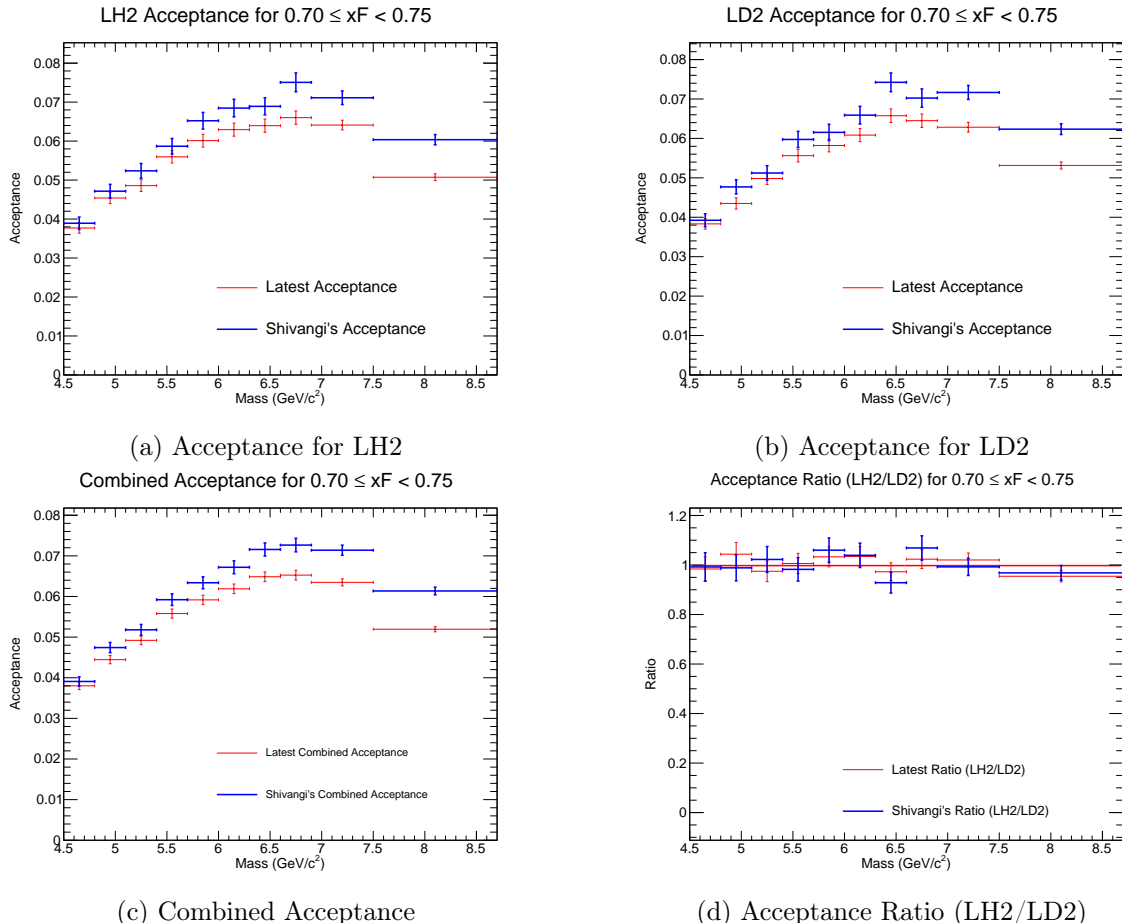


Figure 15: Acceptance plots for $0.70 \leq x_F < 0.75$.

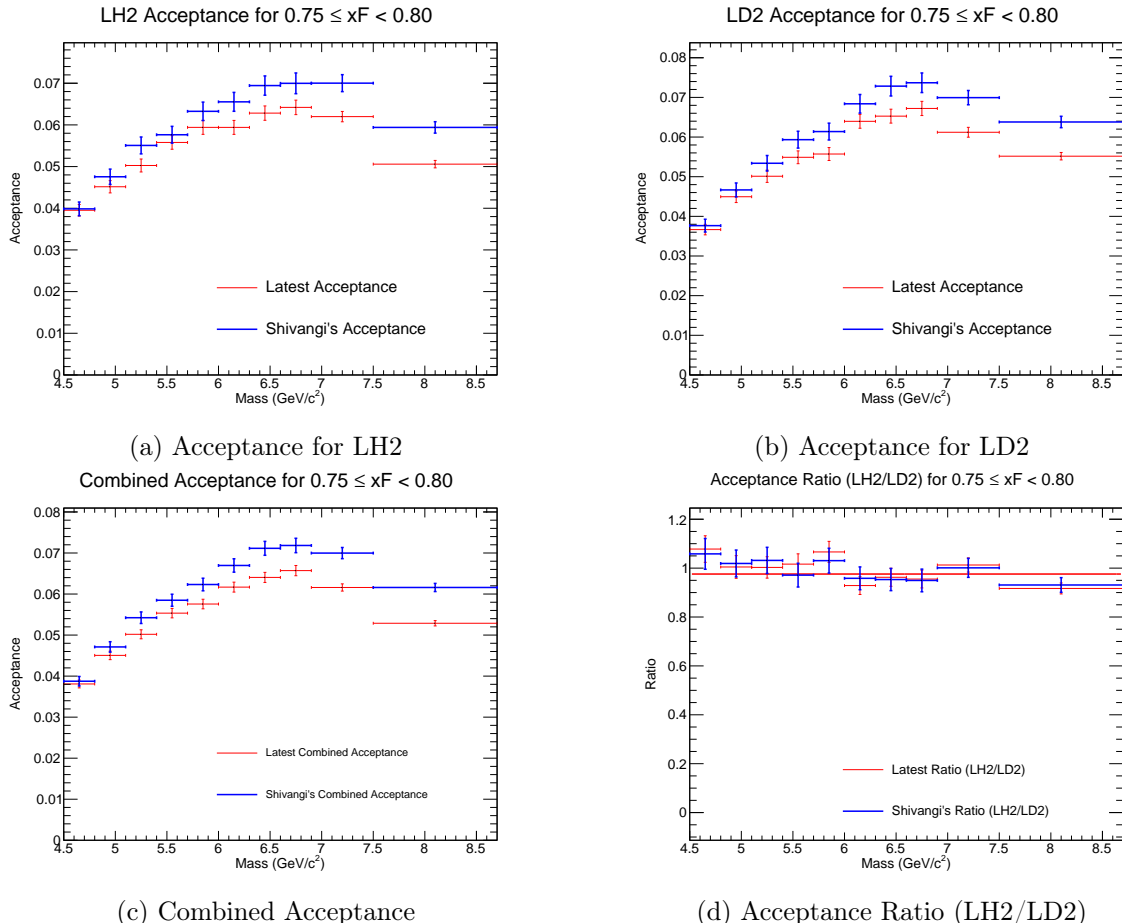


Figure 16: Acceptance plots for $0.75 \leq x_F < 0.80$.

203 **3.2 Reconstruction Efficiency Correction**

204 The track-finding algorithm ("kTracker") has an efficiency that depends on the detector oc-
 205 cupancy; the number of hits from unrelated particles in the detector during an event. This
 206 efficiency is studied using "clean" MC simulations (signal only) and "messy" MC simulations
 207 (signal with background hits overlaid). The reconstruction efficiency, ϵ_{recon} , is defined as the
 208 ratio of events found in the messy sample to those in the clean sample, as a function of an
 209 occupancy-related variable (e.g., D2, the number of hits in Drift Chamber Station 2).

$$\epsilon_{\text{recon}}(\text{D2}, M, x_F) = \frac{N_{\text{reco}}^{\text{messy}}(\text{D2}, M, x_F)}{N_{\text{reco}}^{\text{clean}}(M, x_F)} \quad (6)$$

210 For each kinematic bin of (M, x_F) , an efficiency curve as a function of D2 is generated from
 211 the MC. To obtain a single correction factor for each bin, an average efficiency, $\langle \epsilon \rangle$, is calculated
 212 by weighting this efficiency curve by the D2 distribution of the experimental data in that same
 213 bin.

214 **3.2.1 Uncertainty Propagation**

An important aspect of this procedure is the correct propagation of uncertainties. For each event in the data with a measured D2 value, an efficiency ϵ_i and its uncertainty $\delta\epsilon_i$ are determined by linear interpolation between points on the MC-derived efficiency curve. For a given event i the efficiency will be interpolated:

$$\begin{aligned} \epsilon_i &= \epsilon(D2^-) + \left(\frac{\epsilon(D2^+) - \epsilon(D2^-)}{D2^+ - D2^-} \right) (D2^+ - D2_i) \\ \delta\epsilon_i &= \frac{1}{D2^+ - D2^-} \sqrt{(D2^+ - D2_i)^2 \delta\epsilon(D2^+)^2 + (D2^- - D2_i)^2 \delta\epsilon(D2^-)^2} \end{aligned}$$

215 where $D2_i$ is the value of D2 for the event i , $D2^+$ is the nearest D2 value greater than $D2_i$,
 216 $D2^-$ is the nearest D2 value less than $D2_i$, $\epsilon(D2^\pm)$ is the value of the efficiency at $D2^\pm$, and
 217 $\delta\epsilon(D2^\pm)$ is the uncertainty in $\epsilon(D2^\pm)$

218 The average efficiency $\langle \epsilon \rangle$ for a bin containing N data events is the mean of the individual
 219 efficiencies:

$$\langle \epsilon \rangle = \frac{1}{N} \sum_{i=1}^N \epsilon_i \quad (7)$$

220 The uncertainty on this average, $\delta\langle \epsilon \rangle$, is based on the propagated error from the uncertainty
 221 on the MC-derived efficiency curve itself.

$$\delta_{\text{prop}}\langle \epsilon \rangle = \frac{1}{N} \sqrt{\sum_{i=1}^N (\delta\epsilon_i)^2} \quad (8)$$

222 The final correction applied to the data is $1/\langle \epsilon \rangle$, and its propagated error is given by:

$$\delta(1/\langle \epsilon \rangle) = \frac{\delta_{\text{prop}}\langle \epsilon \rangle}{\langle \epsilon \rangle^2} \quad (9)$$

223 **3.2.2 Efficiency Results**

224 The efficiency curves as a function of D2 were generated for all kinematic bins. The following
 225 pages display these curves, with each page corresponding to a single bin in x_F , showing the
 226 results for all 11 mass bins. **It is clear that some bins have insufficient statistics, and**
 227 **we should perform additional MC simulation in the near future to remedy this.** The
 228 efficiency sometimes exceeds 1.0 due to mistakenly reconstructing dimuon events due to "messy
 229 pick-up events" for some D2 bins.

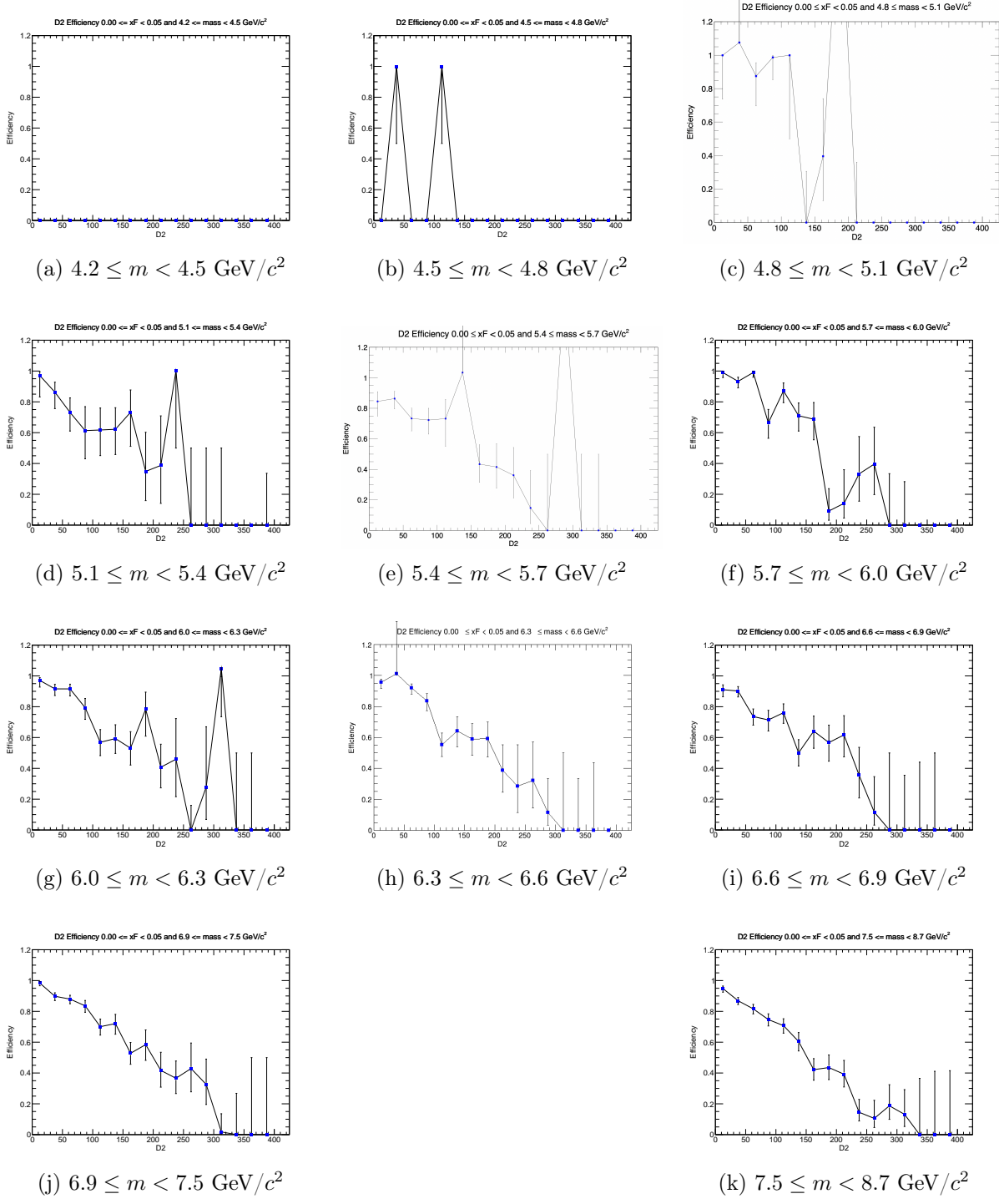


Figure 17: Efficiency plots for the x_F bin $0.00 \leq x_F < 0.05$.

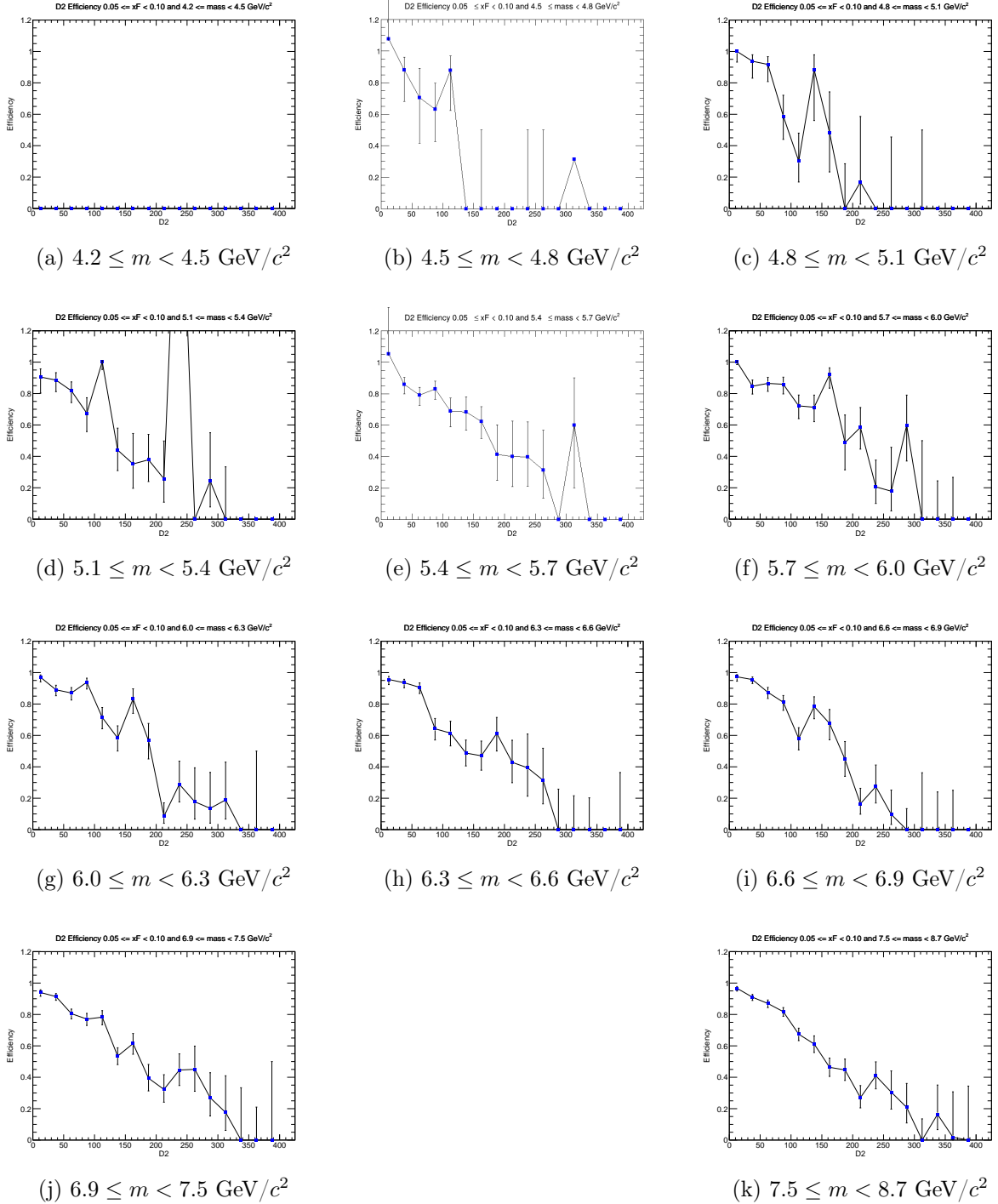


Figure 18: Efficiency plots for the x_F bin $0.05 \leq x_F < 0.10$.

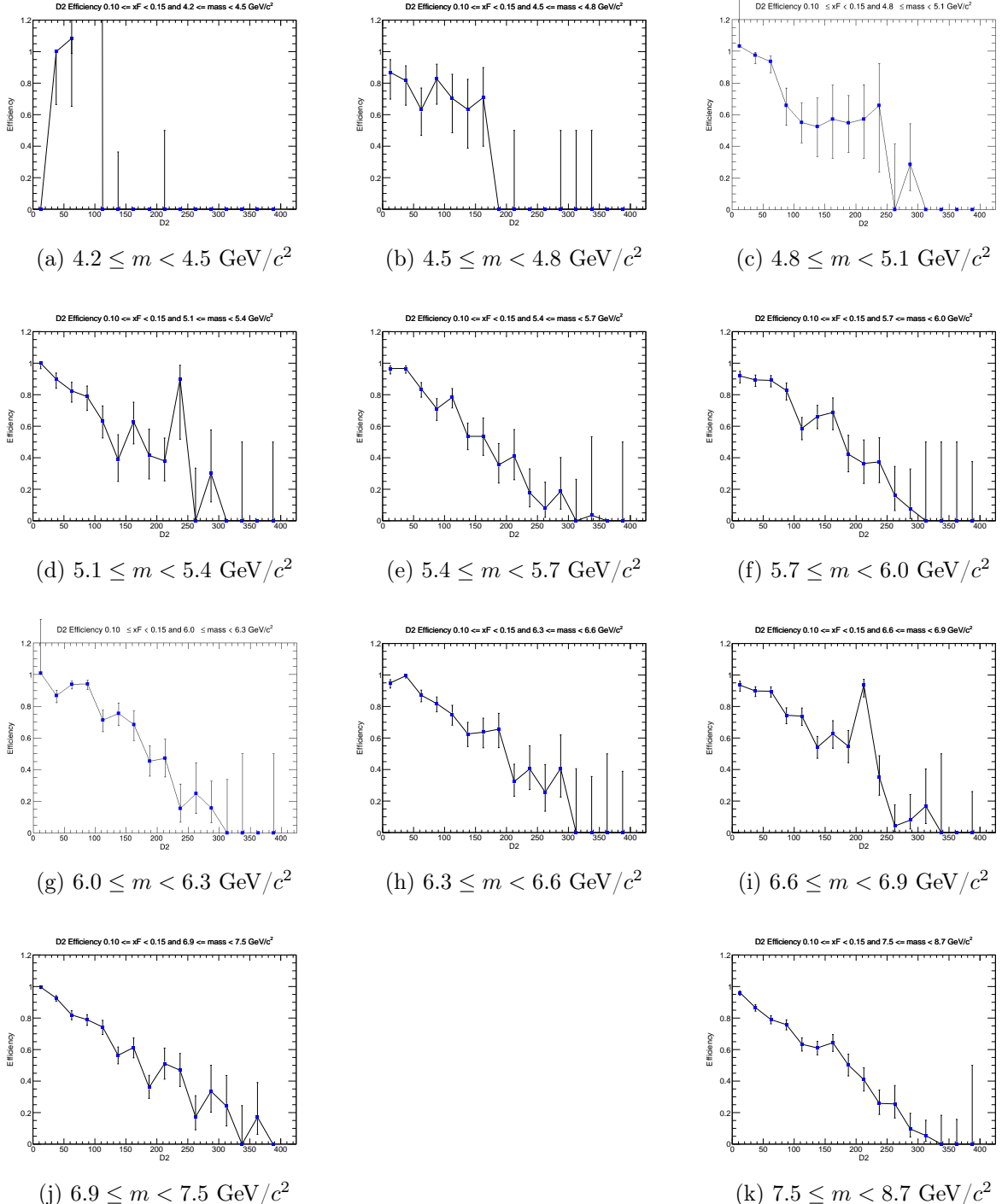


Figure 19: Efficiency plots for the x_F bin $0.10 \leq x_F < 0.15$.

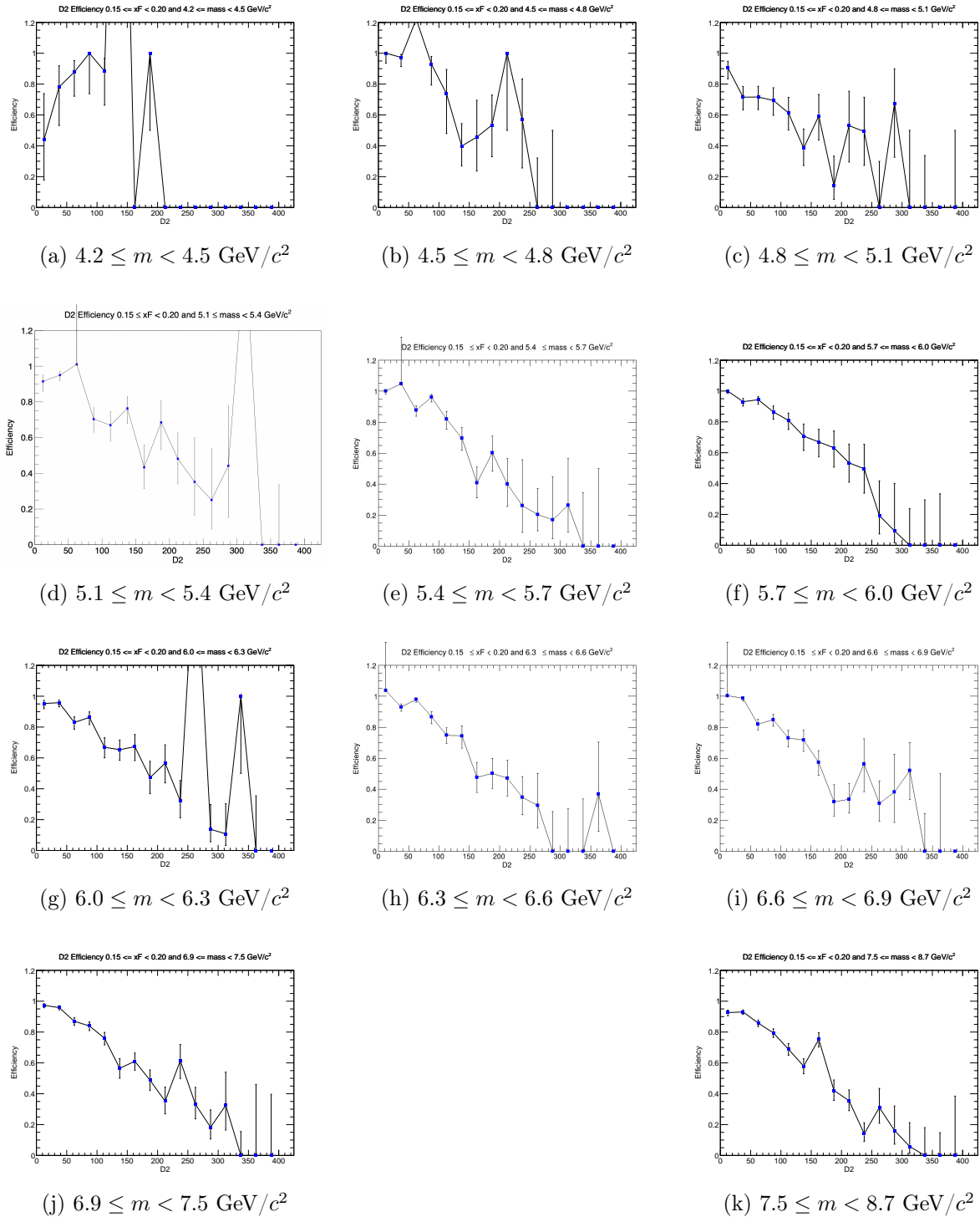


Figure 20: Efficiency plots for the x_F bin $0.15 \leq x_F < 0.20$.

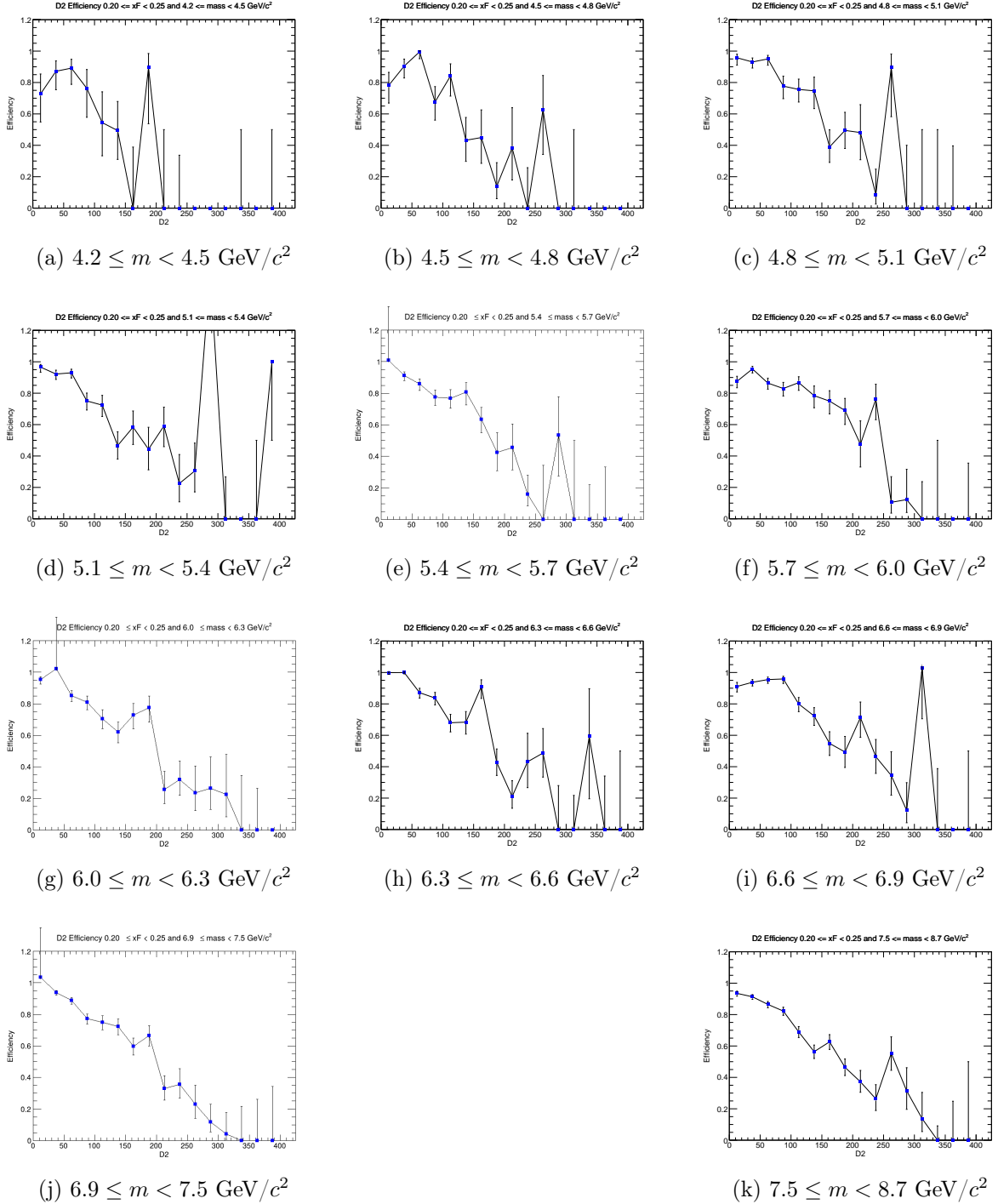


Figure 21: Efficiency plots for the x_F bin $0.20 \leq x_F < 0.25$.

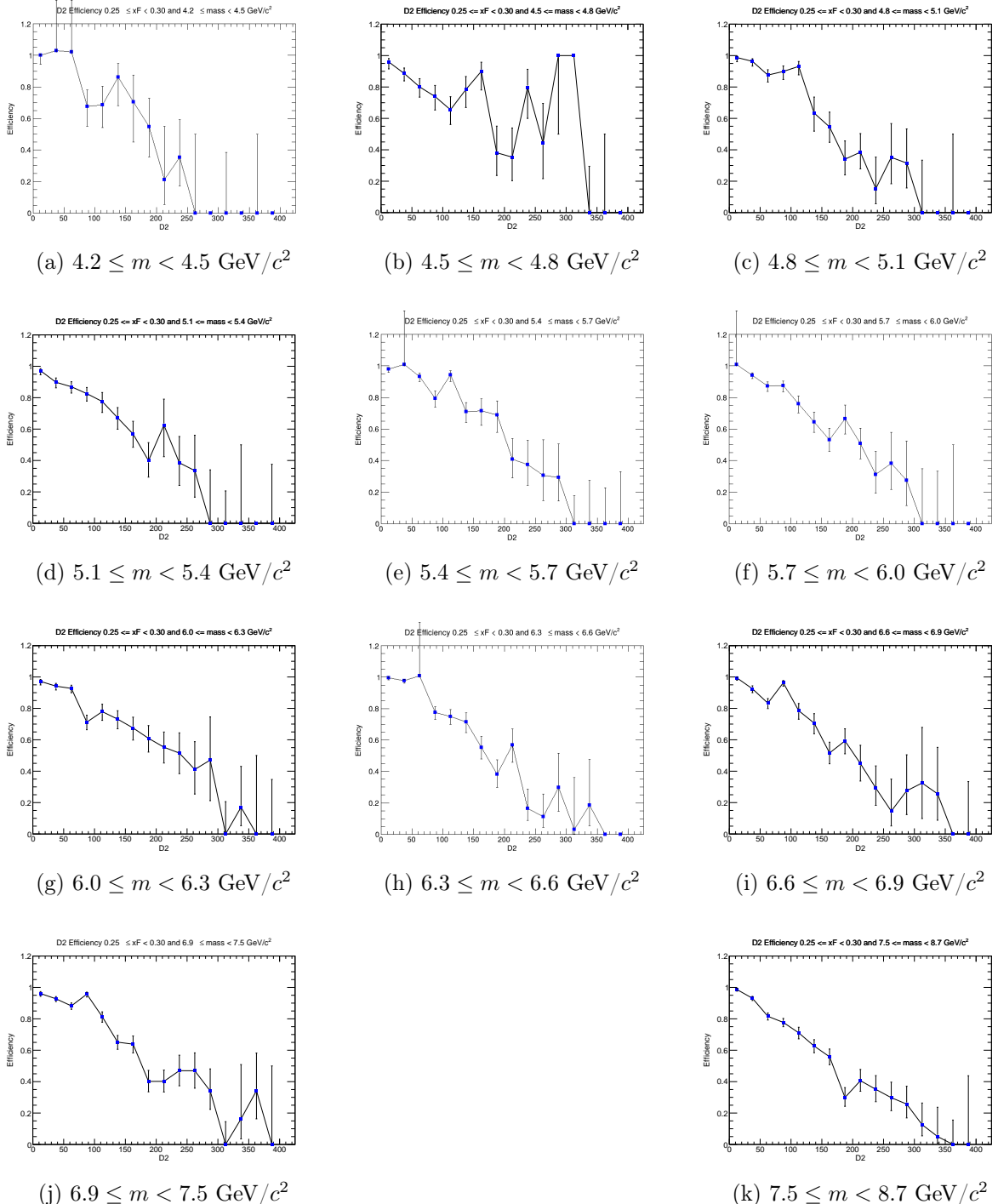


Figure 22: Efficiency plots for the x_F bin $0.25 \leq x_F < 0.30$.

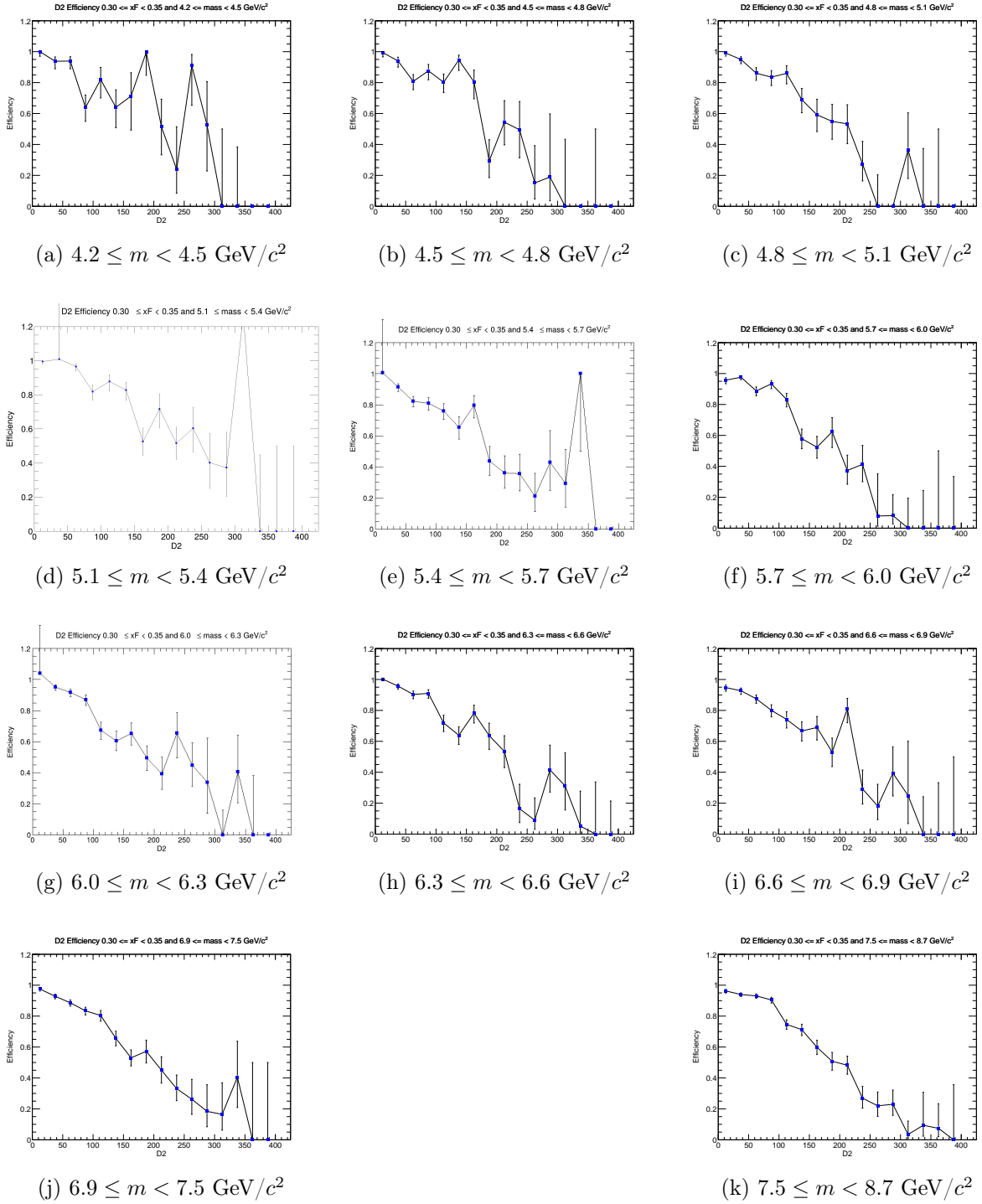


Figure 23: Efficiency plots for the x_F bin $0.30 \leq x_F < 0.35$.

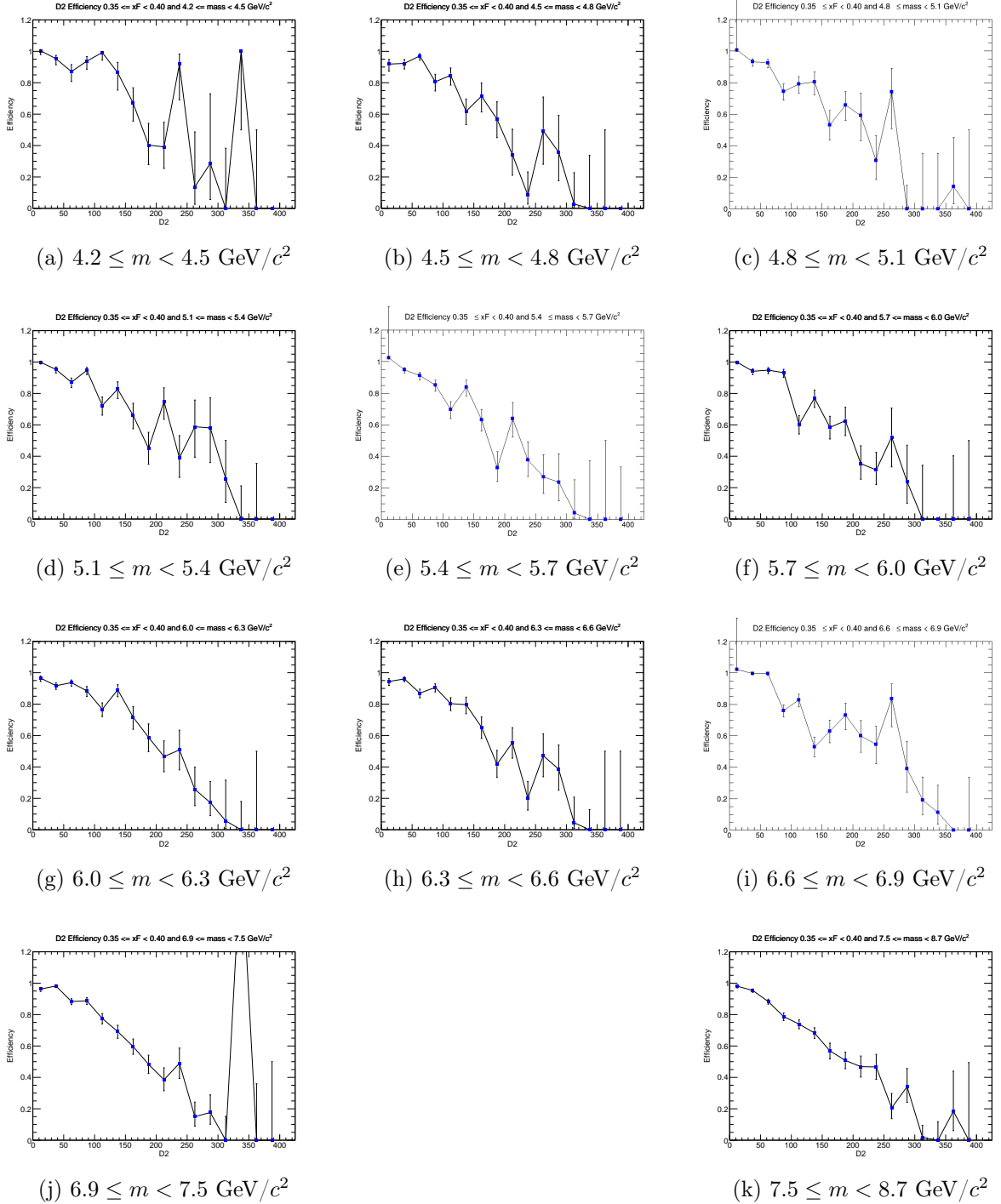


Figure 24: Efficiency plots for the x_F bin $0.35 \leq x_F < 0.40$.

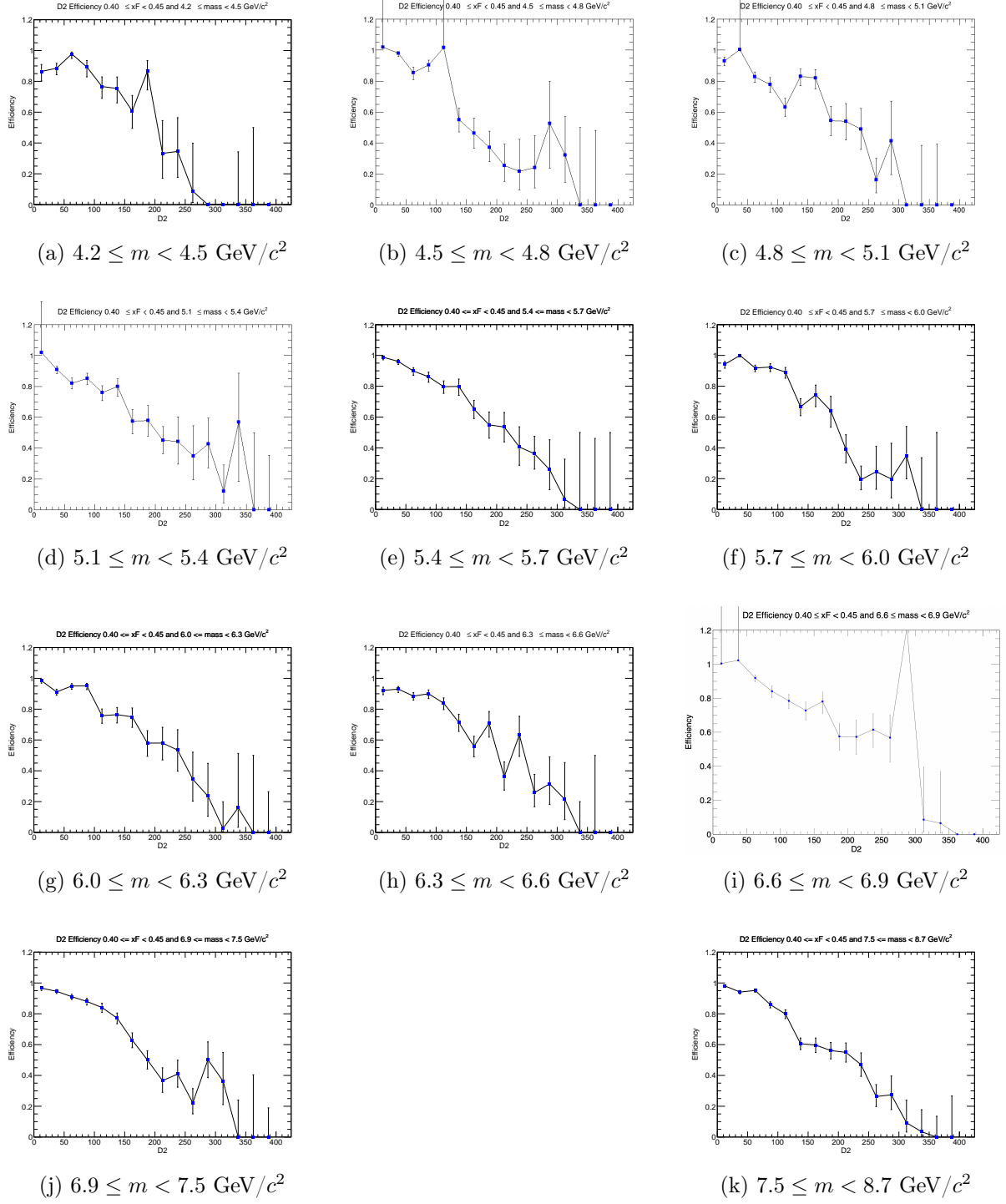


Figure 25: Efficiency plots for the x_F bin $0.40 \leq x_F < 0.45$.

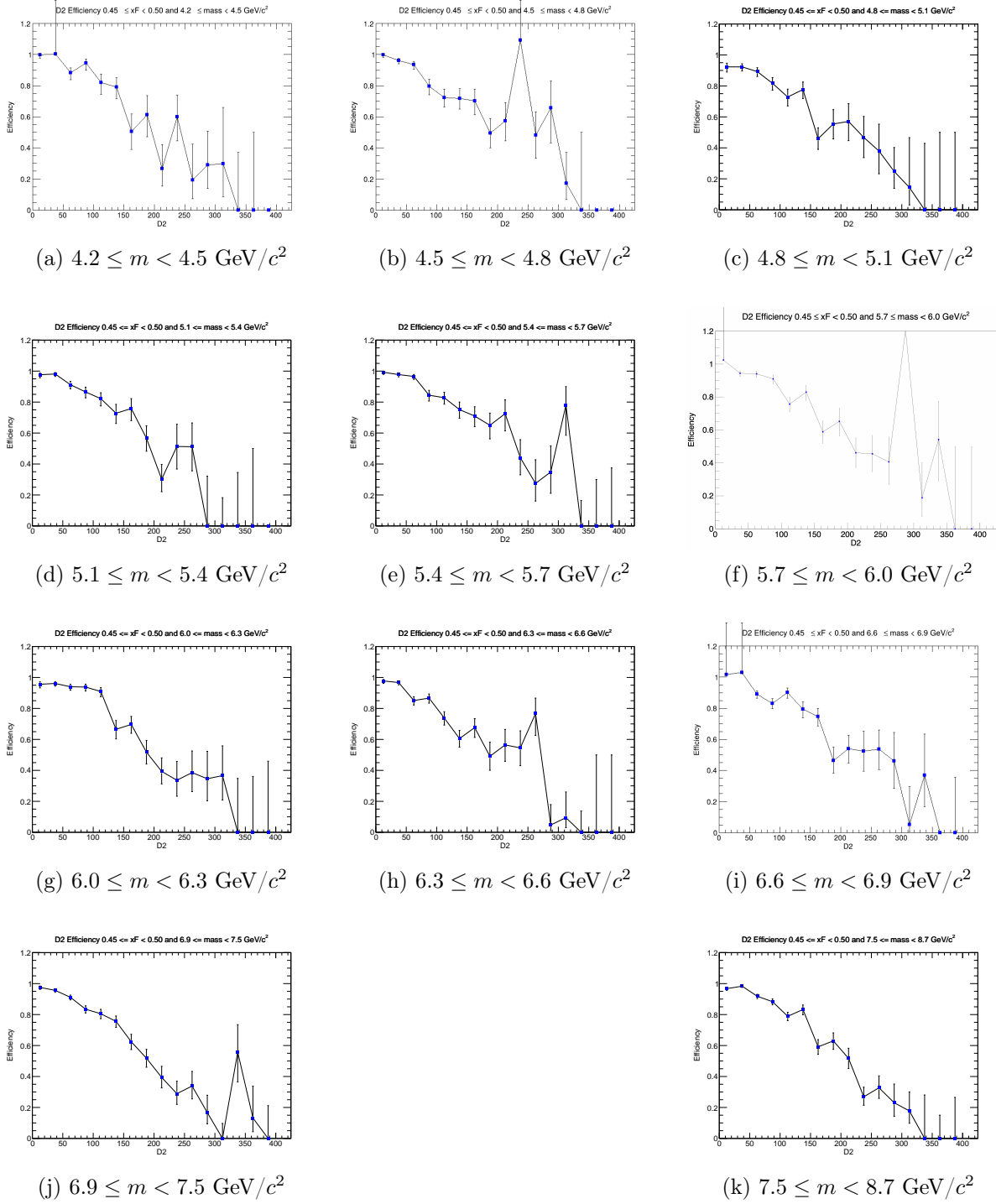


Figure 26: Efficiency plots for the x_F bin $0.45 \leq x_F < 0.50$.

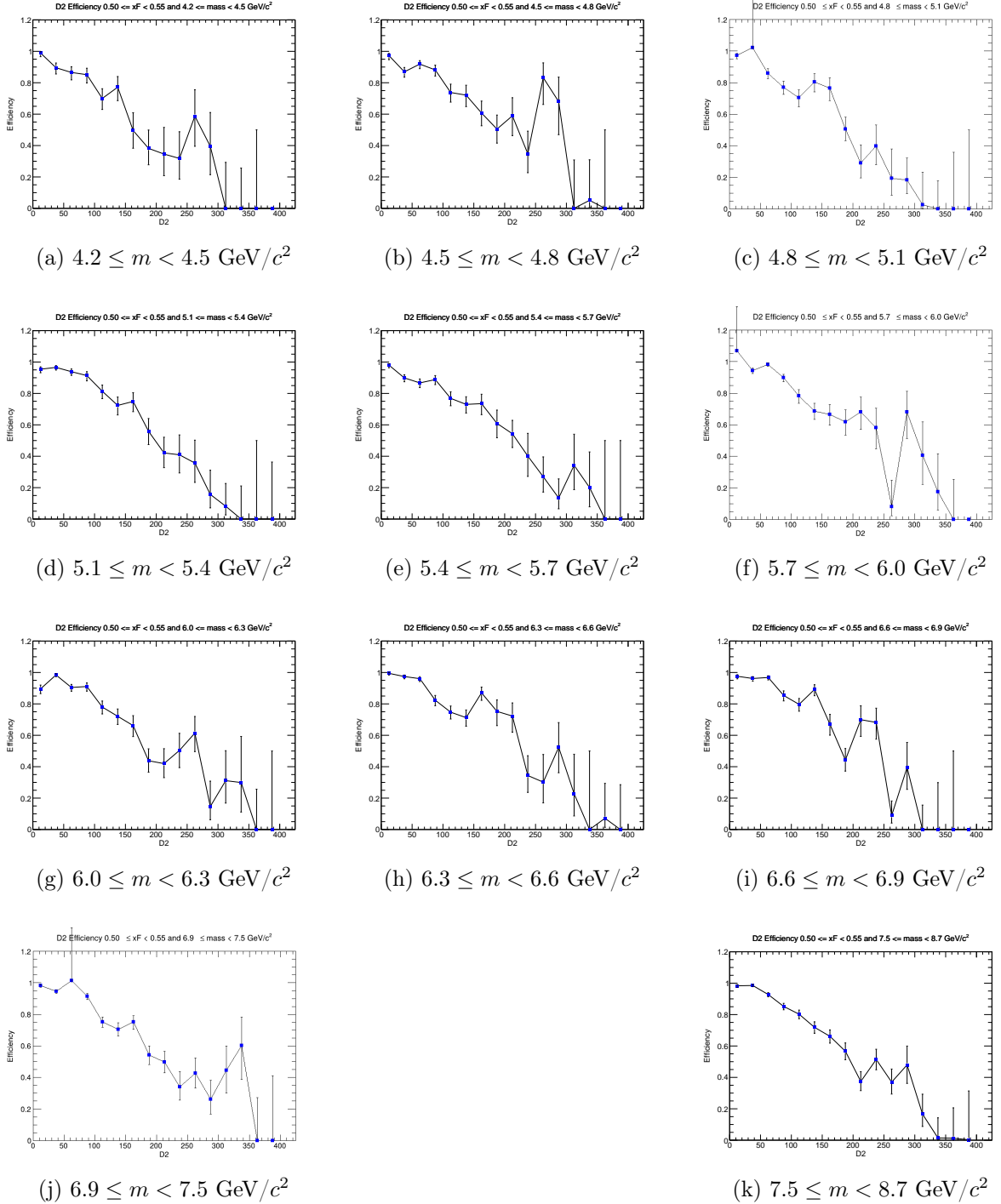


Figure 27: Efficiency plots for the x_F bin $0.50 \leq x_F < 0.55$.

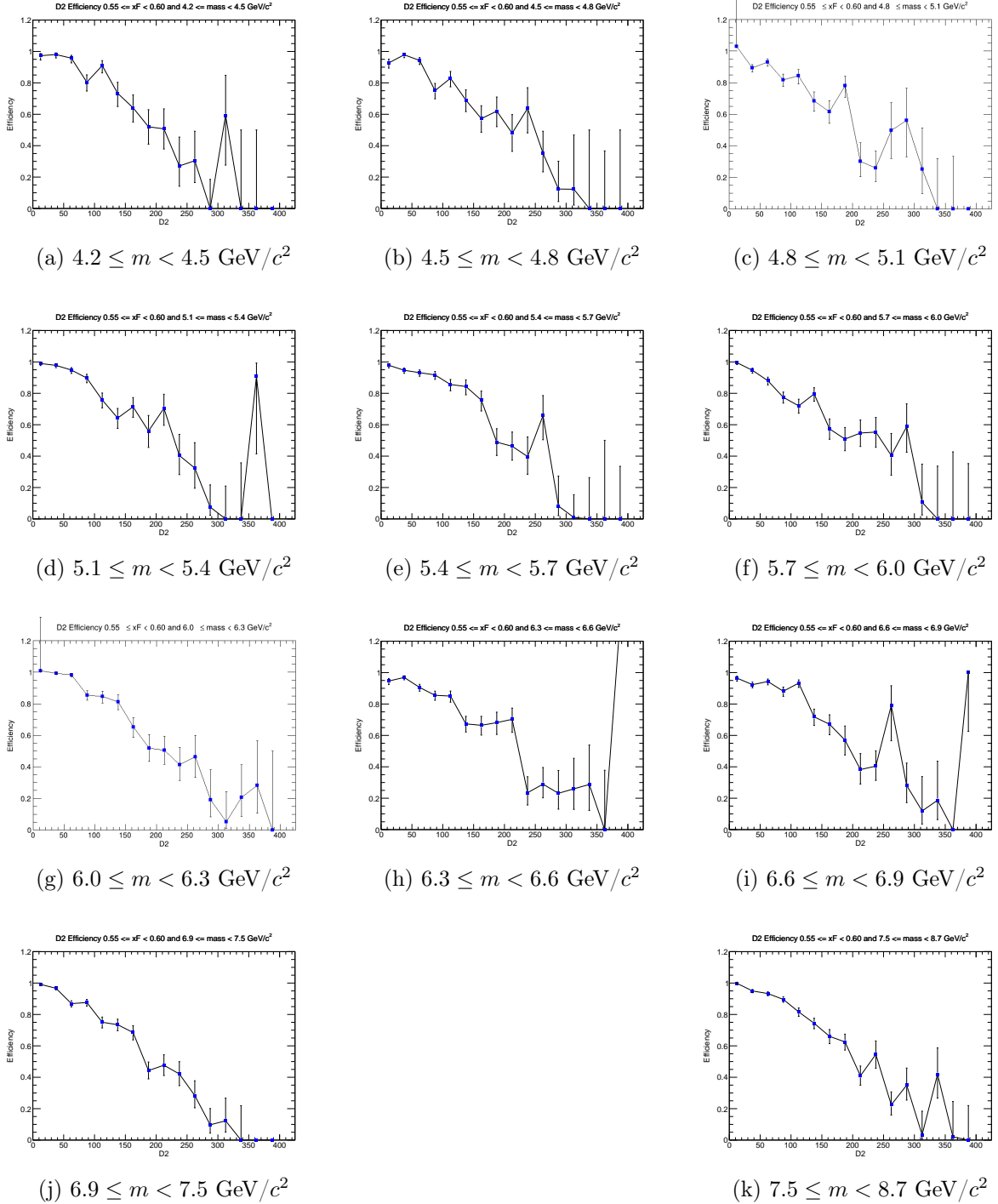


Figure 28: Efficiency plots for the x_F bin $0.55 \leq x_F < 0.60$.

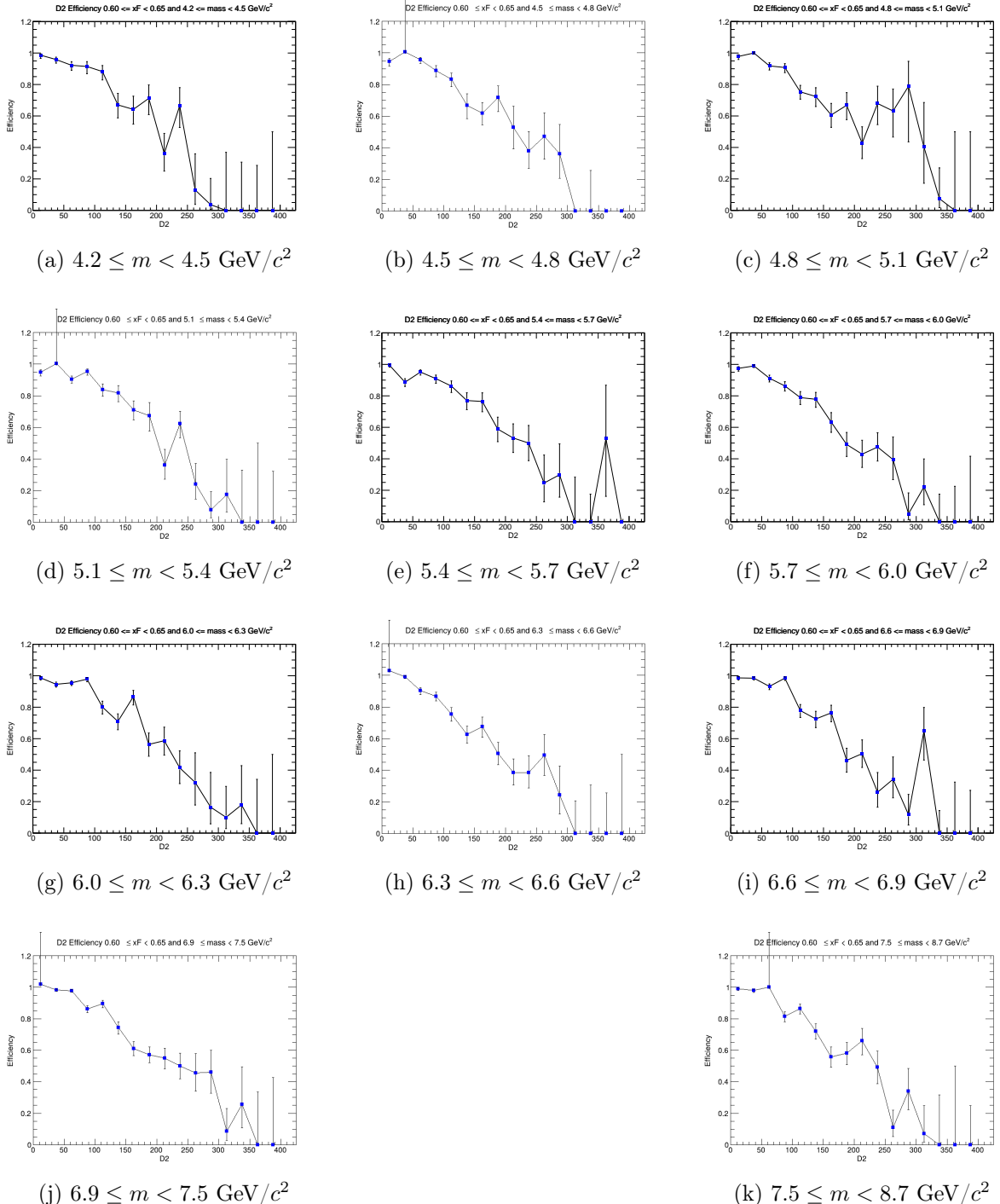


Figure 29: Efficiency plots for the x_F bin $0.60 \leq x_F < 0.65$.

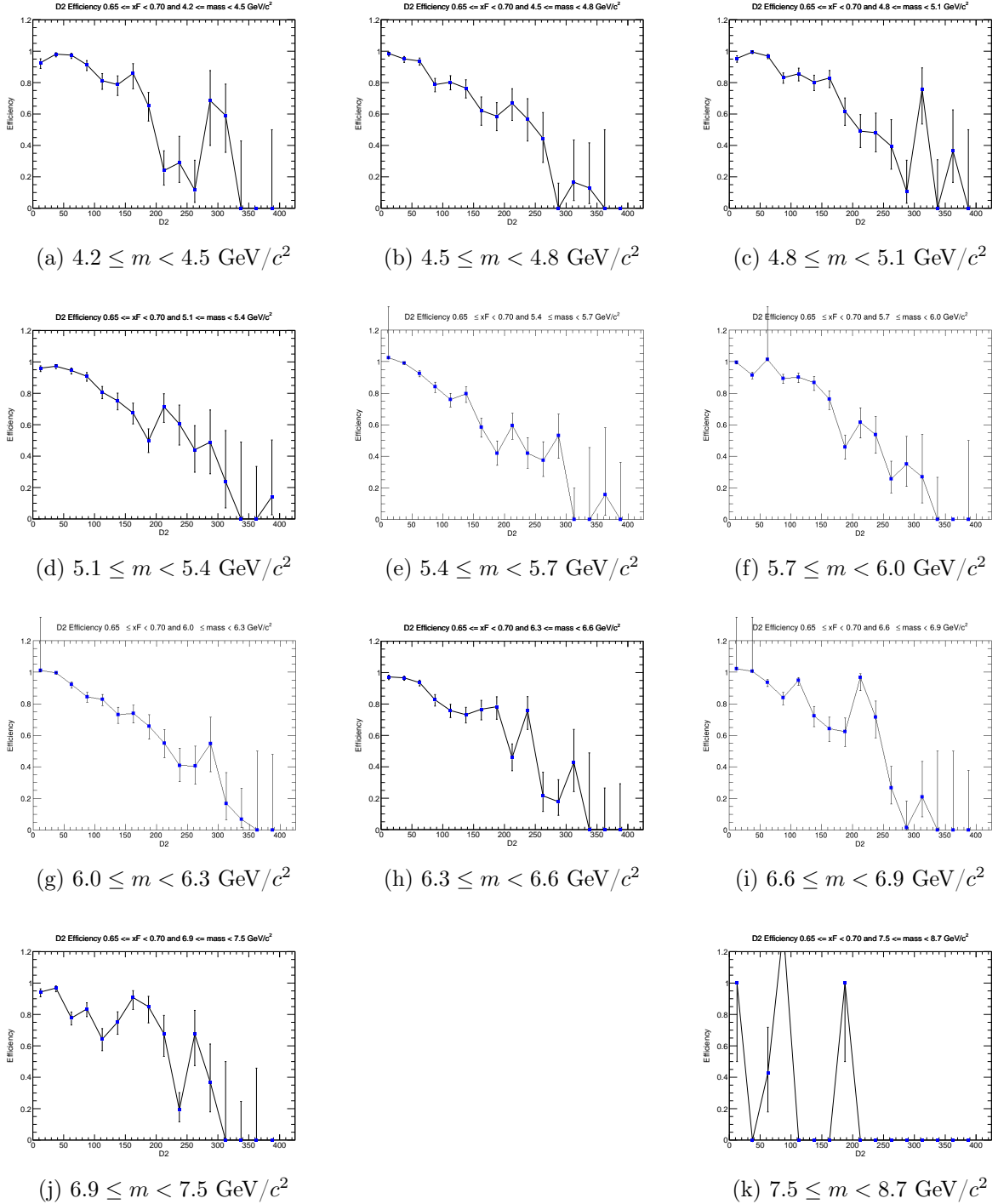


Figure 30: Efficiency plots for the x_F bin $0.65 \leq x_F < 0.70$.

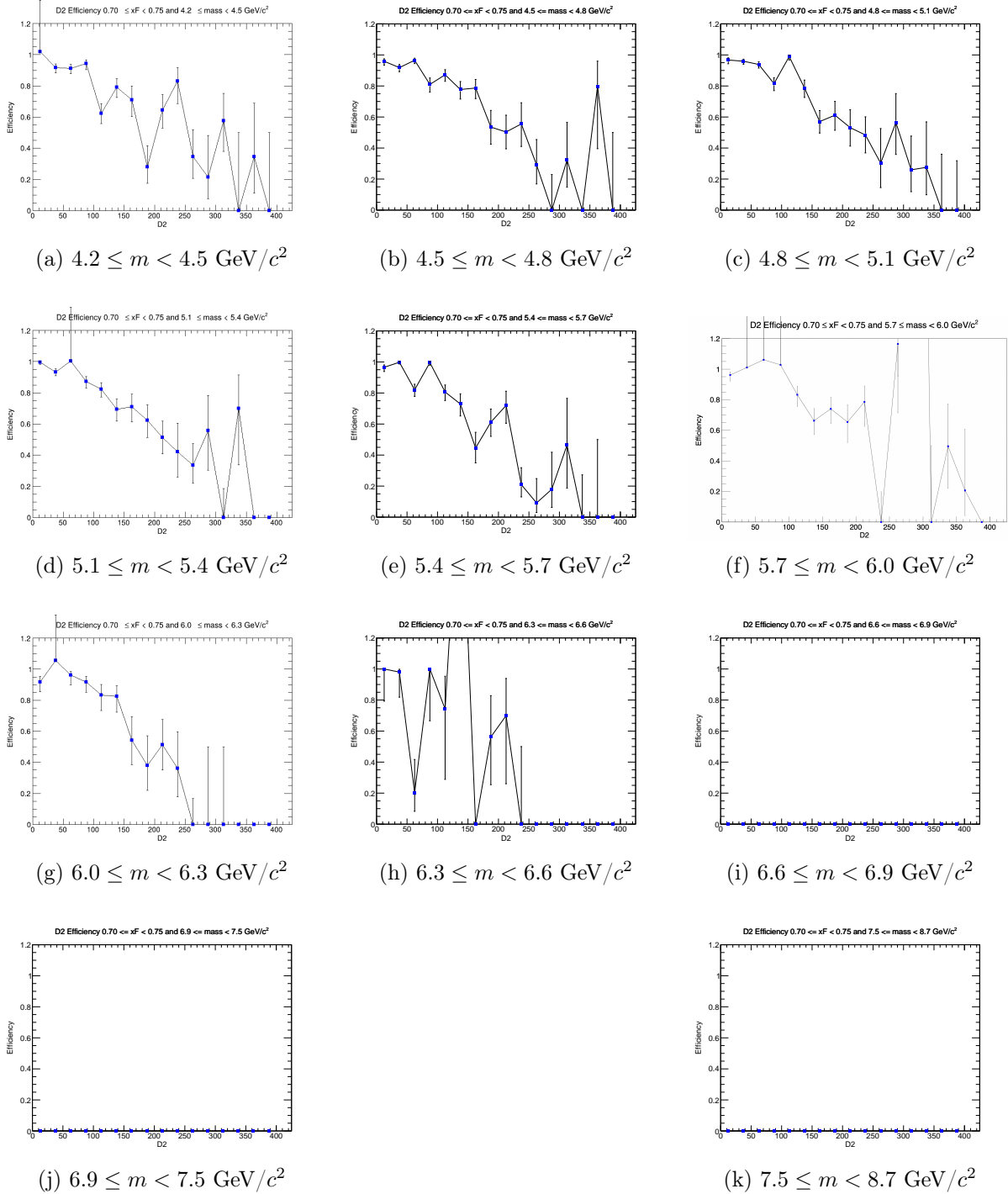


Figure 31: Efficiency plots for the x_F bin $0.70 \leq x_F < 0.75$.

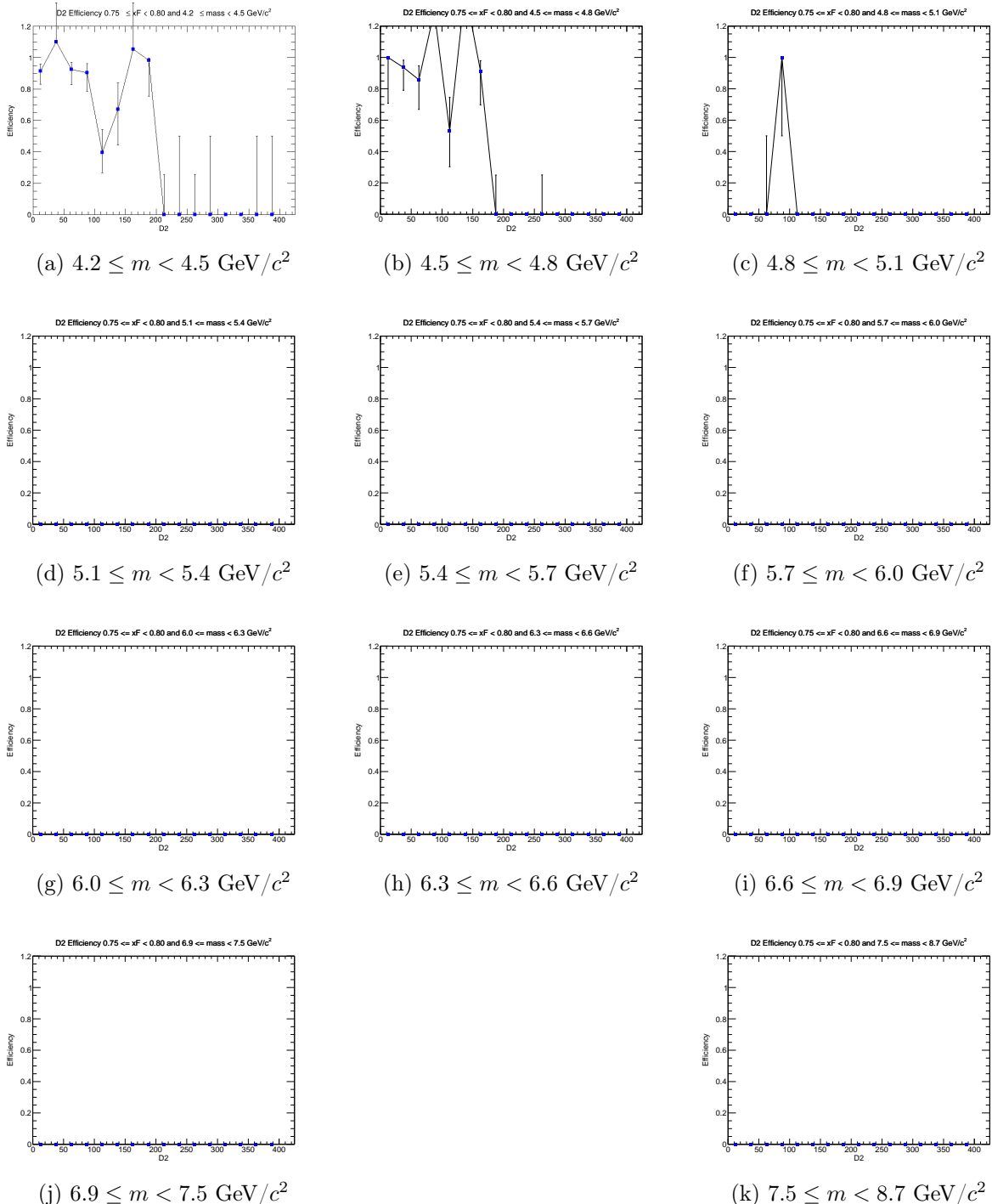


Figure 32: Efficiency plots for the x_F bin $0.75 \leq x_F < 0.80$.

Several bins exhibit unphysical average efficiencies, with some values equal to zero and others exceeding 100%. Therefore, only the bins with valid (0, 100], kTracker efficiencies are included in the final cross section calculation.

Table 1 lists the calculated average efficiencies and their uncertainties for each kinematic bin using the RS-67 LH₂ dataset.

Table 1: Average Efficiency and Errors for Bins in x_F and Mass

x_F Bin	Mass Bin (GeV/c^2)	N_{events}	$\langle \epsilon \rangle$	$\delta_{\text{prop}}(\langle \epsilon \rangle)$	$1/\langle \epsilon \rangle$	$\delta(1/\langle \epsilon \rangle)$
[0.0, 0.05)	[4.2, 4.5)	1	0.0000	0.0000	—	—
[0.0, 0.05)	[4.5, 4.8)	9	0.1378	0.0248	7.258	1.305
[0.0, 0.05)	[4.8, 5.1)	40	0.8807	0.0209	1.135	0.027
[0.0, 0.05)	[5.1, 5.4)	72	0.6521	0.0216	1.534	0.051
[0.0, 0.05)	[5.4, 5.7)	66	0.6728	0.0119	1.486	0.026
[0.0, 0.05)	[5.7, 6.0)	37	0.5828	0.0174	1.716	0.051
[0.0, 0.05)	[6.0, 6.3)	26	0.6369	0.0190	1.570	0.047
[0.0, 0.05)	[6.3, 6.6)	15	0.5970	0.0313	1.675	0.088
[0.0, 0.05)	[6.6, 6.9)	12	0.7055	0.0250	1.417	0.050
[0.0, 0.05)	[6.9, 7.5)	9	0.6253	0.0272	1.599	0.070
[0.0, 0.05)	[7.5, 8.7)	1	0.6066	0.0595	1.649	0.162
[0.05, 0.1)	[4.2, 4.5)	2	0.0000	0.0000	—	—
[0.05, 0.1)	[4.5, 4.8)	39	0.2746	0.0222	3.642	0.294
[0.05, 0.1)	[4.8, 5.1)	81	0.5004	0.0185	1.999	0.074
[0.05, 0.1)	[5.1, 5.4)	95	0.7206	0.0099	1.388	0.019
[0.05, 0.1)	[5.4, 5.7)	77	0.6718	0.0122	1.488	0.027
[0.05, 0.1)	[5.7, 6.0)	53	0.7379	0.0122	1.355	0.022
[0.05, 0.1)	[6.0, 6.3)	39	0.7318	0.0117	1.367	0.022
[0.05, 0.1)	[6.3, 6.6)	25	0.5964	0.0204	1.677	0.057
[0.05, 0.1)	[6.6, 6.9)	5	0.5670	0.0382	1.764	0.119
[0.05, 0.1)	[6.9, 7.5)	7	0.6487	0.0268	1.541	0.064
[0.05, 0.1)	[7.5, 8.7)	6	0.5979	0.0270	1.672	0.075
[0.1, 0.15)	[4.2, 4.5)	31	13.2153	0.0144	0.076	0.000
[0.1, 0.15)	[4.5, 4.8)	96	0.5701	0.0173	1.754	0.053
[0.1, 0.15)	[4.8, 5.1)	137	0.6224	0.0144	1.607	0.037
[0.1, 0.15)	[5.1, 5.4)	132	0.5965	0.0114	1.676	0.032
[0.1, 0.15)	[5.4, 5.7)	87	0.6659	0.0091	1.502	0.021
[0.1, 0.15)	[5.7, 6.0)	76	0.6958	0.0088	1.437	0.018
[0.1, 0.15)	[6.0, 6.3)	52	0.7145	0.0102	1.400	0.020
[0.1, 0.15)	[6.3, 6.6)	28	0.7879	0.0113	1.269	0.018
[0.1, 0.15)	[6.6, 6.9)	10	0.7518	0.0193	1.330	0.034
[0.1, 0.15)	[6.9, 7.5)	11	0.6798	0.0167	1.471	0.036
[0.1, 0.15)	[7.5, 8.7)	7	0.7011	0.0140	1.426	0.029
[0.15, 0.2)	[4.2, 4.5)	82	1.1304	0.0120	0.885	0.009
[0.15, 0.2)	[4.5, 4.8)	167	0.6997	0.0132	1.429	0.027
[0.15, 0.2)	[4.8, 5.1)	231	0.5373	0.0088	1.861	0.030
[0.15, 0.2)	[5.1, 5.4)	201	0.6974	0.0070	1.434	0.014
[0.15, 0.2)	[5.4, 5.7)	113	0.6925	0.0087	1.444	0.018
[0.15, 0.2)	[5.7, 6.0)	94	0.7358	0.0088	1.359	0.016
[0.15, 0.2)	[6.0, 6.3)	67	0.7156	0.0089	1.397	0.017
[0.15, 0.2)	[6.3, 6.6)	35	0.7728	0.0100	1.294	0.017

Continued on next page

Table 1: (Continued)

x_F Bin	Mass Bin (GeV/c^2)	N_{events}	$\langle \epsilon \rangle$	$\delta_{\text{prop}}(\epsilon)$	$1/\langle \epsilon \rangle$	$\delta(1/\langle \epsilon \rangle)$
[0.15, 0.2)	[6.6, 6.9)	16	0.6784	0.0176	1.474	0.038
[0.15, 0.2)	[6.9, 7.5)	12	0.6677	0.0149	1.498	0.033
[0.15, 0.2)	[7.5, 8.7)	3	0.6570	0.0400	1.522	0.093
[0.2, 0.25)	[4.2, 4.5)	181	0.5438	0.0128	1.839	0.043
[0.2, 0.25)	[4.5, 4.8)	281	0.6018	0.0074	1.662	0.021
[0.2, 0.25)	[4.8, 5.1)	269	0.7047	0.0057	1.419	0.012
[0.2, 0.25)	[5.1, 5.4)	206	0.6898	0.0057	1.450	0.012
[0.2, 0.25)	[5.4, 5.7)	143	0.6979	0.0067	1.433	0.014
[0.2, 0.25)	[5.7, 6.0)	106	0.7908	0.0062	1.265	0.010
[0.2, 0.25)	[6.0, 6.3)	54	0.7371	0.0086	1.357	0.016
[0.2, 0.25)	[6.3, 6.6)	46	0.7367	0.0097	1.357	0.018
[0.2, 0.25)	[6.6, 6.9)	21	0.7909	0.0111	1.264	0.018
[0.2, 0.25)	[6.9, 7.5)	10	0.6953	0.0153	1.438	0.032
[0.2, 0.25)	[7.5, 8.7)	6	0.7790	0.0117	1.284	0.019
[0.25, 0.3)	[4.2, 4.5)	363	0.7031	0.0075	1.422	0.015
[0.25, 0.3)	[4.5, 4.8)	402	0.7172	0.0053	1.394	0.010
[0.25, 0.3)	[4.8, 5.1)	316	0.7115	0.0046	1.406	0.009
[0.25, 0.3)	[5.1, 5.4)	243	0.7125	0.0052	1.404	0.010
[0.25, 0.3)	[5.4, 5.7)	179	0.7724	0.0055	1.295	0.009
[0.25, 0.3)	[5.7, 6.0)	89	0.7356	0.0074	1.359	0.014
[0.25, 0.3)	[6.0, 6.3)	60	0.7620	0.0078	1.312	0.013
[0.25, 0.3)	[6.3, 6.6)	38	0.7720	0.0083	1.295	0.014
[0.25, 0.3)	[6.6, 6.9)	26	0.6924	0.0134	1.444	0.028
[0.25, 0.3)	[6.9, 7.5)	24	0.7399	0.0104	1.352	0.019
[0.25, 0.3)	[7.5, 8.7)	2	0.5631	0.0336	1.776	0.106
[0.3, 0.35)	[4.2, 4.5)	542	0.7566	0.0051	1.322	0.009
[0.3, 0.35)	[4.5, 4.8)	488	0.7802	0.0037	1.282	0.006
[0.3, 0.35)	[4.8, 5.1)	381	0.7314	0.0039	1.367	0.007
[0.3, 0.35)	[5.1, 5.4)	271	0.7999	0.0038	1.250	0.006
[0.3, 0.35)	[5.4, 5.7)	185	0.7186	0.0047	1.392	0.009
[0.3, 0.35)	[5.7, 6.0)	93	0.7165	0.0063	1.396	0.012
[0.3, 0.35)	[6.0, 6.3)	60	0.7233	0.0083	1.383	0.016
[0.3, 0.35)	[6.3, 6.6)	45	0.7940	0.0074	1.259	0.012
[0.3, 0.35)	[6.6, 6.9)	25	0.7720	0.0113	1.295	0.019
[0.3, 0.35)	[6.9, 7.5)	19	0.7341	0.0124	1.362	0.023
[0.3, 0.35)	[7.5, 8.7)	9	0.7511	0.0119	1.331	0.021
[0.35, 0.4)	[4.2, 4.5)	625	0.8121	0.0034	1.231	0.005
[0.35, 0.4)	[4.5, 4.8)	543	0.7329	0.0034	1.364	0.006
[0.35, 0.4)	[4.8, 5.1)	402	0.7561	0.0036	1.323	0.006
[0.35, 0.4)	[5.1, 5.4)	281	0.7953	0.0038	1.257	0.006
[0.35, 0.4)	[5.4, 5.7)	147	0.7652	0.0046	1.307	0.008
[0.35, 0.4)	[5.7, 6.0)	110	0.7670	0.0054	1.304	0.009
[0.35, 0.4)	[6.0, 6.3)	68	0.8024	0.0064	1.246	0.010
[0.35, 0.4)	[6.3, 6.6)	43	0.7917	0.0077	1.263	0.012
[0.35, 0.4)	[6.6, 6.9)	20	0.7471	0.0124	1.339	0.022
[0.35, 0.4)	[6.9, 7.5)	19	0.7659	0.0091	1.306	0.016
[0.35, 0.4)	[7.5, 8.7)	8	0.6464	0.0164	1.547	0.039
[0.4, 0.45)	[4.2, 4.5)	652	0.7735	0.0034	1.293	0.006

Continued on next page

Table 1: (Continued)

x_F Bin	Mass Bin (GeV/c^2)	N_{events}	$\langle \epsilon \rangle$	$\delta_{\text{prop}}(\langle \epsilon \rangle)$	$1/\langle \epsilon \rangle$	$\delta(1/\langle \epsilon \rangle)$
[0.4, 0.45)	[4.5, 4.8)	497	0.7426	0.0031	1.347	0.006
[0.4, 0.45)	[4.8, 5.1)	400	0.7471	0.0032	1.339	0.006
[0.4, 0.45)	[5.1, 5.4)	244	0.7470	0.0041	1.339	0.007
[0.4, 0.45)	[5.4, 5.7)	178	0.7796	0.0040	1.283	0.007
[0.4, 0.45)	[5.7, 6.0)	94	0.7949	0.0054	1.258	0.008
[0.4, 0.45)	[6.0, 6.3)	82	0.8039	0.0058	1.244	0.009
[0.4, 0.45)	[6.3, 6.6)	47	0.7396	0.0085	1.352	0.016
[0.4, 0.45)	[6.6, 6.9)	24	0.8323	0.0085	1.202	0.012
[0.4, 0.45)	[6.9, 7.5)	20	0.7353	0.0102	1.360	0.019
[0.4, 0.45)	[7.5, 8.7)	8	0.8233	0.0100	1.215	0.015
[0.45, 0.5)	[4.2, 4.5)	671	0.7745	0.0030	1.291	0.005
[0.45, 0.5)	[4.5, 4.8)	512	0.7618	0.0028	1.313	0.005
[0.45, 0.5)	[4.8, 5.1)	352	0.7306	0.0034	1.369	0.006
[0.45, 0.5)	[5.1, 5.4)	219	0.7627	0.0043	1.311	0.007
[0.45, 0.5)	[5.4, 5.7)	143	0.8074	0.0047	1.239	0.007
[0.45, 0.5)	[5.7, 6.0)	96	0.7845	0.0055	1.275	0.009
[0.45, 0.5)	[6.0, 6.3)	58	0.7846	0.0073	1.275	0.012
[0.45, 0.5)	[6.3, 6.6)	49	0.7242	0.0081	1.381	0.016
[0.45, 0.5)	[6.6, 6.9)	17	0.7580	0.0148	1.319	0.026
[0.45, 0.5)	[6.9, 7.5)	27	0.7951	0.0064	1.258	0.010
[0.45, 0.5)	[7.5, 8.7)	7	0.8274	0.0121	1.209	0.018
[0.5, 0.55)	[4.2, 4.5)	616	0.6899	0.0035	1.449	0.007
[0.5, 0.55)	[4.5, 4.8)	395	0.7404	0.0034	1.351	0.006
[0.5, 0.55)	[4.8, 5.1)	285	0.7299	0.0037	1.370	0.007
[0.5, 0.55)	[5.1, 5.4)	207	0.7855	0.0038	1.273	0.006
[0.5, 0.55)	[5.4, 5.7)	152	0.7783	0.0042	1.285	0.007
[0.5, 0.55)	[5.7, 6.0)	78	0.7854	0.0062	1.273	0.010
[0.5, 0.55)	[6.0, 6.3)	42	0.7132	0.0093	1.402	0.018
[0.5, 0.55)	[6.3, 6.6)	38	0.8216	0.0073	1.217	0.011
[0.5, 0.55)	[6.6, 6.9)	16	0.7818	0.0137	1.279	0.022
[0.5, 0.55)	[6.9, 7.5)	14	0.8153	0.0107	1.227	0.016
[0.5, 0.55)	[7.5, 8.7)	10	0.7404	0.0111	1.351	0.020
[0.55, 0.6)	[4.2, 4.5)	486	0.7795	0.0032	1.283	0.005
[0.55, 0.6)	[4.5, 4.8)	385	0.7572	0.0033	1.321	0.006
[0.55, 0.6)	[4.8, 5.1)	245	0.7574	0.0041	1.320	0.007
[0.55, 0.6)	[5.1, 5.4)	153	0.7870	0.0045	1.271	0.007
[0.55, 0.6)	[5.4, 5.7)	90	0.8021	0.0058	1.247	0.009
[0.55, 0.6)	[5.7, 6.0)	59	0.7335	0.0064	1.363	0.012
[0.55, 0.6)	[6.0, 6.3)	42	0.8234	0.0070	1.214	0.010
[0.55, 0.6)	[6.3, 6.6)	22	0.7949	0.0096	1.258	0.015
[0.55, 0.6)	[6.6, 6.9)	16	0.8082	0.0122	1.237	0.019
[0.55, 0.6)	[6.9, 7.5)	14	0.7432	0.0109	1.346	0.020
[0.55, 0.6)	[7.5, 8.7)	5	0.7910	0.0155	1.264	0.025
[0.6, 0.65)	[4.2, 4.5)	380	0.7973	0.0034	1.254	0.005
[0.6, 0.65)	[4.5, 4.8)	251	0.7772	0.0042	1.287	0.007
[0.6, 0.65)	[4.8, 5.1)	164	0.7728	0.0046	1.294	0.008
[0.6, 0.65)	[5.1, 5.4)	108	0.8356	0.0044	1.197	0.006
[0.6, 0.65)	[5.4, 5.7)	66	0.8310	0.0060	1.203	0.009

Continued on next page

Table 1: (Continued)

x_F Bin	Mass Bin (GeV/c^2)	N_{events}	$\langle \epsilon \rangle$	$\delta_{\text{prop}}(\epsilon)$	$1/\langle \epsilon \rangle$	$\delta(1/\langle \epsilon \rangle)$
[0.6, 0.65)	[5.7, 6.0)	51	0.7211	0.0078	1.387	0.015
[0.6, 0.65)	[6.0, 6.3)	38	0.8297	0.0081	1.205	0.012
[0.6, 0.65)	[6.3, 6.6)	19	0.7875	0.0096	1.270	0.015
[0.6, 0.65)	[6.6, 6.9)	12	0.9017	0.0086	1.109	0.011
[0.6, 0.65)	[6.9, 7.5)	10	0.8154	0.0137	1.226	0.021
[0.6, 0.65)	[7.5, 8.7)	3	0.8549	0.0236	1.170	0.032
[0.65, 0.7)	[4.2, 4.5)	248	0.7996	0.0041	1.251	0.006
[0.65, 0.7)	[4.5, 4.8)	181	0.7809	0.0046	1.281	0.008
[0.65, 0.7)	[4.8, 5.1)	111	0.8258	0.0049	1.211	0.007
[0.65, 0.7)	[5.1, 5.4)	91	0.8077	0.0053	1.238	0.008
[0.65, 0.7)	[5.4, 5.7)	55	0.7491	0.0068	1.335	0.012
[0.65, 0.7)	[5.7, 6.0)	31	0.8202	0.0094	1.219	0.014
[0.65, 0.7)	[6.0, 6.3)	23	0.7967	0.0103	1.255	0.016
[0.65, 0.7)	[6.3, 6.6)	9	0.7798	0.0173	1.282	0.028
[0.65, 0.7)	[6.6, 6.9)	9	0.8424	0.0151	1.187	0.021
[0.65, 0.7)	[6.9, 7.5)	15	0.7883	0.0162	1.269	0.026
[0.65, 0.7)	[7.5, 8.7)	5	0.0786	0.0410	12.717	6.635
[0.7, 0.75)	[4.2, 4.5)	167	0.7450	0.0057	1.342	0.010
[0.7, 0.75)	[4.5, 4.8)	136	0.7774	0.0055	1.286	0.009
[0.7, 0.75)	[4.8, 5.1)	86	0.7999	0.0068	1.250	0.011
[0.7, 0.75)	[5.1, 5.4)	44	0.7882	0.0106	1.269	0.017
[0.7, 0.75)	[5.4, 5.7)	25	0.7779	0.0115	1.286	0.019
[0.7, 0.75)	[5.7, 6.0)	17	0.8597	0.0185	1.163	0.025
[0.7, 0.75)	[6.0, 6.3)	15	0.7732	0.0268	1.293	0.045
[0.7, 0.75)	[6.3, 6.6)	11	0.8705	0.0475	1.149	0.063
[0.7, 0.75)	[6.6, 6.9)	4	0.0000	0.0000	—	—
[0.7, 0.75)	[6.9, 7.5)	3	0.0000	0.0000	—	—
[0.7, 0.75)	[7.5, 8.7)	2	0.0000	0.0000	—	—
[0.75, 0.8)	[4.2, 4.5)	114	0.7278	0.0099	1.374	0.019
[0.75, 0.8)	[4.5, 4.8)	51	0.9280	0.0090	1.078	0.010
[0.75, 0.8)	[4.8, 5.1)	34	0.0947	0.0160	10.559	1.783
[0.75, 0.8)	[5.1, 5.4)	24	0.0000	0.0000	—	—
[0.75, 0.8)	[5.4, 5.7)	18	0.0000	0.0000	—	—
[0.75, 0.8)	[5.7, 6.0)	15	0.0000	0.0000	—	—
[0.75, 0.8)	[6.0, 6.3)	13	0.0000	0.0000	—	—
[0.75, 0.8)	[6.3, 6.6)	4	0.0000	0.0000	—	—
[0.75, 0.8)	[6.6, 6.9)	2	0.0000	0.0000	—	—
[0.75, 0.8)	[6.9, 7.5)	1	0.0000	0.0000	—	—
[0.75, 0.8)	[7.5, 8.7)	2	0.0000	0.0000	—	—
[0.8, 0.85)	[4.2, 4.5)	49	0.0000	0.0000	—	—
[0.8, 0.85)	[4.5, 4.8)	29	0.0000	0.0000	—	—
[0.8, 0.85)	[4.8, 5.1)	22	0.0000	0.0000	—	—
[0.8, 0.85)	[5.1, 5.4)	12	0.0000	0.0000	—	—
[0.8, 0.85)	[5.4, 5.7)	9	0.0000	0.0000	—	—
[0.8, 0.85)	[5.7, 6.0)	8	0.0000	0.0000	—	—
[0.8, 0.85)	[6.0, 6.3)	1	0.0000	0.0000	—	—
[0.8, 0.85)	[6.3, 6.6)	1	0.0000	0.0000	—	—
[0.8, 0.85)	[6.6, 6.9)	2	0.0000	0.0000	—	—

Continued on next page

Table 1: (Continued)

x_F Bin	Mass Bin (GeV/c^2)	N_{events}	$\langle \epsilon \rangle$	$\delta_{\text{prop}}(\epsilon)$	$1/\langle \epsilon \rangle$	$\delta(1/\langle \epsilon \rangle)$
[0.8, 0.85)	[6.9, 7.5)	2	0.0000	0.0000	—	—
[0.8, 0.85)	[7.5, 8.7)	0	—	—	—	—

3.3 Trigger Efficiency

In DocDB 10795 Kenichi performed a trigger efficiency study in support of Hugo’s charmonium analysis. This study showed an efficiency of 0.87 ± 0.10 independent of kinematic bin. This study will need to be redone for the DY region $4.2 < M < 8.0$. For this purposes of this release, however, we have slightly enlarged the range of the error to include the possibility of a lower efficiency. We have adopted the value $\epsilon_{\text{trigger}} = 0.845 \pm 0.125$ temporarily. We note that this will be the largest contributor to the systematic error described in the next section.

4 Systematic Uncertainties

A comprehensive evaluation of systematic uncertainties is essential for a precision cross-section measurement. The main sources of systematic uncertainty in this analysis include:

- **Luminosity Determination:** Uncertainty in the incident proton flux, target density, and length.
- **Acceptance Correction:** Uncertainty stemming from the MC statistics and the physics model used to generate the Drell-Yan events (e.g., the input PDFs).
- **Reconstruction Efficiency:** Uncertainty from the statistics of the clean and messy MC samples, and the method used to average over the data’s occupancy distribution.
- **Background Subtraction:** Uncertainty in the normalization of the empty flask and combinatorial backgrounds.
- **Event Selection:** Variation of the analysis cuts to test the stability of the final result.

A study of the systematic effect of the combinatoric background subtraction is underway (see DocDB 11307), but this is expected to be purely statistical and not systematic.

In this report we have computed a systematic uncertainty from three sources: the reconstruction efficiency, the acceptance, and the trigger efficiency. Those corrections are described in detail in the previous section. In each case we computed the fractional error in the correction and applied that fraction to the corrected yield in Equation 2 to obtain the absolute systematic error. The three systematic errors were added in quadrature. To summarize:

$$\text{Let } C(M, x_F) = \frac{d^2\sigma}{dMdx_F}(M, x_F).$$

$$\text{Then } \sigma_C^{\text{sys,acc}}(M, x_F) = \frac{\delta\epsilon_{\text{acc}}(M, x_F)}{\epsilon_{\text{acc}}(M, x_F)} C(M, x_F),$$

$$\sigma_C^{\text{sys,recon}}(M, x_F) = \frac{\delta\epsilon_{\text{recon}}(M, x_F)}{\epsilon_{\text{recon}}(M, x_F)} C(M, x_F),$$

$$\sigma_C^{\text{sys,trigger}}(M, x_F) = \frac{\delta\epsilon_{\text{trigger}}}{\epsilon_{\text{trigger}}} C(M, x_F), \text{ and}$$

$$\sigma_C^{\text{sys,total}}(M, x_F) = \sqrt{[\sigma_C^{\text{sys,acc}}(M, x_F)]^2 + [\sigma_C^{\text{sys,recon}}(M, x_F)]^2 + [\sigma_C^{\text{sys,trigger}}(M, x_F)]^2}.$$

257 This total systematic error is displayed as an error band in the plots in the next section. Table 2,
258 in the Appendix, lists the systematic uncertainties for each bin.

259 The charmonium paper [3] uses a 10% systematic error associated with the integrated lumi-
260 nosity; we adopt the same value. We have not included this in the plots because it is uniform
261 for every point.

262 5 Results: Double-Differential Cross-Section

263 Following the application of all corrections and background subtraction procedures, the Drell-
264 Yan double-differential cross-section, $M^3 d^2\sigma/(dM dx_F)$, was extracted for the pp collisions at
265 $\sqrt{s} = 15$ GeV. The results are presented in the following figures for all bins of x_F . Table 3, in
266 the Appendix, lists these results.

267 Each figure displays the measured cross-section as a function of the dimuon invariant mass,
268 M . The error bars on the data points represent the statistical uncertainty, while the error
269 bands show the systematic uncertainties. Please note that the 10% global uncertainty due to
270 the integrated luminosity is not included in the error bands.

271 The data are compared with theoretical predictions based on Next-to-Leading Order (NLO)
272 QCD calculations, using the NNPDF4.0 and CT18 NLO PDFs obtained from LHAPDF. These
273 calculations were performed by Hugo and are mentioned in DocDB 10167.

274 Data points do not appear if the efficiency and/or acceptance for that bin was computed to
275 be zero.

Double differential Cross-Section for $0.00 \leq x_F < 0.05$

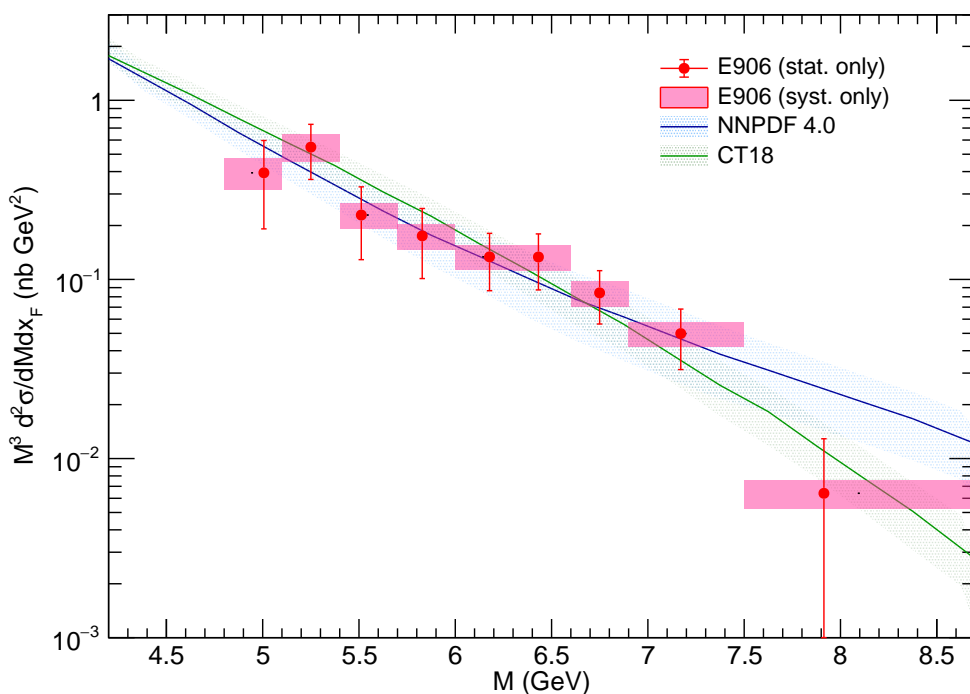


Figure 33: Differential cross-section for x_F bin $0.00 \leq x_F < 0.05$.

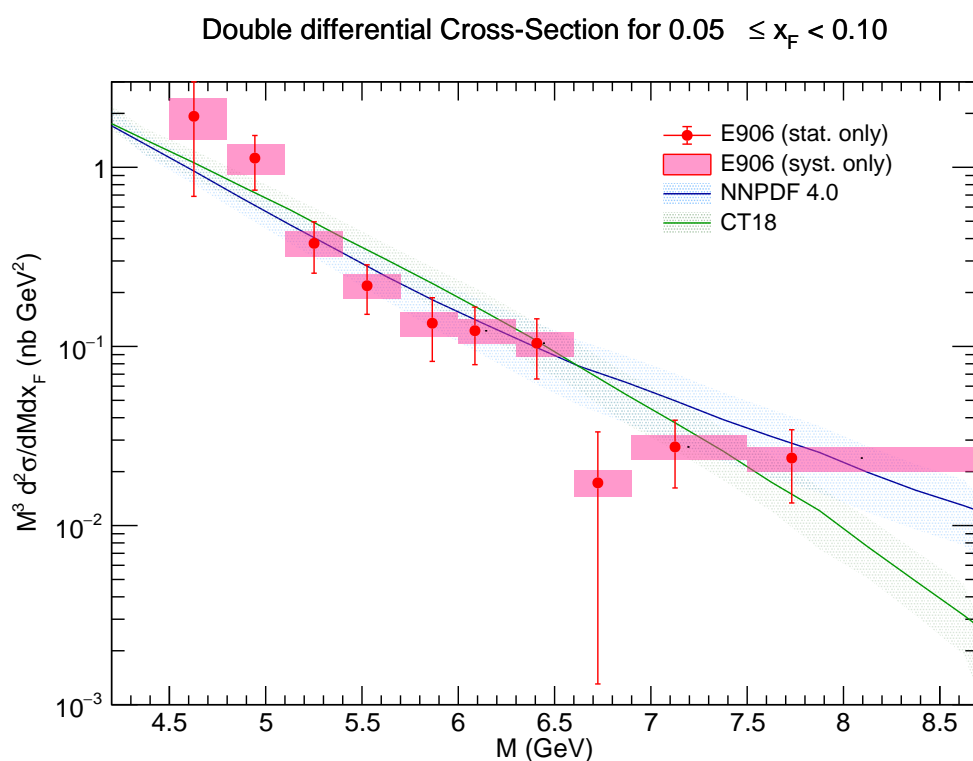


Figure 34: Differential cross-section for x_F bin $0.05 \leq x_F < 0.10$.

Double differential Cross-Section for $0.10 \leq x_F < 0.15$

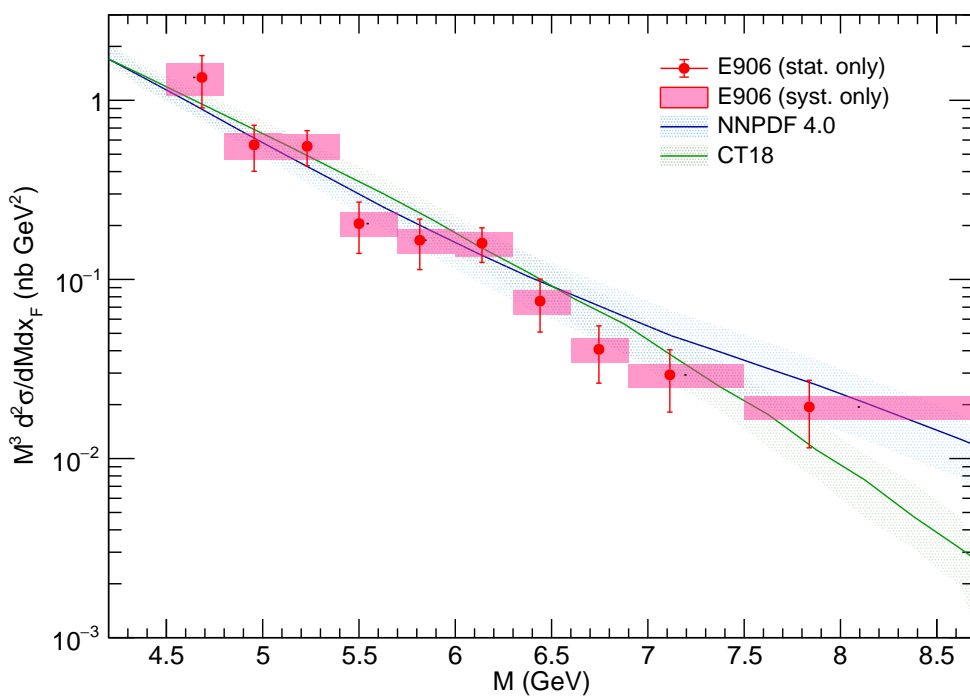


Figure 35: Differential cross-section for x_F bin $0.10 \leq x_F < 0.15$.

Double differential Cross-Section for $0.15 \leq x_F < 0.20$

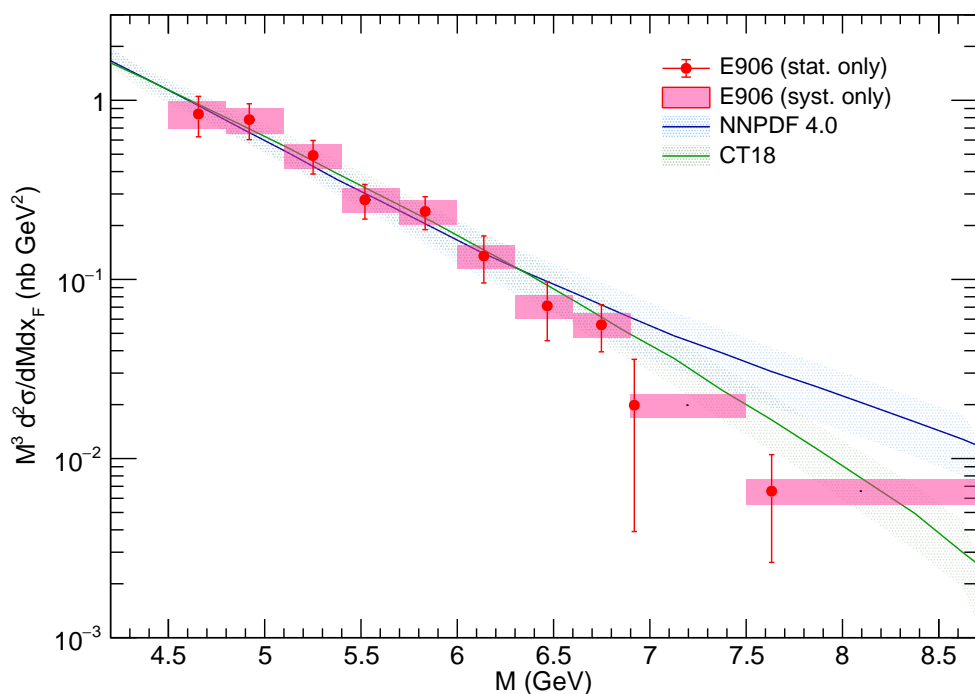


Figure 36: Differential cross-section for x_F bin $0.15 \leq x_F < 0.20$.

Double differential Cross-Section for $0.20 \leq x_F < 0.25$

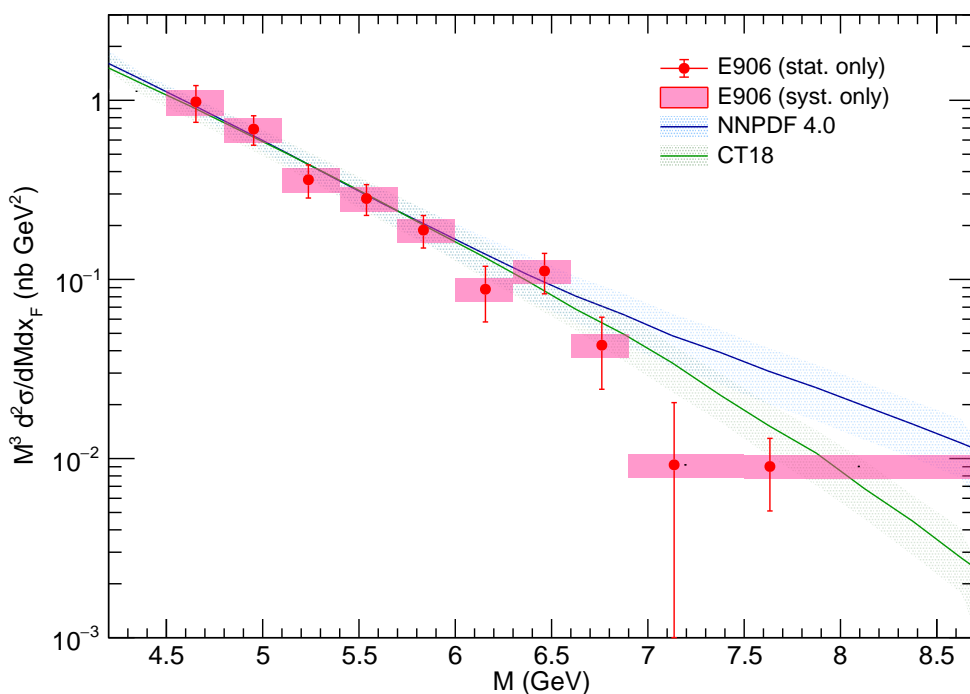


Figure 37: Differential cross-section for x_F bin $0.20 \leq x_F < 0.25$.

Double differential Cross-Section for $0.25 \leq x_F < 0.30$

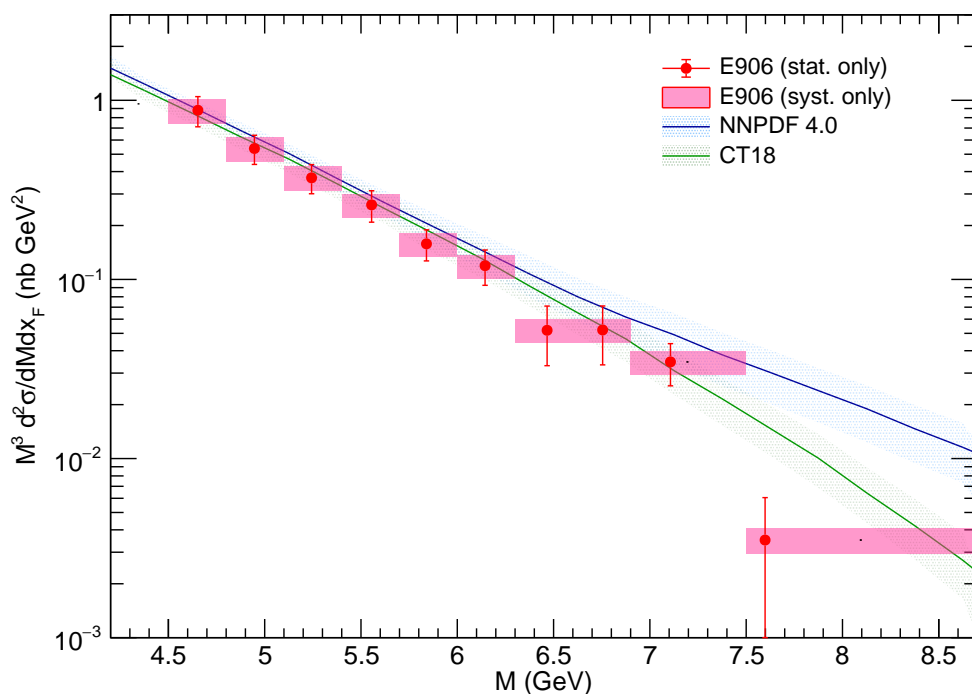


Figure 38: Differential cross-section for x_F bin $0.25 \leq x_F < 0.30$.

Double differential Cross-Section for $0.30 \leq x_F < 0.35$

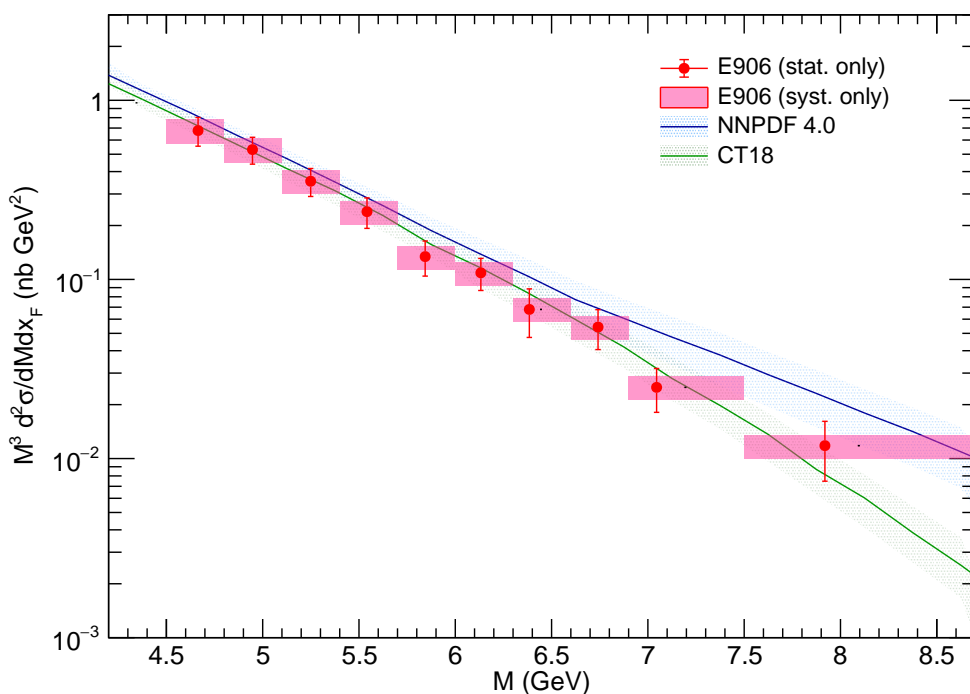


Figure 39: Differential cross-section for x_F bin $0.30 \leq x_F < 0.35$.

Double differential Cross-Section for $0.35 \leq x_F < 0.40$

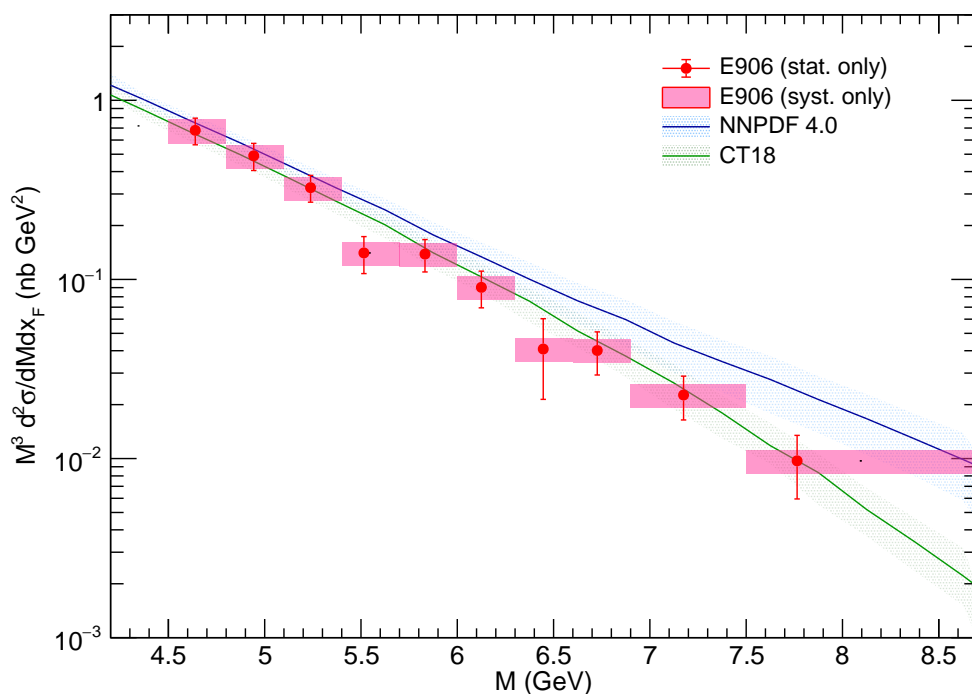


Figure 40: Differential cross-section for x_F bin $0.35 \leq x_F < 0.40$.

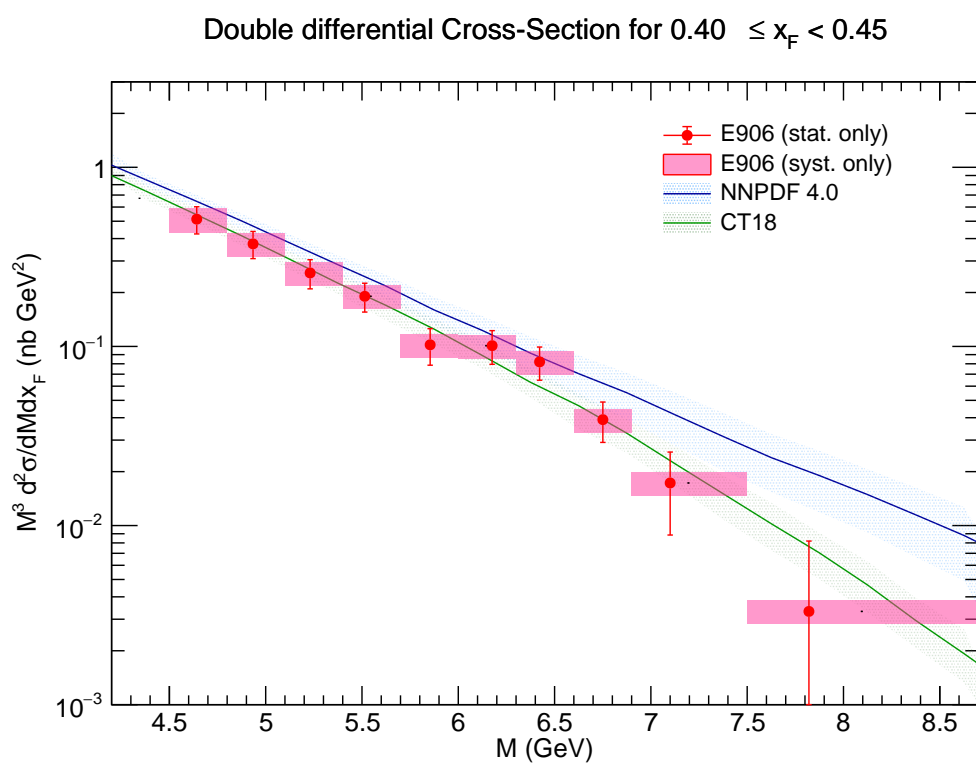


Figure 41: Differential cross-section for x_F bin $0.40 \leq x_F < 0.45$.

Double differential Cross-Section for $0.45 \leq x_F < 0.50$

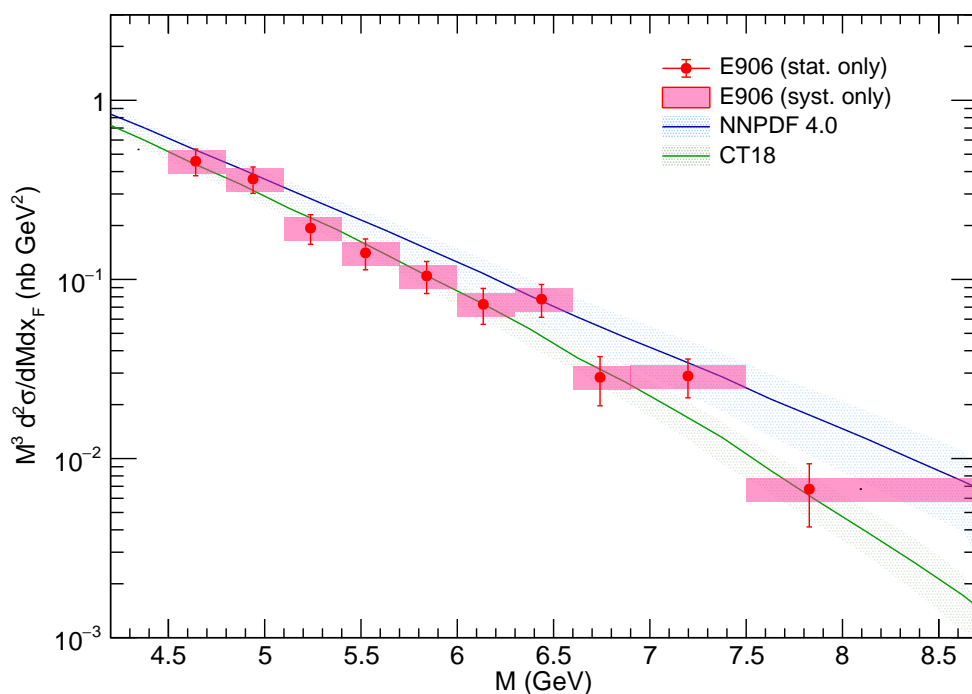


Figure 42: Differential cross-section for x_F bin $0.45 \leq x_F < 0.50$.

Double differential Cross-Section for $0.50 \leq x_F < 0.55$

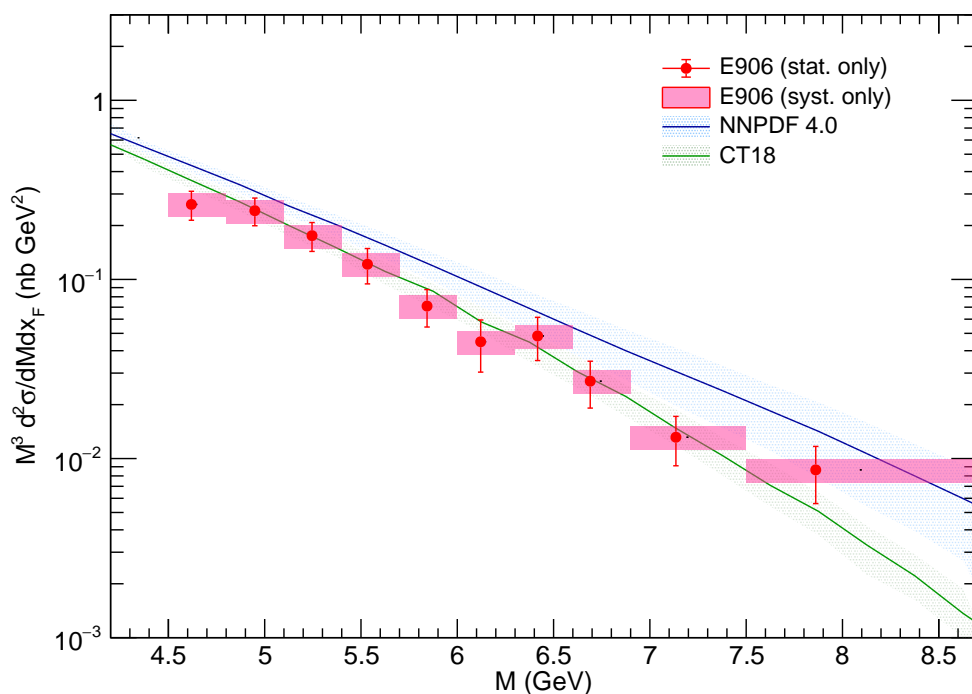


Figure 43: Differential cross-section for x_F bin $0.50 \leq x_F < 0.55$.

Double differential Cross-Section for $0.55 \leq x_F < 0.60$

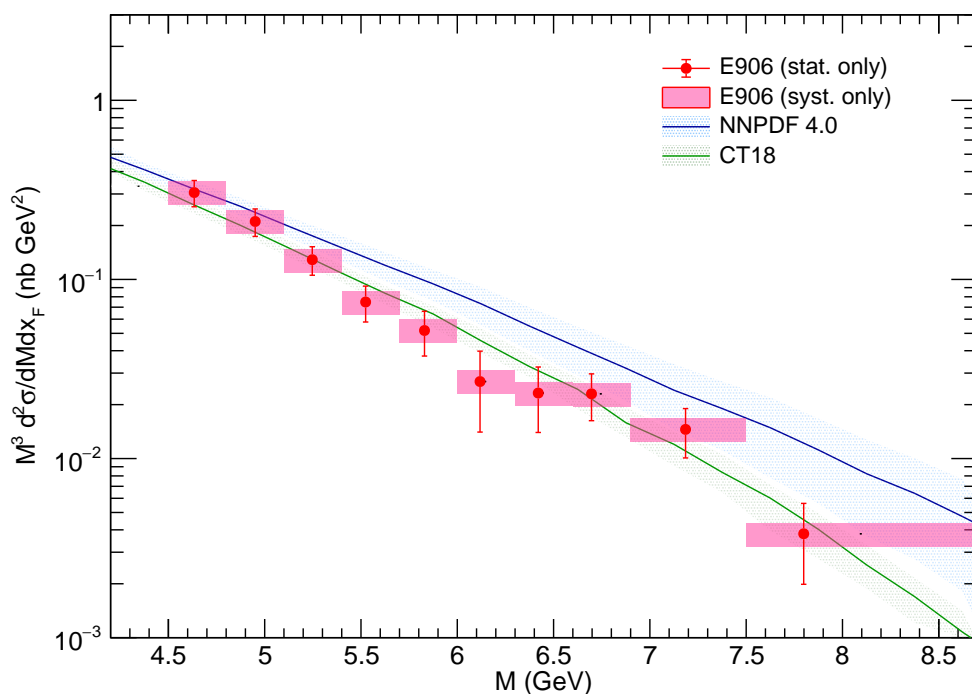


Figure 44: Differential cross-section for x_F bin $0.55 \leq x_F < 0.60$.

Double differential Cross-Section for $0.60 \leq x_F < 0.65$

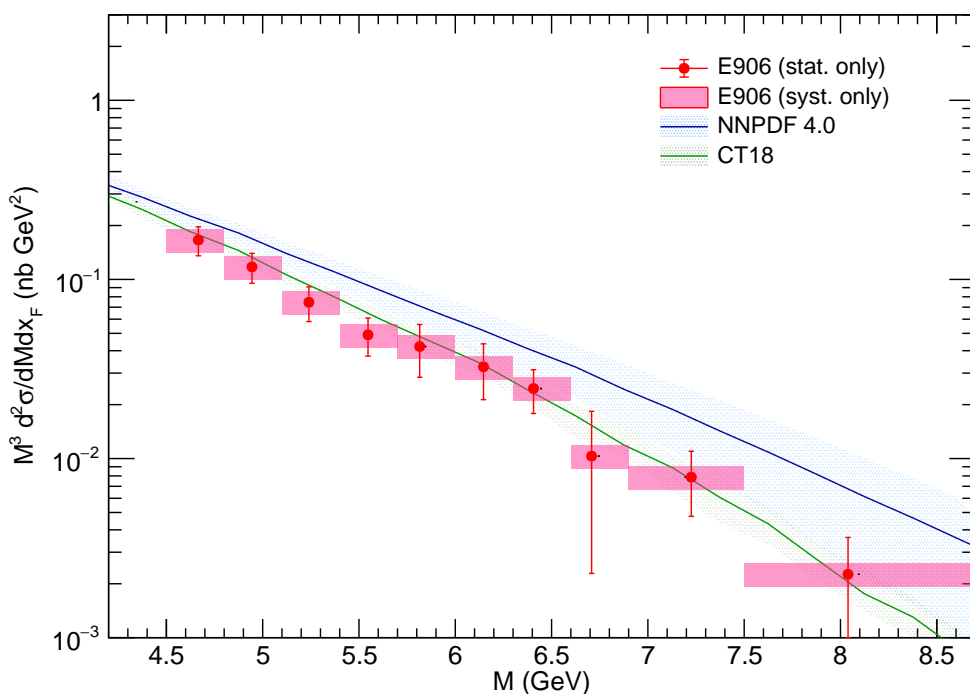


Figure 45: Differential cross-section for x_F bin $0.60 \leq x_F < 0.65$.

Double differential Cross-Section for $0.65 \leq x_F < 0.70$

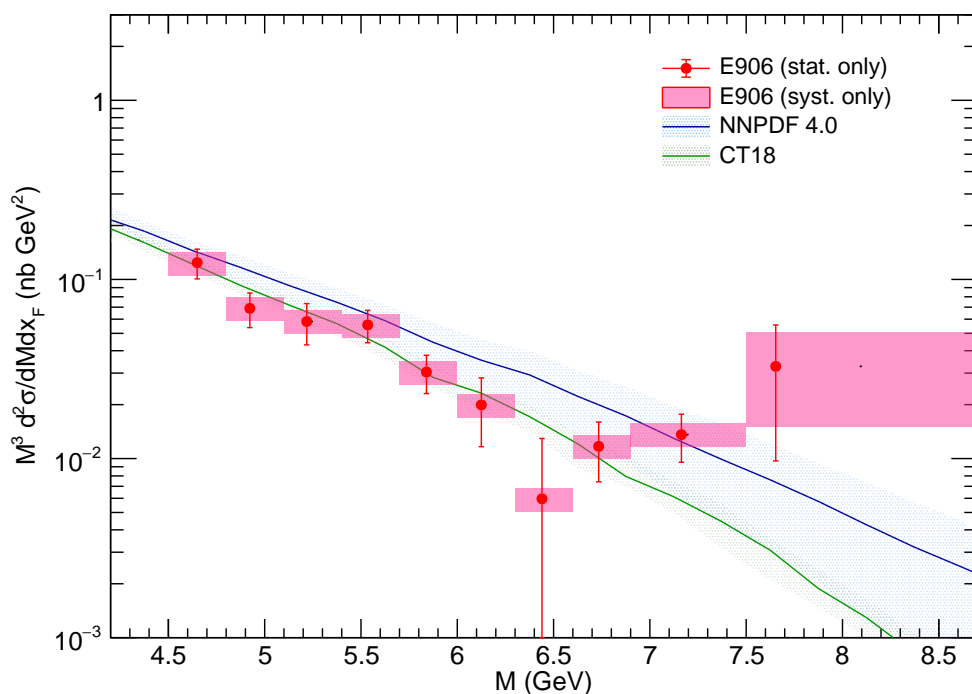


Figure 46: Differential cross-section for x_F bin $0.65 \leq x_F < 0.70$.

Double differential Cross-Section for $0.70 \leq x_F < 0.75$

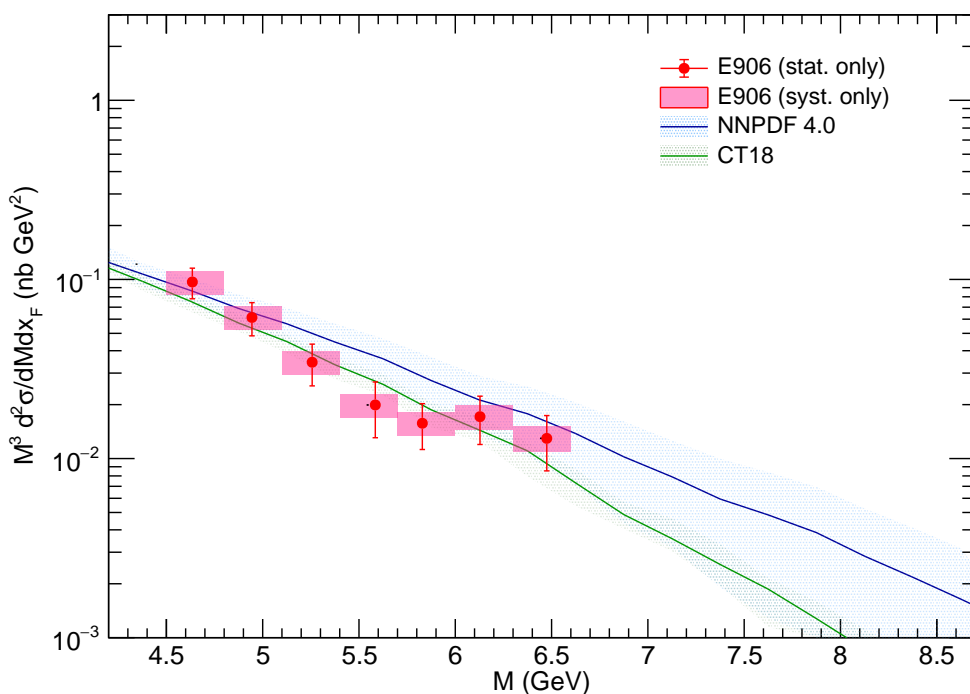


Figure 47: Differential cross-section for x_F bin $0.70 \leq x_F < 0.75$.

Double differential Cross-Section for $0.75 \leq x_F < 0.80$

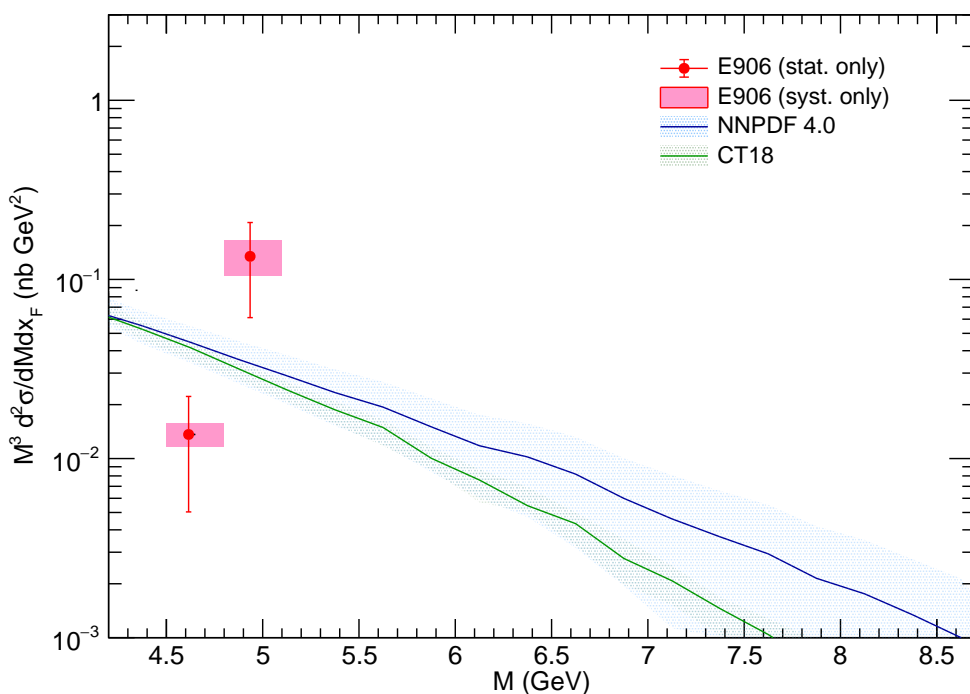


Figure 48: Differential cross-section for x_F bin $0.75 \leq x_F < 0.80$.

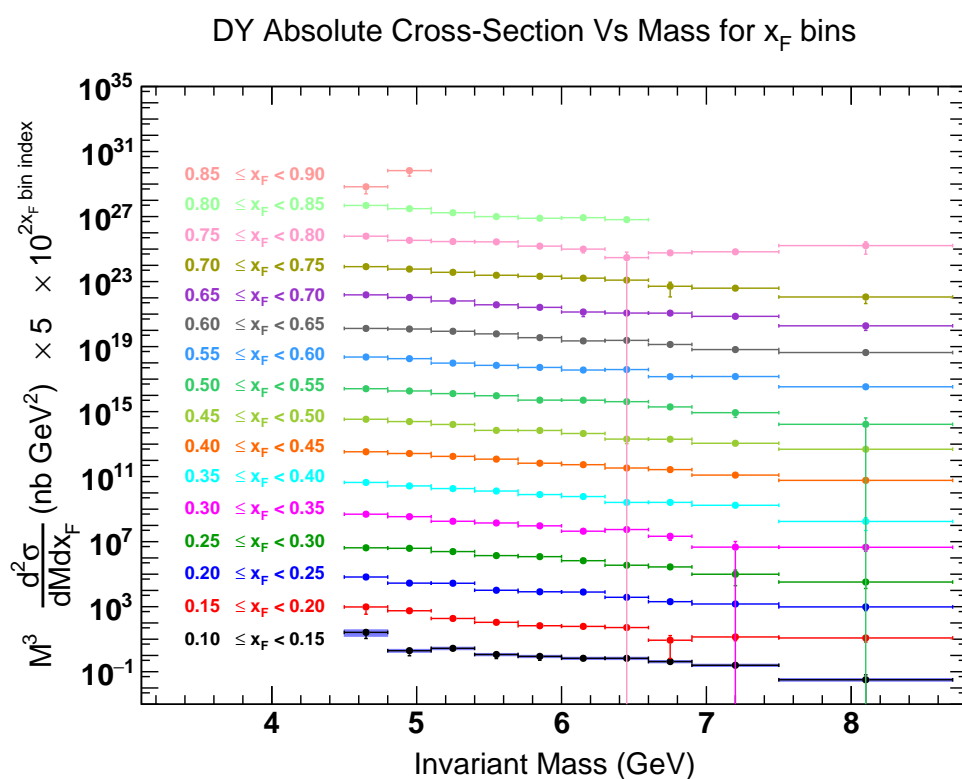


Figure 49: Summary of double differential cross-section measurements

276 **6 Discussion and Conclusion**

277 This analysis presents the first measurement of the absolute Drell-Yan cross-section from the
278 Fermilab SeaQuest experiment for pp collisions at 120 GeV. The preliminary results show reasonable
279 agreement with theoretical predictions from NLO QCD using modern PDF sets, although
280 some tension may be apparent in certain kinematic regions. These data, particularly at high
281 x_F , provide valuable new constraints for global PDF fits.

282 The calculation of the reconstruction efficiency correction (Section 3.2) highlights a key challenge
283 of the analysis. In kinematic bins with low statistics, both in the data and the MC samples,
284 the determination of the efficiency can be unreliable. In some cases, statistical fluctuations lead
285 to calculated efficiencies greater than one or zero, and these bins must be excluded from the
286 final result. Future analyses will benefit from MC samples with higher statistics to mitigate this
287 issue.

288 In conclusion, we have developed a comprehensive framework for the measurement of the
289 absolute Drell-Yan cross-section. The results presented here demonstrate the capability of the
290 SeaQuest experiment to probe the antiquark structure of the nucleon in the large- x domain. The
291 final results from this analysis will provide crucial input for resolving long-standing questions
292 about the non-perturbative structure of the proton.

293 **7 Acknowledgements**

294 The authors wish to express their gratitude to **Kenichi Nakano (University of Virginia)** and
295 **Ching Him Leung (Jefferson Laboratory)** for insightful discussions and valuable feedback.
296 We also thank **Shivangi Prasad (University of Illinois Urbana-Champaign)** and **Harsha
297 Kaluarachchi (New Mexico State University)** for their helpful conversations and support
298 throughout this work.

299 **A Appendix: Event Selection Criteria**

300 The analysis relies on a standard set of selection criteria ("cuts") to identify high-quality dimuon
301 events. These are defined for the positive track (μ^+), negative track (μ^-), and the combined
302 dimuon vertex. The cuts are implemented as TCut objects in the ROOT analysis framework.
303 The parameter `beamOffset` accounts for run-dependent shifts in the beam position.

304 **A.1 Positive Track Cuts (chuckCutsPositive_2111v42)**

```
305 chisq1_target < 15 && pz1_st1 > 9 && pz1_st1 < 75 && nHits1 > 13  
306 && x1_t*x1_t + (y1_t-beamOffset)*(y1_t-beamOffset) < 320  
307 && x1_d*x1_d + (y1_d-beamOffset)*(y1_d-beamOffset) < 1100  
308 && x1_d*x1_d + (y1_d-beamOffset)*(y1_d-beamOffset) > 16  
309 && chisq1_target < 1.5*chisq1_upstream && chisq1_target < 1.5*chisq1_dump  
310 && z1_v < -5 && z1_v > -320 && chisq1/(nHits1-5) < 12  
311 && y1_st1/y1_st3 < 1 && abs(abs(px1_st1-px1_st3)-0.416) < 0.008  
312 && abs(py1_st1-py1_st3) < 0.008 && abs(pz1_st1-pz1_st3) < 0.08  
313 && y1_st1*y1_st3 > 0 && abs(py1_st1)>0.02
```

314 **A.2 Negative Track Cuts (chuckCutsNegative_2111v42)**

```
315 chisq2_target < 15 && pz2_st1 > 9 && pz2_st1 < 75 && nHits2 > 13  
316 && x2_t*x2_t + (y2_t-beamOffset)*(y2_t-beamOffset) < 320  
317 && x2_d*x2_d + (y2_d-beamOffset)*(y2_d-beamOffset) < 1100  
318 && x2_d*x2_d + (y2_d-beamOffset)*(y2_d-beamOffset) > 16  
319 && chisq2_target < 1.5*chisq2_upstream && chisq2_target < 1.5*chisq2_dump  
320 && z2_v < -5 && z2_v > -320 && chisq2/(nHits2-5) < 12  
321 && y2_st1/y2_st3 < 1 && abs(abs(px2_st1-px2_st3)-0.416) < 0.008  
322 && abs(py2_st1-py2_st3) < 0.008 && abs(pz2_st1-pz2_st3) < 0.08  
323 && y2_st1*y2_st3 > 0 && abs(py2_st1)>0.02
```

324 **A.3 Dimuon Cuts (chuckCutsDimuon_2111v42)**

```
325 abs(dx) < 0.25 && abs(dy-beamOffset) < 0.22 && dz > -280 && dz < -5  
326 && abs(dpx) < 1.8 && abs(dpy) < 2 && dpx*dpx + dpy*dpy < 5 && dpz > 38  
327 && dpz < 116 && dx*dx + (dy-beamOffset)*(dy-beamOffset) < 0.06  
328 && abs(trackSeparation) < 270 && chisq_dimuon < 18  
329 && abs(chisq1_target + chisq2_target - chisq_dimuon) < 2  
330 && y1_st3*y2_st3 < 0 && nHits1 + nHits2 > 29 && nHits1St1 + nHits2St1 > 8  
331 && abs(x1_st1+x2_st1) < 42
```

332 **A.4 Physics and Occupancy Cuts**

```
333 // physicsCuts_2111v42  
334 mass > 4.2 && xF > 0 && xF < 0.8 && pt < 5 && pt > 0.1  
335 && abs(pz1_st1-pz2_st1) < 50 && abs(px1_st1-px2_st1) < 3.5  
336 && abs(py1_st1-py2_st1) < 3.5 && pz1_st1 > 15 && pz2_st1 > 15  
337 && pz1_st1 < 75 && pz2_st1 < 75  
338  
339 // occCuts_2111v42  
340 D1 < 150 && D2 < 150 && D3 < 150 && D4 < 150
```

³⁴¹ **B Appendix: Table of Systematic Errors**

Table 2: Detailed Systematic Error calculation for Bins in x_F and Mass

x_F Bin	Mass Bin (GeV)	Trigger Eff.	Acceptance	k-Tracker Eff.	Total Syst.
[0.00 - 0.05)	[4.50 - 4.80)	0.779025	1.873238	0.946767	2.238809
[0.00 - 0.05)	[4.80 - 5.10)	0.058272	0.052304	0.009351	0.078860
[0.00 - 0.05)	[5.10 - 5.40)	0.081048	0.047749	0.018181	0.095809
[0.00 - 0.05)	[5.40 - 5.70)	0.033849	0.013951	0.004059	0.036835
[0.00 - 0.05)	[5.70 - 6.00)	0.025896	0.009169	0.005236	0.027966
[0.00 - 0.05)	[6.00 - 6.30)	0.019771	0.006552	0.003990	0.021207
[0.00 - 0.05)	[6.30 - 6.60)	0.019741	0.006295	0.007003	0.021872
[0.00 - 0.05)	[6.60 - 6.90)	0.012449	0.004049	0.002978	0.013425
[0.00 - 0.05)	[6.90 - 7.50)	0.007375	0.001898	0.002170	0.007919
[0.00 - 0.05)	[7.50 - 8.70)	0.000946	0.000252	0.000628	0.001163
[0.05 - 0.10)	[4.50 - 4.80)	0.284881	0.378813	0.155516	0.498841
[0.05 - 0.10)	[4.80 - 5.10)	0.166470	0.128867	0.041569	0.214586
[0.05 - 0.10)	[5.10 - 5.40)	0.055664	0.025882	0.005169	0.061605
[0.05 - 0.10)	[5.40 - 5.70)	0.032285	0.011302	0.003966	0.034436
[0.05 - 0.10)	[5.70 - 6.00)	0.019937	0.006339	0.002229	0.021039
[0.05 - 0.10)	[6.00 - 6.30)	0.018107	0.005156	0.001957	0.018928
[0.05 - 0.10)	[6.30 - 6.60)	0.015415	0.004246	0.003557	0.016380
[0.05 - 0.10)	[6.60 - 6.90)	0.002562	0.000686	0.001166	0.002897
[0.05 - 0.10)	[6.90 - 7.50)	0.004064	0.000910	0.001134	0.004316
[0.05 - 0.10)	[7.50 - 8.70)	0.003523	0.000764	0.001074	0.003762
[0.10 - 0.15)	[4.50 - 4.80)	0.198459	0.182806	0.040656	0.272868
[0.10 - 0.15)	[4.80 - 5.10)	0.083380	0.040798	0.013031	0.093736
[0.10 - 0.15)	[5.10 - 5.40)	0.081948	0.031238	0.010558	0.088333
[0.10 - 0.15)	[5.40 - 5.70)	0.030329	0.009540	0.002815	0.031918
[0.10 - 0.15)	[5.70 - 6.00)	0.024458	0.006894	0.002083	0.025497
[0.10 - 0.15)	[6.00 - 6.30)	0.023572	0.006173	0.002268	0.024472
[0.10 - 0.15)	[6.30 - 6.60)	0.011184	0.002813	0.001083	0.011583
[0.10 - 0.15)	[6.60 - 6.90)	0.006021	0.001560	0.001047	0.006307
[0.10 - 0.15)	[6.90 - 7.50)	0.004337	0.000867	0.000718	0.004481
[0.10 - 0.15)	[7.50 - 8.70)	0.002871	0.000555	0.000388	0.002950
[0.15 - 0.20)	[4.50 - 4.80)	0.124062	0.075232	0.015770	0.145945
[0.15 - 0.20)	[4.80 - 5.10)	0.115363	0.046469	0.012767	0.125024
[0.15 - 0.20)	[5.10 - 5.40)	0.072817	0.024387	0.004930	0.076950
[0.15 - 0.20)	[5.40 - 5.70)	0.041137	0.011396	0.003480	0.042828
[0.15 - 0.20)	[5.70 - 6.00)	0.035444	0.009302	0.002872	0.036756
[0.15 - 0.20)	[6.00 - 6.30)	0.020001	0.004856	0.001682	0.020651
[0.15 - 0.20)	[6.30 - 6.60)	0.010531	0.002410	0.000921	0.010843
[0.15 - 0.20)	[6.60 - 6.90)	0.008260	0.001887	0.001449	0.008596
[0.15 - 0.20)	[6.90 - 7.50)	0.002937	0.000541	0.000443	0.003019
[0.15 - 0.20)	[7.50 - 8.70)	0.000973	0.000170	0.000400	0.001065
[0.20 - 0.25)	[4.20 - 4.50)	0.166120	0.120909	0.026450	0.207158
[0.20 - 0.25)	[4.50 - 4.80)	0.145103	0.071032	0.012123	0.162010
[0.20 - 0.25)	[4.80 - 5.10)	0.102147	0.034999	0.005624	0.108123
[0.20 - 0.25)	[5.10 - 5.40)	0.053289	0.015003	0.002962	0.055440
[0.20 - 0.25)	[5.40 - 5.70)	0.041865	0.010845	0.002727	0.043332

Cont'd on next page

Table 2: (Continued)

x_F Bin	Mass Bin (GeV)	Trigger Eff.	Acceptance	k-Tracker Eff.	Total Syst.
[0.20 - 0.25)	[5.70 - 6.00)	0.027889	0.006527	0.001469	0.028680
[0.20 - 0.25)	[6.00 - 6.30)	0.013039	0.002957	0.001025	0.013410
[0.20 - 0.25)	[6.30 - 6.60)	0.016485	0.003541	0.001461	0.016924
[0.20 - 0.25)	[6.60 - 6.90)	0.006353	0.001394	0.000605	0.006533
[0.20 - 0.25)	[6.90 - 7.50)	0.001365	0.000229	0.000204	0.001398
[0.20 - 0.25)	[7.50 - 8.70)	0.001336	0.000211	0.000136	0.001359
[0.25 - 0.30)	[4.20 - 4.50)	0.141343	0.072939	0.010257	0.159384
[0.25 - 0.30)	[4.50 - 4.80)	0.130167	0.051529	0.006463	0.140145
[0.25 - 0.30)	[4.80 - 5.10)	0.079605	0.023998	0.003471	0.083216
[0.25 - 0.30)	[5.10 - 5.40)	0.054612	0.014272	0.002683	0.056510
[0.25 - 0.30)	[5.40 - 5.70)	0.038571	0.009218	0.001867	0.039701
[0.25 - 0.30)	[5.70 - 6.00)	0.023376	0.005079	0.001591	0.023974
[0.25 - 0.30)	[6.00 - 6.30)	0.017654	0.003770	0.001225	0.018093
[0.25 - 0.30)	[6.30 - 6.60)	0.007693	0.001519	0.000560	0.007862
[0.25 - 0.30)	[6.60 - 6.90)	0.007726	0.001536	0.001007	0.007941
[0.25 - 0.30)	[6.90 - 7.50)	0.005124	0.000778	0.000489	0.005206
[0.25 - 0.30)	[7.50 - 8.70)	0.000519	0.000076	0.000209	0.000565
[0.30 - 0.35)	[4.20 - 4.50)	0.143223	0.062852	0.006469	0.156541
[0.30 - 0.35)	[4.50 - 4.80)	0.100283	0.033699	0.003193	0.105842
[0.30 - 0.35)	[4.80 - 5.10)	0.078522	0.020901	0.002863	0.081307
[0.30 - 0.35)	[5.10 - 5.40)	0.052272	0.012726	0.001692	0.053826
[0.30 - 0.35)	[5.40 - 5.70)	0.035353	0.007742	0.001569	0.036225
[0.30 - 0.35)	[5.70 - 6.00)	0.019840	0.004222	0.001174	0.020318
[0.30 - 0.35)	[6.00 - 6.30)	0.016108	0.003287	0.001254	0.016488
[0.30 - 0.35)	[6.30 - 6.60)	0.010060	0.002023	0.000634	0.010281
[0.30 - 0.35)	[6.60 - 6.90)	0.008018	0.001569	0.000793	0.008208
[0.30 - 0.35)	[6.90 - 7.50)	0.003694	0.000533	0.000421	0.003756
[0.30 - 0.35)	[7.50 - 8.70)	0.001747	0.000242	0.000186	0.001773
[0.35 - 0.40)	[4.20 - 4.50)	0.106457	0.037922	0.003043	0.113051
[0.35 - 0.40)	[4.50 - 4.80)	0.100531	0.029480	0.003146	0.104811
[0.35 - 0.40)	[4.80 - 5.10)	0.072502	0.018895	0.002326	0.074960
[0.35 - 0.40)	[5.10 - 5.40)	0.048131	0.010864	0.001538	0.049365
[0.35 - 0.40)	[5.40 - 5.70)	0.020800	0.004392	0.000837	0.021275
[0.35 - 0.40)	[5.70 - 6.00)	0.020491	0.004143	0.000980	0.020928
[0.35 - 0.40)	[6.00 - 6.30)	0.013363	0.002624	0.000720	0.013637
[0.35 - 0.40)	[6.30 - 6.60)	0.006047	0.001135	0.000396	0.006165
[0.35 - 0.40)	[6.60 - 6.90)	0.005933	0.001107	0.000667	0.006072
[0.35 - 0.40)	[6.90 - 7.50)	0.003348	0.000459	0.000269	0.003390
[0.35 - 0.40)	[7.50 - 8.70)	0.001436	0.000183	0.000247	0.001469
[0.40 - 0.45)	[4.20 - 4.50)	0.099323	0.033040	0.002941	0.104716
[0.40 - 0.45)	[4.50 - 4.80)	0.075954	0.020641	0.002128	0.078738
[0.40 - 0.45)	[4.80 - 5.10)	0.055286	0.012835	0.001577	0.056778
[0.40 - 0.45)	[5.10 - 5.40)	0.038052	0.008469	0.001399	0.039008
[0.40 - 0.45)	[5.40 - 5.70)	0.028172	0.005715	0.000987	0.028763
[0.40 - 0.45)	[5.70 - 6.00)	0.015105	0.002920	0.000688	0.015400
[0.40 - 0.45)	[6.00 - 6.30)	0.014939	0.002774	0.000734	0.015213
[0.40 - 0.45)	[6.30 - 6.60)	0.012131	0.002291	0.000940	0.012381
[0.40 - 0.45)	[6.60 - 6.90)	0.005773	0.001030	0.000398	0.005877

Cont'd on next page

Table 2: (Continued)

x_F Bin	Mass Bin (GeV)	Trigger Eff.	Acceptance	k-Tracker Eff.	Total Syst.
[0.40 - 0.45)	[6.90 - 7.50)	0.002557	0.000353	0.000241	0.002593
[0.40 - 0.45)	[7.50 - 8.70)	0.000491	0.000061	0.000040	0.000496
[0.45 - 0.50)	[4.20 - 4.50)	0.078635	0.023049	0.002059	0.081969
[0.45 - 0.50)	[4.50 - 4.80)	0.067541	0.017403	0.001706	0.069768
[0.45 - 0.50)	[4.80 - 5.10)	0.053760	0.012443	0.001688	0.055207
[0.45 - 0.50)	[5.10 - 5.40)	0.028610	0.005965	0.001078	0.029245
[0.45 - 0.50)	[5.40 - 5.70)	0.020809	0.004172	0.000821	0.021239
[0.45 - 0.50)	[5.70 - 6.00)	0.015482	0.002928	0.000738	0.015774
[0.45 - 0.50)	[6.00 - 6.30)	0.010741	0.001999	0.000674	0.010946
[0.45 - 0.50)	[6.30 - 6.60)	0.011477	0.002063	0.000873	0.011694
[0.45 - 0.50)	[6.60 - 6.90)	0.004200	0.000754	0.000554	0.004303
[0.45 - 0.50)	[6.90 - 7.50)	0.004274	0.000573	0.000231	0.004319
[0.45 - 0.50)	[7.50 - 8.70)	0.000999	0.000121	0.000098	0.001011
[0.50 - 0.55)	[4.20 - 4.50)	0.091374	0.025832	0.003131	0.095007
[0.50 - 0.55)	[4.50 - 4.80)	0.038797	0.009116	0.001196	0.039872
[0.50 - 0.55)	[4.80 - 5.10)	0.035794	0.007792	0.001215	0.036652
[0.50 - 0.55)	[5.10 - 5.40)	0.025971	0.005366	0.000845	0.026533
[0.50 - 0.55)	[5.40 - 5.70)	0.017990	0.003538	0.000653	0.018346
[0.50 - 0.55)	[5.70 - 6.00)	0.010504	0.001914	0.000561	0.010691
[0.50 - 0.55)	[6.00 - 6.30)	0.006640	0.001204	0.000587	0.006773
[0.50 - 0.55)	[6.30 - 6.60)	0.007154	0.001324	0.000432	0.007288
[0.50 - 0.55)	[6.60 - 6.90)	0.004000	0.000731	0.000474	0.004094
[0.50 - 0.55)	[6.90 - 7.50)	0.001946	0.000254	0.000172	0.001970
[0.50 - 0.55)	[7.50 - 8.70)	0.001279	0.000149	0.000130	0.001294
[0.55 - 0.60)	[4.20 - 4.50)	0.049012	0.013093	0.001356	0.050748
[0.55 - 0.60)	[4.50 - 4.80)	0.045199	0.010565	0.001338	0.046436
[0.55 - 0.60)	[4.80 - 5.10)	0.031162	0.006899	0.001131	0.031937
[0.55 - 0.60)	[5.10 - 5.40)	0.019065	0.003784	0.000735	0.019451
[0.55 - 0.60)	[5.40 - 5.70)	0.011066	0.002143	0.000544	0.011285
[0.55 - 0.60)	[5.70 - 6.00)	0.007673	0.001386	0.000453	0.007810
[0.55 - 0.60)	[6.00 - 6.30)	0.003981	0.000698	0.000228	0.004048
[0.55 - 0.60)	[6.30 - 6.60)	0.003434	0.000599	0.000281	0.003497
[0.55 - 0.60)	[6.60 - 6.90)	0.003400	0.000586	0.000348	0.003468
[0.55 - 0.60)	[6.90 - 7.50)	0.002152	0.000282	0.000214	0.002181
[0.55 - 0.60)	[7.50 - 8.70)	0.000563	0.000065	0.000074	0.000571
[0.60 - 0.65)	[4.20 - 4.50)	0.040173	0.010809	0.001161	0.041617
[0.60 - 0.65)	[4.50 - 4.80)	0.024563	0.005615	0.000889	0.025212
[0.60 - 0.65)	[4.80 - 5.10)	0.017374	0.003688	0.000696	0.017775
[0.60 - 0.65)	[5.10 - 5.40)	0.011024	0.002225	0.000393	0.011254
[0.60 - 0.65)	[5.40 - 5.70)	0.007261	0.001362	0.000352	0.007396
[0.60 - 0.65)	[5.70 - 6.00)	0.006245	0.001139	0.000455	0.006364
[0.60 - 0.65)	[6.00 - 6.30)	0.004809	0.000872	0.000317	0.004898
[0.60 - 0.65)	[6.30 - 6.60)	0.003639	0.000641	0.000299	0.003707
[0.60 - 0.65)	[6.60 - 6.90)	0.001526	0.000273	0.000098	0.001554
[0.60 - 0.65)	[6.90 - 7.50)	0.001164	0.000147	0.000132	0.001181
[0.60 - 0.65)	[7.50 - 8.70)	0.000334	0.000038	0.000062	0.000342
[0.65 - 0.70)	[4.20 - 4.50)	0.024537	0.006446	0.000859	0.025384
[0.65 - 0.70)	[4.50 - 4.80)	0.018367	0.004297	0.000734	0.018877

Cont'd on next page

Table 2: (Continued)

x_F Bin	Mass Bin (GeV)	Trigger Eff.	Acceptance	k-Tracker Eff.	Total Syst.
[0.65 - 0.70)	[4.80 - 5.10)	0.010196	0.002166	0.000407	0.010432
[0.65 - 0.70)	[5.10 - 5.40)	0.008613	0.001753	0.000384	0.008798
[0.65 - 0.70)	[5.40 - 5.70)	0.008247	0.001614	0.000508	0.008419
[0.65 - 0.70)	[5.70 - 6.00)	0.004495	0.000836	0.000349	0.004586
[0.65 - 0.70)	[6.00 - 6.30)	0.002948	0.000528	0.000258	0.003006
[0.65 - 0.70)	[6.30 - 6.60)	0.000881	0.000156	0.000132	0.000905
[0.65 - 0.70)	[6.60 - 6.90)	0.001730	0.000297	0.000210	0.001768
[0.65 - 0.70)	[6.90 - 7.50)	0.002013	0.000264	0.000280	0.002049
[0.65 - 0.70)	[7.50 - 8.70)	0.004838	0.000546	0.017062	0.017743
[0.70 - 0.75)	[4.20 - 4.50)	0.018003	0.004826	0.000928	0.018662
[0.70 - 0.75)	[4.50 - 4.80)	0.014316	0.003395	0.000682	0.014729
[0.70 - 0.75)	[4.80 - 5.10)	0.009071	0.001949	0.000519	0.009293
[0.70 - 0.75)	[5.10 - 5.40)	0.005102	0.001052	0.000465	0.005230
[0.70 - 0.75)	[5.40 - 5.70)	0.002947	0.000565	0.000295	0.003015
[0.70 - 0.75)	[5.70 - 6.00)	0.002329	0.000432	0.000339	0.002393
[0.70 - 0.75)	[6.00 - 6.30)	0.002535	0.000456	0.000594	0.002644
[0.70 - 0.75)	[6.30 - 6.60)	0.001917	0.000343	0.000707	0.002072
[0.75 - 0.80)	[4.20 - 4.50)	0.012861	0.003466	0.001181	0.013372
[0.75 - 0.80)	[4.50 - 4.80)	0.002016	0.000478	0.000132	0.002076
[0.75 - 0.80)	[4.80 - 5.10)	0.019900	0.004388	0.022716	0.030517

³⁴² **C Appendix: Table of $M^3 \frac{d^2\sigma}{dMdx_F}$ Cross-Section Values**

Table 3: Detailed cross-section calculation for Bins in x_F and Mass

x_F Bin	Mass Bin (GeV)	Bin Center (GeV)	Bin Average (GeV)	Cross-Section (nb-GeV 2)	stat. error (nb-GeV 2)	syst. error (nb-GeV 2)
[0.00, 0.05)	[4.5, 4.8)	4.650	4.740	5.266×10^0	3.059×10^0	2.239×10^0
[0.00, 0.05)	[4.8, 5.1)	4.950	5.006	3.939×10^{-1}	2.024×10^{-1}	7.886×10^{-2}
[0.00, 0.05)	[5.1, 5.4)	5.250	5.250	5.479×10^{-1}	1.864×10^{-1}	9.581×10^{-2}
[0.00, 0.05)	[5.4, 5.7)	5.550	5.512	2.288×10^{-1}	9.988×10^{-2}	3.684×10^{-2}
[0.00, 0.05)	[5.7, 6.0)	5.850	5.828	1.751×10^{-1}	7.393×10^{-2}	2.797×10^{-2}
[0.00, 0.05)	[6.0, 6.3)	6.150	6.178	1.336×10^{-1}	4.716×10^{-2}	2.121×10^{-2}
[0.00, 0.05)	[6.3, 6.6)	6.450	6.432	1.334×10^{-1}	4.608×10^{-2}	2.187×10^{-2}
[0.00, 0.05)	[6.6, 6.9)	6.750	6.749	8.415×10^{-2}	2.777×10^{-2}	1.343×10^{-2}
[0.00, 0.05)	[6.9, 7.5)	7.200	7.171	4.985×10^{-2}	1.846×10^{-2}	7.919×10^{-3}
[0.00, 0.05)	[7.5, 8.7)	8.100	7.914	6.397×10^{-3}	6.502×10^{-3}	1.163×10^{-3}
[0.05, 0.10)	[4.5, 4.8)	4.650	4.627	1.926×10^0	1.237×10^0	4.988×10^{-1}
[0.05, 0.10)	[4.8, 5.1)	4.950	4.944	1.125×10^0	3.799×10^{-1}	2.146×10^{-1}
[0.05, 0.10)	[5.1, 5.4)	5.250	5.251	3.763×10^{-1}	1.199×10^{-1}	6.160×10^{-2}
[0.05, 0.10)	[5.4, 5.7)	5.550	5.526	2.182×10^{-1}	6.716×10^{-2}	3.444×10^{-2}
[0.05, 0.10)	[5.7, 6.0)	5.850	5.865	1.348×10^{-1}	5.227×10^{-2}	2.104×10^{-2}
[0.05, 0.10)	[6.0, 6.3)	6.150	6.086	1.224×10^{-1}	4.329×10^{-2}	1.893×10^{-2}
[0.05, 0.10)	[6.3, 6.6)	6.450	6.408	1.042×10^{-1}	3.840×10^{-2}	1.638×10^{-2}
[0.05, 0.10)	[6.6, 6.9)	6.750	6.725	1.732×10^{-2}	1.601×10^{-2}	2.897×10^{-3}
[0.05, 0.10)	[6.9, 7.5)	7.200	7.125	2.747×10^{-2}	1.126×10^{-2}	4.316×10^{-3}
[0.05, 0.10)	[7.5, 8.7)	8.100	7.731	2.382×10^{-2}	1.045×10^{-2}	3.762×10^{-3}
[0.10, 0.15)	[4.5, 4.8)	4.650	4.685	1.342×10^0	4.340×10^{-1}	2.729×10^{-1}
[0.10, 0.15)	[4.8, 5.1)	4.950	4.956	5.636×10^{-1}	1.621×10^{-1}	9.374×10^{-2}
[0.10, 0.15)	[5.1, 5.4)	5.250	5.231	5.540×10^{-1}	1.229×10^{-1}	8.833×10^{-2}
[0.10, 0.15)	[5.4, 5.7)	5.550	5.500	2.050×10^{-1}	6.525×10^{-2}	3.192×10^{-2}
[0.10, 0.15)	[5.7, 6.0)	5.850	5.816	1.653×10^{-1}	5.186×10^{-2}	2.550×10^{-2}
[0.10, 0.15)	[6.0, 6.3)	6.150	6.139	1.593×10^{-1}	3.486×10^{-2}	2.447×10^{-2}
[0.10, 0.15)	[6.3, 6.6)	6.450	6.440	7.560×10^{-2}	2.478×10^{-2}	1.158×10^{-2}
[0.10, 0.15)	[6.6, 6.9)	6.750	6.746	4.070×10^{-2}	1.434×10^{-2}	6.307×10^{-3}
[0.10, 0.15)	[6.9, 7.5)	7.200	7.114	2.932×10^{-2}	1.115×10^{-2}	4.481×10^{-3}
[0.10, 0.15)	[7.5, 8.7)	8.100	7.838	1.941×10^{-2}	7.930×10^{-3}	2.950×10^{-3}
[0.15, 0.20)	[4.5, 4.8)	4.650	4.656	8.386×10^{-1}	2.133×10^{-1}	1.459×10^{-1}
[0.15, 0.20)	[4.8, 5.1)	4.950	4.920	7.798×10^{-1}	1.766×10^{-1}	1.250×10^{-1}
[0.15, 0.20)	[5.1, 5.4)	5.250	5.251	4.922×10^{-1}	1.046×10^{-1}	7.695×10^{-2}
[0.15, 0.20)	[5.4, 5.7)	5.550	5.520	2.781×10^{-1}	6.083×10^{-2}	4.283×10^{-2}
[0.15, 0.20)	[5.7, 6.0)	5.850	5.833	2.396×10^{-1}	5.007×10^{-2}	3.676×10^{-2}
[0.15, 0.20)	[6.0, 6.3)	6.150	6.138	1.352×10^{-1}	3.967×10^{-2}	2.065×10^{-2}
[0.15, 0.20)	[6.3, 6.6)	6.450	6.467	7.119×10^{-2}	2.568×10^{-2}	1.084×10^{-2}
[0.15, 0.20)	[6.6, 6.9)	6.750	6.748	5.584×10^{-2}	1.640×10^{-2}	8.596×10^{-3}
[0.15, 0.20)	[6.9, 7.5)	7.200	6.919	1.985×10^{-2}	1.594×10^{-2}	3.019×10^{-3}
[0.15, 0.20)	[7.5, 8.7)	8.100	7.632	6.576×10^{-3}	3.945×10^{-3}	1.065×10^{-3}
[0.20, 0.25)	[4.2, 4.5)	4.350	4.347	1.123×10^0	3.376×10^{-1}	2.072×10^{-1}
[0.20, 0.25)	[4.5, 4.8)	4.650	4.653	9.809×10^{-1}	2.274×10^{-1}	1.620×10^{-1}
[0.20, 0.25)	[4.8, 5.1)	4.950	4.953	6.905×10^{-1}	1.291×10^{-1}	1.081×10^{-1}

Cont'd on next page

Table 3: (Continued)

x_F Bin	Mass Bin (GeV)	Bin Center (GeV)	Bin Average (GeV)	Cross-Section (nb-GeV 2)	stat. error (nb-GeV 2)	syst. error (nb-GeV 2)
[0.20, 0.25)	[5.1, 5.4)	5.250	5.237	3.602×10^{-1}	7.549×10^{-2}	5.544×10^{-2}
[0.20, 0.25)	[5.4, 5.7)	5.550	5.539	2.830×10^{-1}	5.529×10^{-2}	4.333×10^{-2}
[0.20, 0.25)	[5.7, 6.0)	5.850	5.835	1.885×10^{-1}	3.880×10^{-2}	2.868×10^{-2}
[0.20, 0.25)	[6.0, 6.3)	6.150	6.157	8.814×10^{-2}	3.025×10^{-2}	1.341×10^{-2}
[0.20, 0.25)	[6.3, 6.6)	6.450	6.463	1.114×10^{-1}	2.832×10^{-2}	1.692×10^{-2}
[0.20, 0.25)	[6.6, 6.9)	6.750	6.761	4.295×10^{-2}	1.858×10^{-2}	6.533×10^{-3}
[0.20, 0.25)	[6.9, 7.5)	7.200	7.136	9.224×10^{-3}	1.130×10^{-2}	1.398×10^{-3}
[0.20, 0.25)	[7.5, 8.7)	8.100	7.634	9.030×10^{-3}	3.932×10^{-3}	1.359×10^{-3}
[0.25, 0.30)	[4.2, 4.5)	4.350	4.390	9.555×10^{-1}	2.055×10^{-1}	1.594×10^{-1}
[0.25, 0.30)	[4.5, 4.8)	4.650	4.653	8.799×10^{-1}	1.686×10^{-1}	1.401×10^{-1}
[0.25, 0.30)	[4.8, 5.1)	4.950	4.947	5.381×10^{-1}	9.957×10^{-2}	8.322×10^{-2}
[0.25, 0.30)	[5.1, 5.4)	5.250	5.243	3.692×10^{-1}	6.835×10^{-2}	5.651×10^{-2}
[0.25, 0.30)	[5.4, 5.7)	5.550	5.555	2.607×10^{-1}	5.198×10^{-2}	3.970×10^{-2}
[0.25, 0.30)	[5.7, 6.0)	5.850	5.840	1.580×10^{-1}	3.113×10^{-2}	2.397×10^{-2}
[0.25, 0.30)	[6.0, 6.3)	6.150	6.144	1.193×10^{-1}	2.663×10^{-2}	1.809×10^{-2}
[0.25, 0.30)	[6.3, 6.6)	6.450	6.466	5.200×10^{-2}	1.901×10^{-2}	7.862×10^{-3}
[0.25, 0.30)	[6.6, 6.9)	6.750	6.755	5.223×10^{-2}	1.888×10^{-2}	7.941×10^{-3}
[0.25, 0.30)	[6.9, 7.5)	7.200	7.107	3.464×10^{-2}	9.170×10^{-3}	5.206×10^{-3}
[0.25, 0.30)	[7.5, 8.7)	8.100	7.598	3.508×10^{-3}	2.544×10^{-3}	5.647×10^{-4}
[0.30, 0.35)	[4.2, 4.5)	4.350	4.355	9.682×10^{-1}	1.855×10^{-1}	1.565×10^{-1}
[0.30, 0.35)	[4.5, 4.8)	4.650	4.665	6.779×10^{-1}	1.236×10^{-1}	1.058×10^{-1}
[0.30, 0.35)	[4.8, 5.1)	4.950	4.947	5.308×10^{-1}	9.068×10^{-2}	8.131×10^{-2}
[0.30, 0.35)	[5.1, 5.4)	5.250	5.249	3.533×10^{-1}	6.288×10^{-2}	5.383×10^{-2}
[0.30, 0.35)	[5.4, 5.7)	5.550	5.542	2.390×10^{-1}	4.623×10^{-2}	3.623×10^{-2}
[0.30, 0.35)	[5.7, 6.0)	5.850	5.844	1.341×10^{-1}	2.975×10^{-2}	2.032×10^{-2}
[0.30, 0.35)	[6.0, 6.3)	6.150	6.133	1.089×10^{-1}	2.213×10^{-2}	1.649×10^{-2}
[0.30, 0.35)	[6.3, 6.6)	6.450	6.384	6.800×10^{-2}	2.056×10^{-2}	1.028×10^{-2}
[0.30, 0.35)	[6.6, 6.9)	6.750	6.741	5.420×10^{-2}	1.360×10^{-2}	8.208×10^{-3}
[0.30, 0.35)	[6.9, 7.5)	7.200	7.045	2.497×10^{-2}	6.858×10^{-3}	3.756×10^{-3}
[0.30, 0.35)	[7.5, 8.7)	8.100	7.919	1.181×10^{-2}	4.331×10^{-3}	1.773×10^{-3}
[0.35, 0.40)	[4.2, 4.5)	4.350	4.337	7.196×10^{-1}	1.297×10^{-1}	1.131×10^{-1}
[0.35, 0.40)	[4.5, 4.8)	4.650	4.640	6.796×10^{-1}	1.152×10^{-1}	1.048×10^{-1}
[0.35, 0.40)	[4.8, 5.1)	4.950	4.943	4.901×10^{-1}	8.446×10^{-2}	7.496×10^{-2}
[0.35, 0.40)	[5.1, 5.4)	5.250	5.238	3.254×10^{-1}	5.543×10^{-2}	4.937×10^{-2}
[0.35, 0.40)	[5.4, 5.7)	5.550	5.515	1.406×10^{-1}	3.281×10^{-2}	2.127×10^{-2}
[0.35, 0.40)	[5.7, 6.0)	5.850	5.832	1.385×10^{-1}	2.843×10^{-2}	2.093×10^{-2}
[0.35, 0.40)	[6.0, 6.3)	6.150	6.125	9.033×10^{-2}	2.093×10^{-2}	1.364×10^{-2}
[0.35, 0.40)	[6.3, 6.6)	6.450	6.446	4.087×10^{-2}	1.947×10^{-2}	6.165×10^{-3}
[0.35, 0.40)	[6.6, 6.9)	6.750	6.727	4.011×10^{-2}	1.084×10^{-2}	6.072×10^{-3}
[0.35, 0.40)	[6.9, 7.5)	7.200	7.175	2.263×10^{-2}	6.209×10^{-3}	3.390×10^{-3}
[0.35, 0.40)	[7.5, 8.7)	8.100	7.764	9.710×10^{-3}	3.761×10^{-3}	1.469×10^{-3}
[0.40, 0.45)	[4.2, 4.5)	4.350	4.351	6.714×10^{-1}	1.212×10^{-1}	1.047×10^{-1}
[0.40, 0.45)	[4.5, 4.8)	4.650	4.642	5.134×10^{-1}	8.883×10^{-2}	7.874×10^{-2}
[0.40, 0.45)	[4.8, 5.1)	4.950	4.934	3.737×10^{-1}	6.449×10^{-2}	5.678×10^{-2}
[0.40, 0.45)	[5.1, 5.4)	5.250	5.231	2.572×10^{-1}	4.759×10^{-2}	3.901×10^{-2}
[0.40, 0.45)	[5.4, 5.7)	5.550	5.514	1.904×10^{-1}	3.491×10^{-2}	2.876×10^{-2}
[0.40, 0.45)	[5.7, 6.0)	5.850	5.854	1.021×10^{-1}	2.355×10^{-2}	1.540×10^{-2}

Cont'd on next page

Table 3: (Continued)

x_F Bin	Mass Bin (GeV)	Bin Center (GeV)	Bin Average (GeV)	Cross-Section (nb-GeV 2)	stat. error (nb-GeV 2)	syst. error (nb-GeV 2)
[0.40, 0.45)	[6.0, 6.3)	6.150	6.176	1.010×10^{-1}	2.152×10^{-2}	1.521×10^{-2}
[0.40, 0.45)	[6.3, 6.6)	6.450	6.422	8.200×10^{-2}	1.722×10^{-2}	1.238×10^{-2}
[0.40, 0.45)	[6.6, 6.9)	6.750	6.751	3.902×10^{-2}	9.905×10^{-3}	5.877×10^{-3}
[0.40, 0.45)	[6.9, 7.5)	7.200	7.100	1.729×10^{-2}	8.435×10^{-3}	2.593×10^{-3}
[0.40, 0.45)	[7.5, 8.7)	8.100	7.821	3.316×10^{-3}	4.877×10^{-3}	4.960×10^{-4}
[0.45, 0.50)	[4.2, 4.5)	4.350	4.344	5.316×10^{-1}	9.382×10^{-2}	8.197×10^{-2}
[0.45, 0.50)	[4.5, 4.8)	4.650	4.642	4.566×10^{-1}	7.742×10^{-2}	6.977×10^{-2}
[0.45, 0.50)	[4.8, 5.1)	4.950	4.940	3.634×10^{-1}	6.084×10^{-2}	5.521×10^{-2}
[0.45, 0.50)	[5.1, 5.4)	5.250	5.238	1.934×10^{-1}	3.633×10^{-2}	2.925×10^{-2}
[0.45, 0.50)	[5.4, 5.7)	5.550	5.523	1.407×10^{-1}	2.747×10^{-2}	2.124×10^{-2}
[0.45, 0.50)	[5.7, 6.0)	5.850	5.841	1.047×10^{-1}	2.125×10^{-2}	1.577×10^{-2}
[0.45, 0.50)	[6.0, 6.3)	6.150	6.135	7.260×10^{-2}	1.647×10^{-2}	1.095×10^{-2}
[0.45, 0.50)	[6.3, 6.6)	6.450	6.437	7.758×10^{-2}	1.612×10^{-2}	1.169×10^{-2}
[0.45, 0.50)	[6.6, 6.9)	6.750	6.741	2.839×10^{-2}	8.681×10^{-3}	4.303×10^{-3}
[0.45, 0.50)	[6.9, 7.5)	7.200	7.198	2.889×10^{-2}	7.053×10^{-3}	4.319×10^{-3}
[0.45, 0.50)	[7.5, 8.7)	8.100	7.828	6.752×10^{-3}	2.599×10^{-3}	1.011×10^{-3}
[0.50, 0.55)	[4.2, 4.5)	4.350	4.353	6.177×10^{-1}	1.029×10^{-1}	9.501×10^{-2}
[0.50, 0.55)	[4.5, 4.8)	4.650	4.620	2.623×10^{-1}	4.829×10^{-2}	3.987×10^{-2}
[0.50, 0.55)	[4.8, 5.1)	4.950	4.949	2.420×10^{-1}	4.259×10^{-2}	3.665×10^{-2}
[0.50, 0.55)	[5.1, 5.4)	5.250	5.246	1.756×10^{-1}	3.222×10^{-2}	2.653×10^{-2}
[0.50, 0.55)	[5.4, 5.7)	5.550	5.534	1.216×10^{-1}	2.718×10^{-2}	1.835×10^{-2}
[0.50, 0.55)	[5.7, 6.0)	5.850	5.843	7.100×10^{-2}	1.676×10^{-2}	1.069×10^{-2}
[0.50, 0.55)	[6.0, 6.3)	6.150	6.121	4.488×10^{-2}	1.451×10^{-2}	6.773×10^{-3}
[0.50, 0.55)	[6.3, 6.6)	6.450	6.417	4.836×10^{-2}	1.310×10^{-2}	7.288×10^{-3}
[0.50, 0.55)	[6.6, 6.9)	6.750	6.690	2.704×10^{-2}	7.906×10^{-3}	4.094×10^{-3}
[0.50, 0.55)	[6.9, 7.5)	7.200	7.135	1.315×10^{-2}	4.040×10^{-3}	1.970×10^{-3}
[0.50, 0.55)	[7.5, 8.7)	8.100	7.861	8.646×10^{-3}	3.042×10^{-3}	1.294×10^{-3}
[0.55, 0.60)	[4.2, 4.5)	4.350	4.348	3.313×10^{-1}	5.895×10^{-2}	5.075×10^{-2}
[0.55, 0.60)	[4.5, 4.8)	4.650	4.634	3.055×10^{-1}	5.112×10^{-2}	4.644×10^{-2}
[0.55, 0.60)	[4.8, 5.1)	4.950	4.951	2.106×10^{-1}	3.677×10^{-2}	3.194×10^{-2}
[0.55, 0.60)	[5.1, 5.4)	5.250	5.247	1.289×10^{-1}	2.334×10^{-2}	1.945×10^{-2}
[0.55, 0.60)	[5.4, 5.7)	5.550	5.524	7.481×10^{-2}	1.696×10^{-2}	1.129×10^{-2}
[0.55, 0.60)	[5.7, 6.0)	5.850	5.830	5.187×10^{-2}	1.452×10^{-2}	7.810×10^{-3}
[0.55, 0.60)	[6.0, 6.3)	6.150	6.118	2.691×10^{-2}	1.286×10^{-2}	4.048×10^{-3}
[0.55, 0.60)	[6.3, 6.6)	6.450	6.420	2.321×10^{-2}	9.228×10^{-3}	3.497×10^{-3}
[0.55, 0.60)	[6.6, 6.9)	6.750	6.697	2.299×10^{-2}	6.715×10^{-3}	3.468×10^{-3}
[0.55, 0.60)	[6.9, 7.5)	7.200	7.185	1.455×10^{-2}	4.465×10^{-3}	2.181×10^{-3}
[0.55, 0.60)	[7.5, 8.7)	8.100	7.799	3.803×10^{-3}	1.816×10^{-3}	5.711×10^{-4}
[0.60, 0.65)	[4.2, 4.5)	4.350	4.357	2.716×10^{-1}	4.774×10^{-2}	4.162×10^{-2}
[0.60, 0.65)	[4.5, 4.8)	4.650	4.666	1.660×10^{-1}	3.053×10^{-2}	2.521×10^{-2}
[0.60, 0.65)	[4.8, 5.1)	4.950	4.945	1.174×10^{-1}	2.239×10^{-2}	1.777×10^{-2}
[0.60, 0.65)	[5.1, 5.4)	5.250	5.240	7.452×10^{-2}	1.633×10^{-2}	1.125×10^{-2}
[0.60, 0.65)	[5.4, 5.7)	5.550	5.547	4.908×10^{-2}	1.178×10^{-2}	7.396×10^{-3}
[0.60, 0.65)	[5.7, 6.0)	5.850	5.815	4.222×10^{-2}	1.379×10^{-2}	6.364×10^{-3}
[0.60, 0.65)	[6.0, 6.3)	6.150	6.146	3.251×10^{-2}	1.119×10^{-2}	4.898×10^{-3}
[0.60, 0.65)	[6.3, 6.6)	6.450	6.406	2.460×10^{-2}	6.754×10^{-3}	3.707×10^{-3}
[0.60, 0.65)	[6.6, 6.9)	6.750	6.708	1.032×10^{-2}	8.032×10^{-3}	1.554×10^{-3}

Cont'd on next page

Table 3: (Continued)

x_F Bin	Mass Bin (GeV)	Bin Center (GeV)	Bin Average (GeV)	Cross-Section (nb-GeV 2)	stat. error (nb-GeV 2)	syst. error (nb-GeV 2)
[0.60, 0.65)	[6.9, 7.5)	7.200	7.225	7.869×10^{-3}	3.112×10^{-3}	1.181×10^{-3}
[0.60, 0.65)	[7.5, 8.7)	8.100	8.039	2.259×10^{-3}	1.368×10^{-3}	3.421×10^{-4}
[0.65, 0.70)	[4.2, 4.5)	4.350	4.324	1.659×10^{-1}	3.011×10^{-2}	2.538×10^{-2}
[0.65, 0.70)	[4.5, 4.8)	4.650	4.650	1.242×10^{-1}	2.342×10^{-2}	1.888×10^{-2}
[0.65, 0.70)	[4.8, 5.1)	4.950	4.923	6.892×10^{-2}	1.510×10^{-2}	1.043×10^{-2}
[0.65, 0.70)	[5.1, 5.4)	5.250	5.219	5.822×10^{-2}	1.511×10^{-2}	8.798×10^{-3}
[0.65, 0.70)	[5.4, 5.7)	5.550	5.535	5.575×10^{-2}	1.145×10^{-2}	8.419×10^{-3}
[0.65, 0.70)	[5.7, 6.0)	5.850	5.840	3.039×10^{-2}	7.325×10^{-3}	4.586×10^{-3}
[0.65, 0.70)	[6.0, 6.3)	6.150	6.125	1.993×10^{-2}	8.279×10^{-3}	3.006×10^{-3}
[0.65, 0.70)	[6.3, 6.6)	6.450	6.440	5.959×10^{-3}	6.988×10^{-3}	9.048×10^{-4}
[0.65, 0.70)	[6.6, 6.9)	6.750	6.734	1.170×10^{-2}	4.284×10^{-3}	1.768×10^{-3}
[0.65, 0.70)	[6.9, 7.5)	7.200	7.164	1.361×10^{-2}	4.073×10^{-3}	2.049×10^{-3}
[0.65, 0.70)	[7.5, 8.7)	8.100	7.654	3.270×10^{-2}	2.300×10^{-2}	1.774×10^{-2}
[0.70, 0.75)	[4.2, 4.5)	4.350	4.334	1.217×10^{-1}	2.425×10^{-2}	1.866×10^{-2}
[0.70, 0.75)	[4.5, 4.8)	4.650	4.635	9.677×10^{-2}	1.880×10^{-2}	1.473×10^{-2}
[0.70, 0.75)	[4.8, 5.1)	4.950	4.944	6.132×10^{-2}	1.289×10^{-2}	9.293×10^{-3}
[0.70, 0.75)	[5.1, 5.4)	5.250	5.257	3.449×10^{-2}	9.039×10^{-3}	5.230×10^{-3}
[0.70, 0.75)	[5.4, 5.7)	5.550	5.585	1.992×10^{-2}	6.850×10^{-3}	3.015×10^{-3}
[0.70, 0.75)	[5.7, 6.0)	5.850	5.829	1.574×10^{-2}	4.508×10^{-3}	2.393×10^{-3}
[0.70, 0.75)	[6.0, 6.3)	6.150	6.128	1.714×10^{-2}	5.156×10^{-3}	2.644×10^{-3}
[0.70, 0.75)	[6.3, 6.6)	6.450	6.475	1.296×10^{-2}	4.424×10^{-3}	2.072×10^{-3}
[0.75, 0.80)	[4.2, 4.5)	4.350	4.347	8.694×10^{-2}	1.875×10^{-2}	1.337×10^{-2}
[0.75, 0.80)	[4.5, 4.8)	4.650	4.615	1.363×10^{-2}	8.592×10^{-3}	2.076×10^{-3}
[0.75, 0.80)	[4.8, 5.1)	4.950	4.935	1.345×10^{-1}	7.332×10^{-2}	3.052×10^{-2}

³⁴³ **References**

- ³⁴⁴ [1] S. D. Drell and T.-M. Yan, *Massive Lepton-Pair Production in Hadron-Hadron Collisions*
³⁴⁵ *at High Energies*, Phys. Rev. Lett. **25**, 316 (1970).
- ³⁴⁶ [2] S. Pate and C. Kuruppu, *An alternative proposal for determining DY yields*, DocDB 11322
- ³⁴⁷ [3] C.H. Leung et al., *Measurement of J/ψ and $\psi(2S)$ production in $p+p$ and $p+d$ interactions*
³⁴⁸ *at 120 GeV*, Physics Letters B **858**, 139032 (2024).